Good tidings for red tides?

Responses of toxic and calcareous dinoflagellates to global change

Dissertation zur Erlangung des akademischen Grades eines
Doktors der Naturwissenschaften
Dr. rer. nat.

Am Fachbereich 2 (Biologie/Chemie)

Vorgelegt von Tim Eberlein, März 2017

“An investment in knowledge always pays the best interest“

Benjamin Franklin (1706–1790)

Contents

Acknowledgements

The success of this thesis is based upon many pillars.

My biggest thanks go to my supervisors Björn Rost and Dedmer Van de Waal, who have the gift to inspire people with science as well as to guide them pleasantly through their PhD, always conveying fun with science work.

I thank Uwe John for his criticisms as a member of my PhD committee and furthermore for the nice time in Kristineberg.

I very much acknowledge the help I received from the PhytoChange group as well as the Biogeoscience section regarding help in setting up experiments, keeping them running and doing the sampling.

I thank the POLMAR duo Claudia & Claudia for the excellent organization of the graduate school, which allowed me to take part in very helpful and interesting courses.

I am glad of having had the opportunity in attending the Kristineberg study in 2013 as part of the BioAcid phase II, which were a really nice time and such a cool experiment on which I very often reminisce about.

Special thanks go to my family and friends, who encouraged me to keep going, especially in stressful times such as the last year of teaching at a secondary school.

Für meine liebe Oma Lia Eberlein.

Summary

Atmospheric CO_2 partial pressure (pCO_2) rises at a yet unprecedented rate, which enhances the uptake of CO_2 by the surface ocean and concomitantly lowers the pH. Due to the latter, these changes are often referred to as 'ocean acidification' (OA). In the last decades, consequences of OA on marine phytoplankton have been intensively studied from cellular to ecosystem level. These investigations have, however, largely focused on coccolithophores, diatoms and cyanobacteria. Little is known about the responses of dinoflagellates to OA, even though they represent an important component of phytoplankton assemblages. Moreover, owing to their type II RubisCO, a carboxylating enzyme with very low affinities for its substrate CO_2, dinoflagellates may be particularly sensitive to changes in CO_2 concentrations.

In my first publication, I therefore investigated the impact of OA on two dinoflagellate species, the calcareous *Scrippsiella trochoidea* and the paralytic shellfish poisoning (PSP) toxin producing *Alexandrium fundyense* (previously *A. tamarense*). The results show that, besides species-specific differences, growth characteristics remained largely unaltered with rising pCO_2 (*Publication I*). To understand these responses, several aspects of inorganic carbon (C_i) acquisition were investigated, revealing effective yet differently expressed carbon concentrating mechanisms (CCMs). These CCMs were moreover adjusted to the respective CO_2 environment, which enabled both species to keep their growth rates relatively unaffected over a broad range of pCO_2.

In addition to OA, rising CO_2 causes global warming, which in turn will lead to a rise in sea surface temperatures. Consequences will be an enhanced thermal stratification and a lowered nutrient resupply from nutrient-rich deep waters. Nutrient limitation may alter the response of dinoflagellates towards elevated pCO_2. In Publication II, I therefore investigated the effects of

rising CO_2 and nitrogen (N) limitation on *S. trochoidea* and *A. fundyense*. The findings indicate a close coupling between C and N assimilation and showed a CO_2-dependent increase in N assimilation in both species. Although N-rich compounds per cell were highest at high pCO_2, this came at the expense of higher N requirements and lower N affinities, which will reduce the competitive ability of both species that potentially translate to changes in the phytoplankton community composition in a future ocean.

To test the effect of OA on the productivity of phytoplankton in a natural community, a five months mesocosm study was conducted at the coast of the Swedish North Sea (*Publication III*). Besides early spring blooms of diatoms, dinoflagellate blooms often occur in these waters in late summer. During the experimental phase from March until July, we observed two major phytoplankton bloom events, which were both dominated by diatoms. Dinoflagellates usually overwinter as resting cysts in the sediment and as the applied mesocosms were closed in early spring, the initial inoculum of dinoflagellates was low. Weekly attempts to introduce seed populations of dinoflagellates to the mesocosms were not effective enough for species to subsist in these systems. Concerning the overall phytoplankton community, impacts of OA on primary production were generally small, though total primary production increased during the second phytoplankton bloom when nutrients were depleted to very low concentrations.

In conclusion, OA seems to have an effect on the photosynthetic activity of marine dinoflagellates, and furthermore cause changes in various physiological processes also related to nutrient acquisition. Even though these changes may appear ‘small’, at least when compared to OA-responses of other taxa, they can nonetheless influence the competitive abilities of species, especially when being exposed to nutrient limitation. On an ecosystem level, OA therefore has the potential to stimulate primary production and alter the phytoplankton community structure in coastal waters, especially at times when the availability of nutrients is limited.

Zusammenfassung

Der erdgeschichtlich beispiellose Anstieg im atmosphärischen CO_2-Partialdruck (pCO_2) führt zu einer erhöhten CO_2-Aufnahme der Ozeane und damit einhergehend einer Absenkung des pH-Wertes. Letzterer Prozess wird als „Ozeanversauerung“ bezeichnet, dessen Auswirkungen von der zellulärern Ebene bis hin zu ganzen Ökosystemen in den letzten Jahrzehnten intensiv untersucht wurden. Die meisten Studien haben sich hierbei auf Vertreter der Coccolithophoriden, Diatomeen und Cyanobakterien konzentriert. Vergleichsweise wenig ist über die Reaktionen von Dinoflagellaten auf Ozeanversauerung bekannt, obwohl diese Gruppe auch eine wichtige Komponente der Phytoplanktongemeinschaften darstellt. Durch den Typ II RubisCO, einem carboxylierenden Enzym mit besonders niedriger Affinität zu seinem Substrat CO_2, könnten Dinoflagellaten besonders stark auf Veränderungen im pCO_2 reagieren.

Für meine erste Publikation untersuchte ich deswegen den Einfluss von Ozeanversauerung auf zwei Dinoflagellaten, die kalzifizierende Art *Scrippsiella trochoidea* und die *paralytic shellfish poisoning* (PSP)-Toxine produzierende Alge *Alexandrium fundyense* (zuvor *A. tamarense*). Die Ergebnisse zeigen artenspezifische Unterschiede im Wachstumsverhalten, welche sich aber nur geringfügig unter steigenden CO_2-Konzentrationen verändern. Um diese Beobachtungen besser zu verstehen, wurden physiologische Untersuchungen zur Kohlenstoffaufnahme durchgeführt, die für beide Arten effektive, aber unterschiedlich regulierte Kohlenstoffkonzentrierungsmechanismen (CCM) ergaben. Diese CCMs ermöglichen es ihnen relativ unabhängig von den CO_2-Bedingungen in ihrer Umgebung zu wachsen.

Neben der Ozeanversauerung wirkt sich der Anstieg im atmosphärischen pCO_2 auch auf die globale Erwärmung und damit die Meeresoberflächentemperatur aus. Durch eine stärkere Stratifizierung wird vorrausichtlich weniger nährstoffreiches Wasser aus den Tiefen der Ozeane

an die Wasseroberfläche gelangen. Nährstofflimitierung könnten wiederum die Auswirkungen von OA auf Dinoflagellaten beeinflussen. In meiner zweiten Publikation untersuchte ich daher den kombinierten Einfluss von OA und Nitratlimitierung auf *S. trochoidea* und *A. fundyense*. Die Ergebnisse zeigen, dass die Assimilation von Kohlenstoff und Stickstoff stark miteinander verknüpft ist und sich die Stickstoffassimilierung mit steigendem CO_2-Gehalt in beiden Arten erhöht. Der CO_2-bedingte Anstieg in zellulären stickstoffreichen Verbindungen hatte jedoch einen höheren Stickstoffbedarf und niedrigere Affinitäten bei der Stickstoffaufnahme zur Folge. Diese Veränderungen können die Konkurrenzfähigkeit beider Arten beeinflussen und folglich Auswirkungen auf die Artenzusammensetzung zukünftiger Algenblüten haben.

Um den Effekt von Ozeanversauerung auf die Produktivität einer natürlichen Planktongemeinschaft zu testen, wurde eine 5-monatige Studie mit sogenannten Mesokosmen an der schwedischen Nordseeküste durchgeführt. Neben Algenblüten von Diatomeen im Frühling zeigen sich Blüten von Dinoflagllaten oft erst im Spätsommer. Während des Experimentes von März bis Juli konnten zwei von Diatomeen dominierte Algenblüten beobachtet werden. Dinoflagellaten überwintern als Zysten im Sediment und als die Mesokosmen im zum Frühlingsanfang hin geschlossen wurden, war die Anzahl an Dinoflagellaten sehr gering. Wöchentliche Versuche, Dinoflagellaten in die Mesokosmen einzubringen brachten nicht den erhofften Erfolg. Hinsichtlich der Phytoplanktongemeinschaft lässt sich festhalten, dass der Effekt der Ozeanversauerung nur einen geringen positiven Effekt auf die Primärproduktion hatte, und dies auch nur in der zweiten Algenblüte unter Nähstofflimitierung.

Es lässt sich abschließend festhalten, dass Ozeanversauerung Veränderungen in der Photosyntheseaktivität und weitere physiologische Prozesse hinsichtlich der Nährstoffaufnahme bei Algen hervorrufen kann. Verglichen mit anderen Taxa mögen diese Veränderungen klein wirken, doch sie können einen großen Einfluss auf die Konkurrenzfähigkeit der Arten haben, was

gerade unter Nährstofflimitierung zum Tragen kommt. Auf der Ebene eines Ökosystems kann Ozeanversauerung Einfluss auf die ganze Lebensgemeinschaft in Küstenregionen nehmen und besonders bei geringem Nährstoffangebot die Primärproduktion erhöhen und Artenzusammensetzung der Algengemeinschaft verändern.

1. Introduction

Preface

What makes planet Earth a 'habitable' planet? To answer this question in detail would surely go beyond the scope of this thesis. Basically, it is because of the relative distance between the earth and the sun, and the natural greenhouse gases such as water vapor, carbon dioxide (CO_2), ozone, and other elements including methane (CH_4) and nitrous oxide (N_2O), which keep the atmosphere relatively warm and insulated (NASA 1994). Altogether, these greenhouse gases make less than 0.1 % of the atmosphere, with the other 99.9 % being composed of nitrogen (N_2), oxygen (O_2), and to a lesser extent argon. This already indicates that small changes in atmospheric trace gas composition may have a strong impact on the global climate system.

1.1 Past - present - future of atmospheric CO_2 partial pressure

Ice core data reveals detailed insights into the atmospheric composition and the climate system to 800,000 years before present (Petit et al. 1999; Lüthi et al. 2008). This record also provides the natural variability in trace gases such as CO_2, which partial pressure (pCO_2) has varied between 180 and 300 µatm during glacial and interglacial cycles, respectively.

With the beginning of the Industrial Revolution less than 250 years ago, anthropogenic release of greenhouse gases, such as CO_2 from burning of fossil fuels, or NH_4 and N_2O from changes in land-use, have since then altered the atmospheric composition (IPCC 2013). Although climate can strongly vary, e.g. through volcanic eruptions or changes in solar variability, the observed changes exceed the signal of natural variability, being inevitably human-induced and on a time scale with no known precedent in the past (Karl et al. 2003).

Regarding CO_2, which is the most important contributor to anthropogenic forcing of climate change, pCO_2 values increased from pre-industrial levels of about 280 µatm towards 400 µatm CO_2 at present-day (Fig. 1; http://www.esrl.noaa.gov/ gmd/ccgg/trends/; Mauna Loa CO_2, November 2016). Although estimated pCO_2 values for 2100 vary, ranging from 800 to 1150 µatm (IPCC 2013), most models predict at least a doubling compared to today's CO_2 concentrations.

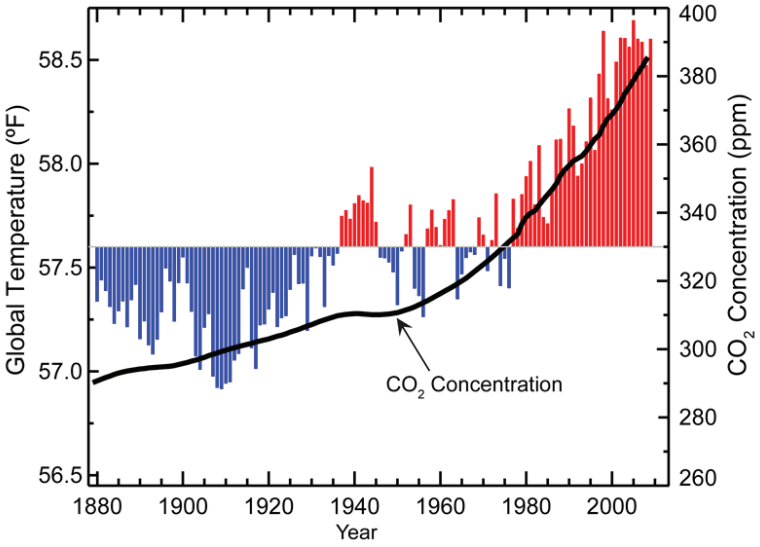

Fig. 1: Global temperature (°F) and CO_2 concentrations (parts per million; ppm) from 1880 until 2010. Temperature values represent the annual mean, with blue bars being below and red bars being above the baseline calculated from the 1961 to 1990. Figure from ncdc.noaa.gov.

One traceable response of the climate system to the anthropogenic CO_2 release is global warming (Karl et al. 2003). Over the last 100 years, global temperatures have increased by about 0.8 °C, with a rate of about 0.2 °C per decade over the last three decades (Fig. 1; Hansen et al. 2006). Ecological responses to climate change, ranging from polar to tropical systems, are already visible today (Walther et al. 2002). The predicted increase in global

temperatures of around 4 °C until 2100 (A1FI scenario; IPCC 2013) will further impose strong changes on the structure and functioning of ecosystems.

1.2 Implications of rising pCO_2 on the oceans

The release of CO_2 into the atmosphere and the associated global warming also affect the oceans, which cover 71 % of the earth's surface (http://www.noaa.gov/ocean.html). The oceans act as buffer in two ways, absorbing both heat and CO_2 from the atmosphere. Levitus et al. (2012) estimated that during the period from 1955 to 2010, the upper 2000 m of the oceans have warmed on average by about 0.1 °C. Although this increase seems small, putting the absorbed heat into perspective by transferring it into the lower 10 km of the atmosphere this would result in a temperature increase of 36 °C (Levitus et al. 2012). With the expected increase in atmospheric temperatures of up to 4 °C until 2100 (IPCC 2013), the oceans will absorb even more heat, which will alter physical, chemical as well as biological processes. In the low- and mid-latitude oceans, for instance, an increased vertical stratification may decrease the nutrient re-supply from nutrient-rich ocean bottom waters and, as most phytoplankton need a vertical nutrient transport to uphold productivity (Behrenfeld et al. 2006), thereby lowering primary production (Le Quéré et al. 2003; Sarmiento et al. 2004; Polovina et al. 2008).

Besides heat buffering, the oceans have a capacity to sequester large amounts of CO_2. From 1800 to 1994, this resulted in the uptake of around one third of anthropogenic CO_2 released into the atmosphere (Sabine and Feely 2007). Without the oceanic CO_2 uptake, concentrations in the atmosphere would have already exceeded 450 µatm at present-day (Doney et al. 2009). By taking up CO_2 from the atmosphere, however, the ocean surface waters become more acidic, which is commonly referred to as 'ocean acidification' (OA;

Caldeira and Wickett 2003) or *'the other CO_2 problem'* (Henderson 2006; Doney et al. 2009). Its effect on ecological processes, such as biodiversity or productivity, has since then been the focus of many studies. From 2004 until present, the number of publications on OA increased exponentially from about 20 to over 500 articles per year, respectively (Riebesell and Gattuso 2015).

1.3 Carbonate chemistry of seawater

CO_2 in the surface oceans equilibrates with the atmosphere through air-sea gas exchange. Besides atmospheric CO_2 levels, fluxes of CO_2 between ocean and atmosphere depend on the temperature- and salinity-dependent solubility constant K_0 (according to *Henry's law*). Unlike many other gases, such as O_2 and N_2, CO_2 does not only dissolve in water, but reacts with H_2O molecules and dissociates into several inorganic carbon (C_i) forms. In seawater, CO_2 (aq) and H_2O lead to the formation of carbonic acid (H_2CO_3), which due to its instability dissociates into bicarbonate (HCO_3^-) and carbonate (CO_3^{2-}) ions and protons (H^+) (Eq. 1).

$$CO_2(aq) + H_2O \rightleftharpoons H_2CO_3 \overset{K_1}{\rightleftharpoons} HCO_3^- + H^+ \overset{K_2}{\rightleftharpoons} CO_3^{2-} + H^+ \qquad \text{Eq. 1}$$

where K_1 and K_2 are the temperature-, salinity-, and pressure-dependent equilibrium constants of carbonic acid. The sum of the C_i forms is defined as dissolved inorganic carbon (DIC), but the relative contribution of each C_i form to DIC varies. As H_2CO_3 accounts for less than 0.3 % of CO_2 (aq) and both forms cannot chemically be distinguished from each other, H_2CO_3 is commonly subsumed in the term CO_2 (Zeebe and Wolf-Gladrow 2001). At a typical surface seawater pH of around 8.1 (with T=25 °C, S=35), CO_2 contributes about 1 % to DIC, HCO_3^- about 90 %, and CO_3^{2-} about 9 %.

Besides its dependency on temperature, salinity, and pressure, the contribution of the C_i forms to total DIC depends on total alkalinity (TA), which is also referred to as the proton buffer capacity of the water. TA can furthermore be defined as the excess of H^+ acceptors over H^+ donors with respect to a zero level of H^+ (Dickson 1981). Wolf-Gladrow et al. (2007) expressed TA in an *explicit conservative* way in terms of charge neutrality of major ions and acid base species:

$$\begin{aligned} TA_{ec} = {} & [Na^+] + 2[Mg^{2+}] + 2[Ca^{2+}] + [K^+] + 2[Sr^{2+}] + \ldots \\ & - [Cl^-] - [Br^-] - [NO_3^-] - \ldots \\ & + [TPO_4] + [TNH_3] - 2[TSO_4] - [THF] - [THNO_2] \end{aligned} \qquad \text{Eq. 2}$$

The advantage of the latter definition is that it permits to judge consequences of biological processes on TA. For instance, calcification (i.e. the production of $CaCO_3$) will remove two positive charges from solution (i.e. Ca^{2+}) and thereby decreases TA by two units. Assimilation of one unit nitrate, on the other hand, increases TA by one unit (Eq. 2). These effects are illustrated in Figure 2.

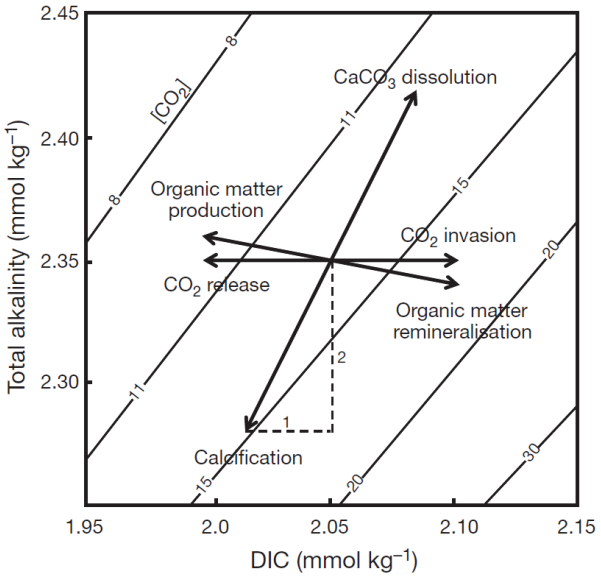

Fig. 2: Effects of biotic and abiotic processes on total alkalinity (TA) and dissolved inorganic carbon (DIC) concentrations in marine seawater. After Zeebe and Wolf-Gladrow (2001).

Increased CO_2 emissions will alter the dissolution of CO_2 in seawater, leading to a decrease in CO_3^{2-} and an increase in CO_2 (aq), HCO_3^- and H^+, the latter being the decisive factor for the drop in seawater pH. Until 2100, seawater pH is projected to decrease by 0.3 units from around 8.1 to 7.8 (Fig. 3; IPCC 2013).

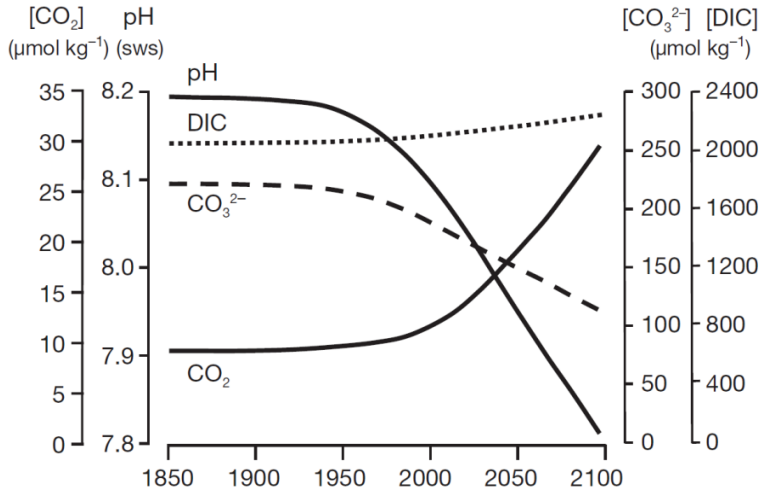

Fig. 3: Anticipated changes in carbonate chemistry in the surface ocean layer as a result from increasing atmospheric CO_2 concentrations, based on the IS92a Scenario (IPCC 1992). Modified after Wolf-Gladrow et al. (1999).

1.4 The ocean carbon cycle

Through air-sea gas exchange, CO_2 equilibrates between the atmosphere and the surface ocean over timescales of weeks to months (Falkowski et al. 2000). Biological activity in the upper mixed layer can strongly alter surface ocean DIC concentrations. Below 300 m depth, concentrations notably increase relative to surface ocean DIC, which can be attributed to the *solubility pump* and *biological pumps* (Volk and Hoffert 1985; Sarmiento et al. 1995). Here, the term 'pump' indicates transportation of carbon to depth building a vertical DIC gradient. CO_2 is more soluble in cold waters, promoting dissolution of CO_2 in seawater at high latitudes. This cold, dense, and CO_2-rich surface water sinks to the depths of the oceans. Once it is transported laterally, the overlaying lighter waters prevent re-equilibration with the atmosphere (Falkowski et al. 2000). Yet, this process explains only a quarter of the observed vertical DIC gradient. The remaining 75 % can be attributed to the biological pumps. Primary production in the surface layer leads to the fixation of roughly 45 gigatons inorganic carbon per year and thereby reduces surface ocean DIC concentrations (Falkowski et al. 1998). While most of the organic matter is remineralized in the surface, up to 11 gigatons organic carbon (i.e. about 25 %) is exported into deeper layers and out of the upper mixed layer (Schlitzer 2000), while only 1 to 3 % of reaches the ocean floor, building up carbon-rich sediments (De La Rocha and Passow 2007).

Phytoplankton are relatively flexible in terms of dealing with different nutrient conditions. Still, formation of particulate organic matter requires the supply of nutrients in a certain proportion in the oceans and therefore nutrient availability strongly impacts biochemical cycles (Smetacek 1999). The Redfield ratio denotes the mean elemental ratio in marine phytoplankton of 106 (carbon) : 16 (nitrogen) : 1 (phosphorus) and the same N : P ratio in ocean deep waters (Redfield 1958; Redfield et al. 1963). Deviations from the Redfield ratio

are often used as an indication for metabolic demands or nutrient limitations by organisms (Sterner & Elser 2002; Klausmeier et al. 2004). Nitrogen and phosphorus are key nutrients required for the maintenance of metabolic processes and thus growth. Their surface concentrations, however, are low in large areas of the present-day oceans (e.g. nitrate; Fig. 4) and often limit primary production (Elser et al. 2007; Moore et al. 2013).

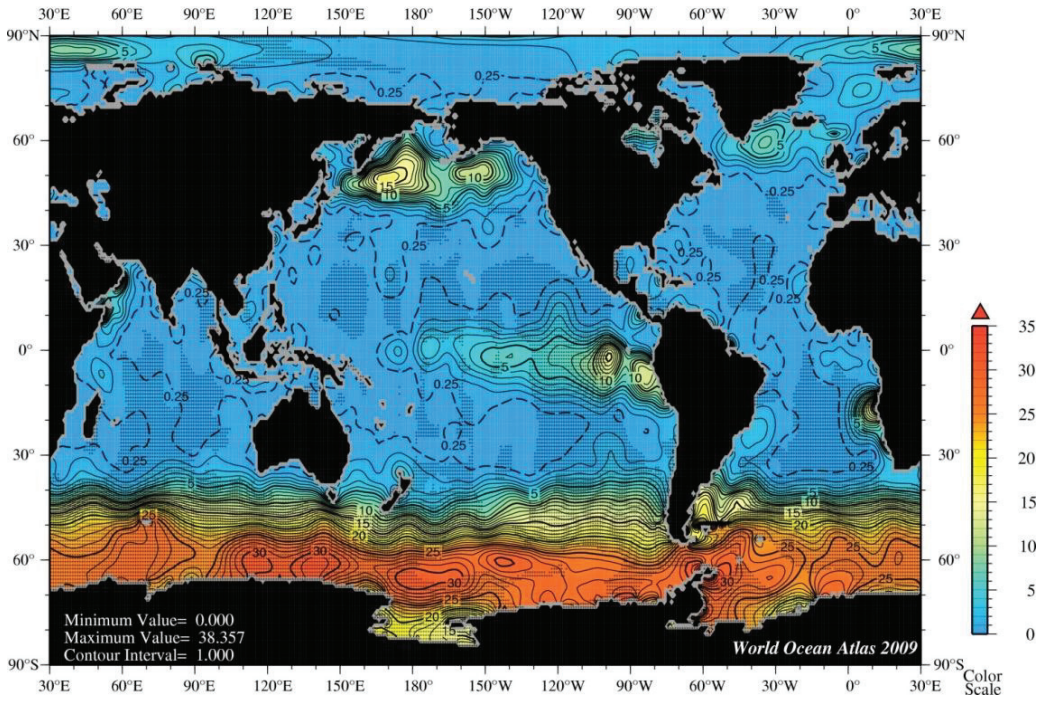

Fig. 4: Average nitrate concentrations (µmol L^{-1}) in the upper 10 meter of the world oceans from July to September, ranging from almost zero in the tropics and subtropics to about 15 in the Arctic and 40 µmol L^{-1} in the Antarctic. From *World Ocean Atlas 2009*.

1.5 The ocean nitrogen cycle

In the oceanic nitrogen pool, 95 % is present in the form of dissolved dinitrogen (N_2), which is an inert molecule and only accessible to diazotrophs (Capone et al. 1997; Mahaffey et al. 2005). The remaining 5 % comprises more reactive forms, e.g. nitrate (NO_3^-), nitrite (NO_2^-), ammonium (NH_4^+), and dissolved organic nitrogen forms. Metabolism from most phytoplankton species rely on the availability of NO_3^-, NO_2^-, and NH_4^+ as nitrogen sources, which due to their low abundance often limit primary production in the open oceans. NO_3^- is supplied to the surface oceans via upwelling events of NO_3^--rich bottom waters that are formed through remineralization of sunken particulate organic matter in the deep oceans (Voss et al. 2013). Once upwelled, these suddenly available NO_3^- molecules (new nutrients) are considered to support "new" production. Another process supporting new production is provided by N_2-fixating diazotrophs. In warm, oligotrophic regions, diazotrophs can be responsible for more than 50 % of net production (Capone et al. 1997). At end of a phytoplankton spring bloom, new production can be as high as 80 %, while the remaining 20 % of particulate organic matter originates from recycled nitrogen (mainly NH_4^+) in the surface oceans (Eppley and Peterson 1979). In contrast to new production, a recycling of nutrients in the food web in the upper mixed layer will not alter net production and is thus termed "regenerated" production (Dugdale and Goering 1967).

It is crucial to understand the cycling of major nutrients in the oceans in order to understand the carbon cycle and *vice versa*. The knowledge of a connection between them reaches back to the classical paper of Redfield (1958) and shows the interweaving of biologically required nutrients such as carbon, nitrogen and phosphorus. Being part of global change, the increase in thermal stratification and the accompanied decrease in nutrient re-supply from ocean deep waters (Le Quéré et al. 2003; Sarmiento et al. 2004) may shift the

ratio between new and regenerated production. New production could decrease (Beman et al. 2011; Hutchins et al. 2009), while regenerated production, based on NH_4^+ could become more prominent. Either way, regions of NO_3^--limited growth may expand in a future ocean, thereby having a tremendous effect on the biogeochemical cycle of carbon.

1. 6 Marine primary production and limitations therein

Marine phytoplankton convert solar energy into chemical energy that is used to fix CO_2 into organic compounds. They form the base of the marine food web and account for about 50 % of the global primary production (Falkowski et al. 1998). Briefly, C_i enters the Calvin cycle as CO_2 via the enzyme Ribulose-1,5-bisphosphate carboxylase/ oxygenase (RubisCO), where it is linked to Ribulose-1,5-bisphosphate yielding two molecules of 3-phosphoglycerate. Using photochemically derived ATP and NADPH, 3-phosphoglycerate is transformed into the two molecules of the carbohydrate glyceraldehyde-3-phosphate of which one is exported from the Calvin cycle. Through an oxygenase reaction, RubisCO is also able to link O_2 to Ribulose-1,5-bisphosphate, producing 2-phosphoglycolat. Although two molecules of 2-phosphoglycolat can be recycled into one molecule of 3-phosphoglycerate, this process of photorespiration is very energy-demanding and produces CO_2 as well as NH_3 (Badger et al. 1998). Regarding the latter, NH_3 can either get lost from the amino acid pool or once more be assimilated, a process that requires again energy.

By producing energy-carrying carbohydrates, phytoplankton make the otherwise inaccessible and energy-poor C_i accessible to other organisms and provide the basis for the food web. Marine phytoplankton possess different forms of RubisCO, which vary in their affinity for CO_2 and sensitivity to O_2. Among the main eukaryotic phytoplankton groups, type I RubisCO is the most common form and comprises eight large and eight small subunits, which are encoded in the plastid and the nucleus, respectively. Dinoflagellates feature a type II RubisCO, which consists of only eight large subunits and coincidently exhibit very low CO_2 affinities compared to type I (Morse et al. 1995; Badger et al. 1998). One reason for this low affine RubisCO may be due to the fact that dinoflagellates evolved around 400 million years ago, when CO_2 concentrations in the atmosphere were about

eight times higher compared to present-day CO_2 concentrations (Beardall and Raven 2004). Under these conditions, such poor affinities apparently came without any significant disadvantages. In contrast, haptophytes and diatoms (based on fossils) evolved more recently, their origin dates back to 200 million and 150 million years ago, respectively (Berner 1997; Falkowski and Raven 1997). At that time, CO_2 concentrations decreased already by more than half compared to 400 million years ago.

With the low equilibrium CO_2 concentrations relative to total DIC concentrations and the low diffusion rate of CO_2 in water, the effectiveness of C fixation in marine phytoplankton was expected to be very low, particularly in dinoflagellates (Colman et al. 2002; Dason et al. 2004). In the past decades, however, studies showed that many species do possess different mechanisms to overcome these risks of C limitation by deploying so-called carbon concentrating mechanisms (CCMs). These CCMs enable species to reach saturation in C fixation already at much lower CO_2 concentrations than the affinity of their RubisCO would actually support (Fig. 5; Beardall and Raven 2004; Giordano et al. 2005).

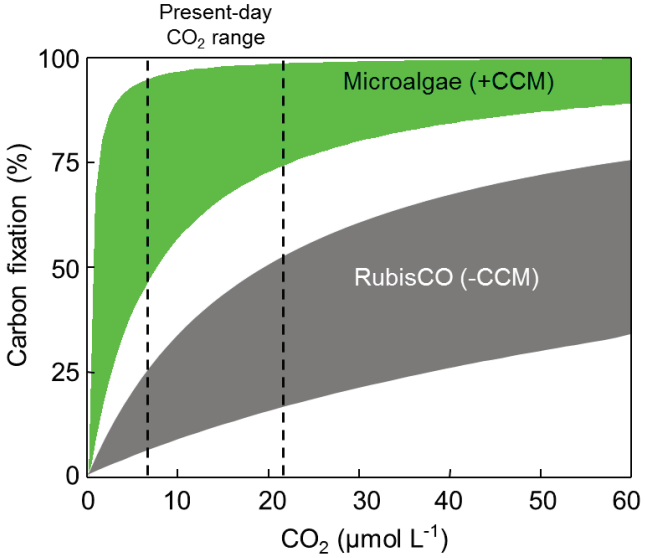

Fig. 5: Schematic overview of carbon fixation by phytoplankton (green; including a CCM) or isolated RubisCO (grey) in response to increasing CO_2 availability. The range of present-day CO_2 concentrations is marked by dotted lines. Modified after Beardall and Raven (2004).

CCMs may involve active CO_2 and HCO_3^- uptake, as well as means to decrease CO_2 leakage from the cell. The usage of carbonic anhydrase (CA) may further support the accumulation of C_i in the cell. More specifcally, CA can be extracellular, where it accelerates the equlibration of CO_2 and HCO_3^- in boundary layer of the cell. This may be favorable particularly for CO_2-using phytoplankton, as it preserves the availability of CO_2 for uptake. Inside the cell, CA falilates CO_2 at the side of RubisCO and is involved in means to reduce the loss of C_i from the cell.

Within the group of dinoflagellates, effective CCMs were found (Leggat et al. 1999; Rost et al. 2006; Ratti et al. 2007). With respect to the type II RubisCO and its low CO_2 affinity and low CO_2 to O_2 sensitivity, this mechanism may be crucial for dinoflagellates to persist under present-day CO_2 concentrations. Yet, depending on the mode, CCMs require most of the energy resources of a cell implying that the investment in C_i acquisition may have a profound effect on the fitness of species and the costs for growth (Raven et al. 2004). In view of the annual succession of phytoplankton, dinoflagellates bloom relatively late in low-nutrient and less turbulent waters (Margalef 1978), indicating that within this group of phytoplankton, other traits may play a vital role in its persistence as well.

1.7 Harmful algal blooms in a future ocean

Many dinoflagellate species have the ability to form harmful algal blooms (HABs; Burkholder 1998; Granéli and Turner 2006). It has to be noted, however, that the HAB criteria represent more a societal concept than a scientific definition, and comprise algal blooms with the potential to cause injury to human health or socioeconomic interests, or components of aquatic ecosystems (Anderson et al. 2012*a*). Among the group of

dinoflagellates, the genus *Alexandrium* and *Dinophysis* are classified as very toxic, causing "paralytic shellfish poisoning" (PSP) and "diarrhetic shellfish poisoning", respectively. With regard to diversity, distribution, and toxin production, *Alexandrium* is considered as one the most important HAB species having biggest impact on human intoxications and death from contaminated shellfish (Anderson et al. 2012*b*). This can be attributed to the production of saxitoxin (STX) and its analogues, most importantly neosaxitoxin (NEO), and the less toxic gonyautoxins (GTX 1-4) (Anderson et al. 2012*b*). The fact that toxin analogues vary in their toxicity (Wiese et al. 2010) makes it important to determine both total toxin production and toxin composition when determining the threat from HAB species. The success of cosmopolitan dinoflagellates such as the genus *Alexandrium* is, however, not only facilitated by their ability to produce toxic and allelopathic compounds, but furthermore the result of their vast genetic and phenotypic diversity and their capability to form resting cysts (Masseret et al. 2009; John et al. 2014). In addition, many dinoflagellate species can actively prevent nutrient limitation on a short-term basis through mixotrophy (Jeong et al. 2005) and by exhibiting a swim strategy (MacIntyre et al. 1997). Formation of (temporary) cysts has also been observed in many species and allows them to survive unfavorable nutrient conditions as well as predator-prey interactions (Fistarol et al. 2004).

In the last decades, the frequency of PSP toxin producing HABs have strongly increased (Fig. 6; Anderson et al. 2012*a*). While the occurrence of HAB events could in some cases be directly linked to eutrophication (Glibert et al. 2008), in other cases it could not and may be attributed to the increase in monitoring effort as well as the greater awareness due to the steady increase in shellfish farming (Anderson et al. 2008). An increase in the frequency of HABs may also derive from the anticipated changes in ocean carbonate chemistry, i.e. enhanced growth and photosynthesis of HAB species as a result of increasing CO_2

availability (Fu et al. 2012) or lowered pH values (Hansen et al. 2007). CCMs are active processes demanding for ATP, and with an increasing availability of CO_2, the energetic costs for C acquisition and transport are expected to decrease, resulting in more energy being available for other growth processes (Beardall and Giordano 2002). The few studies, which investigated the responses of OA on toxin production and toxin composition in HAB species show differential effects, indicating that underlying processes are not yet well understood (Fu et al. 2012; Kremp et al. 2012; Van de Waal et al. 2014). Toxin levels in algae were furthermore shown to vary depending on the nutrient concentrations in the water. The production of PSP toxins, for instance, strongly depends on nitrogen or phosphorus availability (Boyer et al. 1987; Cembella 1998; Van de Waal et al. 2013).

With respect to the genetic and phenotypic diversity and the various traits found among dinoflagellate species (e.g. mixotrophy, formation of resting cysts, swim strategy), there is a big knowledge gap of how OA and other environmental drivers involved in global change may favor the occurrence, frequency and magnitude of HABs (Wells et al. 2015). The interplay of OA and N limitation for example, has so far not been tested on dinoflagellates, which makes predictions for the future ocean in the end imprecise.

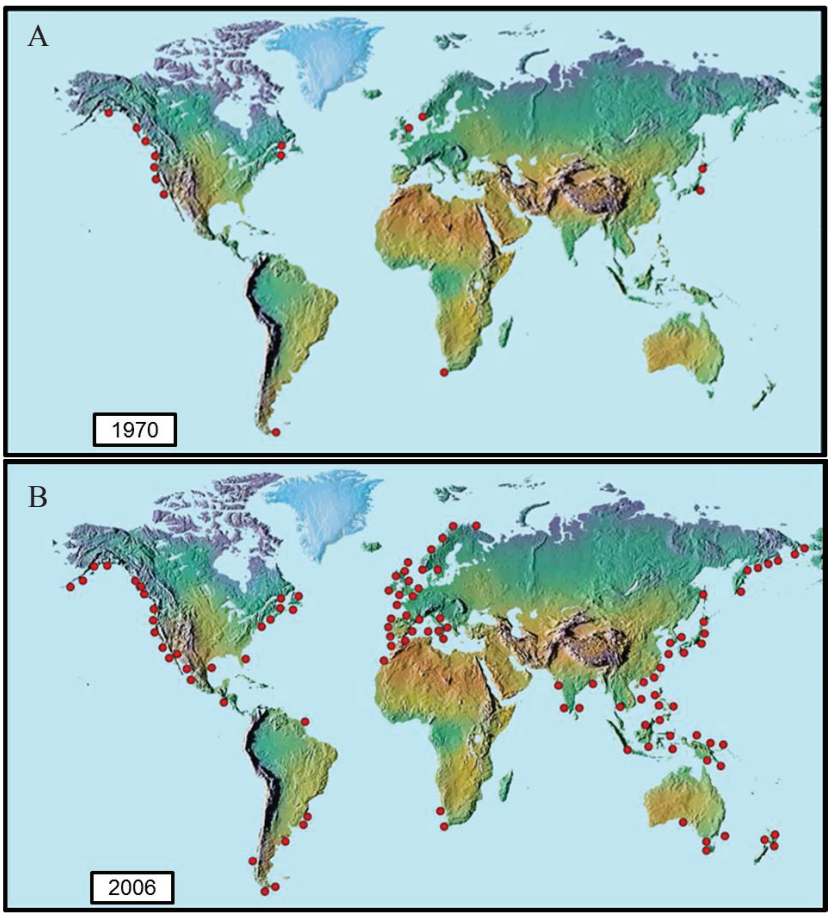

Fig. 6: Harmful algal bloom events (red dots) of paralytic shellfish poisoning toxins worldwide until 1970 (A) and 2006 (B). From *U.S. National office for Harmful Algal Blooms*.

1.8 Aim of this thesis

In the last decades, the number of studies investigating the effects of OA on marine biota has strongly enhanced our knowledge e.g. on CO_2-dependent regulation of the C acquisition in phytoplankton. Yet, there is a strong imbalance of studies between the major groups of phytoplankton. For instance, still relatively little is known about the group of dinoflagellates. While earlier work suggested that this taxon may be particularly prone to C limitation (Coleman et al. 2002), more recent studies determined effective CCMs in many species, allowing them to overcome potential C limitation during photosynthesis (Rost et al. 2006).

In the first study of this thesis, responses of two ecologically important dinoflagellates species (i.e. the toxic *Alexandrium fundyense* and calcifying *Scrippsiella trochoidea*) towards increasing pCO_2 were therefore tested. To understand the measured growth responses and furthermore to characterize their specific CCMs, membrane-inlet mass spectrometry (MIMS) was performed. This approach yields rates for physiological key processes such as photosynthetic O_2 evolution, respiration, CO_2 and HCO_3^- fluxes, as well as CA activities. Unravelling these processes provided the basis for explaining their responsiveness towards different pCO_2 conditions.

The second study was motivated by observations that global change also involves an increase in thermal stratification of the surface oceans, reducing nutrient re-supply with nutrient-rich deep waters. Thus, responses of both dinoflagellate species to OA combined with N limitation were tested using chemostat incubations. In a high CO_2 environment, down-regulation of costly and under these conditions partly 'expendable' processes, such as CCMs, may allow for a reallocation of energy into other cellular processes. Under N limitation, this led to CO_2-dependent changes in N assimilation, which affected elemental

composition, N affinity as well as toxicity. Such changes may have strong ecological consequences for future HAB events.

A third study assessed the effects of OA on primary production during a five-month period in an outdoor mesocosm experiment of a coastal North Sea phytoplankton community. My motivation was to 'zoom out' from my previous approach of investigating single cell processes, and to acknowledge that the oceans comprise *more than a 2 L bottle*. The duration of the experiment was designed to allow for changes to occur in species composition, abundance, and succession, and thus leading to a restructuring in a coastal marine food web. The findings suggest that OA may have a stimulating effect on the productivity and biomass build-up of phytoplankton during two consecutive bloom events, though the effects were small and mainly present under severe N limitation. OA also led to a change in the phytoplankton community structure (Bach et al. 2016). So, although effects of OA on primary production were small, it may restructure phytoplankton communities in the future coastal North Sea with likely consequences for higher trophic levels.

2. Publications

2.1 List of publications

Eberlein, T., D. B. Van de Waal, and B. Rost. 2014. Differential effects of ocean acidification on carbon acquisition in two bloom-forming dinoflagellate species. Physiol. Plant. 151: 468–479

Eberlein, T., D. B. Van de Waal, K. M. Brandenburg, U. John, M. Voss, E. P. Achterberg, and B. Rost. 2016. Interactive effects of ocean acidification and nitrogen limitation on two bloom-forming dinoflagellate species. Mar. Ecol. Prog. Ser. 543: 127–140

Eberlein, T., S. Wohlrab, B. Rost, U. John, L. Bach, U. Riebesell, and D. B. Van de Waal. 2016. Impacts of ocean acidification on primary production in a coastal North Sea phytoplankton community. *accepted for PLoS ONE*.

Declaration of own contribution

Tim Eberlein, Dr. Björn Rost and Dr. Dedmer Van de Waal developed the experiments of the three manuscripts. The first author performed most of the practical work, accomplished the analyses, and wrote the drafts of the manuscripts. These drafts were discussed with all co-authors and manuscripts were then finalized by the first author.

2.2 Publication I

Differential effects of ocean acidification on carbon acquisition in two bloom-forming dinoflagellate species.

Physiologia Plantarum
An International Journal fo

Physiologia Plantarum 151: 468–479. 2014 ISSN 0031-9317

Differential effects of ocean acidification on carbon acquisition in two bloom-forming dinoflagellate species

Tim Eberlein[a,*], Dedmer B. Van de Waal[a,b] and Björn Rost[a]

[a]Department of Marine Biogeoscience, Alfred Wegener Institute for Polar and Marine Research, Bremerhaven, Germany
[b]Department of Aquatic Ecology, Netherlands Institute of Ecology (NIOO-KNAW), 6700 AB Wageningen, The Netherlands

Correspondence
*Corresponding author,
e-mail: Tim.Eberlein@awi.de

Received 30 September 2013;
revised 18 November 2013

doi:10.1111/ppl.12137

Dinoflagellates represent a cosmopolitan group of phytoplankton with the ability to form harmful algal blooms. Featuring a Ribulose-1,5-bisphosphate carboxylase/oxygenase (RubisCO) with very low CO_2 affinities, photosynthesis of this group may be particularly prone to carbon limitation and thus benefit from rising atmospheric CO_2 partial pressure (pCO_2) under ocean acidification (OA). Here, we investigated the consequences of OA on two bloom-forming dinoflagellate species, the calcareous *Scrippsiella trochoidea* and the toxic *Alexandrium tamarense*. Using dilute batch incubations, we assessed growth characteristics over a range of pCO_2 (i.e. 180–1200 µatm). To understand the underlying physiology, several aspects of inorganic carbon acquisition were investigated by membrane-inlet mass spectrometry. Our results show that both species kept growth rates constant over the tested pCO_2 range, but we observed a number of species-specific responses. For instance, biomass production and cell size decreased in *S. trochoidea*, while *A. tamarense* was not responsive to OA in these measures. In terms of oxygen fluxes, rates of photosynthesis and respiration remained unaltered in *S. trochoidea* whereas respiration increased in *A. tamarense* under OA. Both species featured efficient carbon concentrating mechanisms (CCMs) with a CO_2-dependent contribution of HCO_3^- uptake. In *S. trochoidea*, the CCM was further facilitated by exceptionally high and CO_2-independent carbonic anhydrase activity. Comparing both species, a general trade-off between maximum rates of photosynthesis and respective affinities is indicated. In conclusion, our results demonstrate effective CCMs in both species, yet very different strategies to adjust their carbon acquisition. This regulation in CCMs enables both species to maintain growth over a wide range of ecologically relevant pCO_2.

Abbreviations – CA, carbonic anhydrase; CCM, carbon concentrating mechanism; Chl *a*, chlorophyll *a*; C_i, inorganic carbon; CO_3^{2-}, carbonate ion; DBS, dextran-bound sulphonamide; DIC, dissolved inorganic carbon; eCA, extracellular carbonic anhydrase; HCO_3^-, bicarbonate; HEPES, 4-(2-hydroxylethyl)-1-piperazine-ethanesulfonic acid; $K_{1/2}$, half-saturation concentration; MIMS, membrane-inlet mass spectrometry; OA, ocean acidification; pCO_2, atmospheric CO_2 partial pressure; PFD, photon flux density; PIC, particulate inorganic carbon; POC, particulate organic carbon; PON, particulate organic nitrogen; PST, paralytic shellfish poisoning toxins; RubisCO, Ribulose-1,5-bisphosphate carboxylase/oxygenase; TA, total alkalinity.

Introduction

Since the Industrial Revolution, alterations in fossil fuel combustion and land-use have caused atmospheric CO_2 partial pressure (pCO_2) to increase from approximately 280 toward approximately 395 µatm at present-day, and is predicted to reach values of approximately 900 µatm by the end of the 21st century (IPCC 2007). Regarding the oceans, elevated pCO_2 causes an increase in CO_2 and bicarbonate (HCO_3^-) concentrations, while carbonate ion concentrations (CO_3^{2-}) decrease. These changes in the speciation of dissolved inorganic carbon (DIC) result in lowered pH values, a phenomenon also known as ocean acidification (OA; Wolf-Gladrow et al. 1999, Caldeira and Wickett 2003). OA and associated changes in the carbonate chemistry have been shown to impact marine organisms in many ways (Fabry et al. 2008). Especially for phytoplankton, being the base of the marine food web and the driver of the biological carbon pumps, such changes may have far reaching consequences (Falkowski et al. 1998, Doney et al. 2009).

Phytoplankton take up inorganic carbon and fix CO_2 into organic compounds by Ribulose-1,5-bisphosphate carboxylase/oxygenase (RubisCO). This enzyme generally features low affinities for CO_2, and a competing reaction with O_2 further reduces its overall efficiency (Badger et al. 1998). To overcome these catalytic limitations imposed by RubisCO, phytoplankton developed so-called carbon concentrating mechanisms (CCMs). Common features of a CCM include active uptake of CO_2 and HCO_3^- as well as means to reduce the CO_2 leakage (Giordano et al 2005, Rost et al. 2006). CCMs may further involve carbonic anhydrase (CA), an enzyme which accelerates the otherwise slow interconversion between CO_2 and HCO_3^-. The mode and cost of CCMs will to a great extent determine the sensitivity of phytoplankton toward OA (Rost et al. 2008, Reinfelder 2011).

The functioning of CCMs has been intensively studied in various phytoplankton species. In diatoms, CCMs were generally downregulated with increasing pCO_2 as reflected by lowered photosynthetic affinities for CO_2 and DIC (Burkhardt et al. 2001, Trimborn et al. 2008). Often, these changes were also accompanied by lowered contribution of HCO_3^- uptake or decreased activities of extracellular CA (eCA). In other taxa such as the coccolithophore *Emiliania huxleyi* or the cyanobacterium *Trichodesmium*, affinities for CO_2 and DIC were also downregulated under OA, yet eCA activity did not seem to play a role in the functioning of their CCMs (Rost et al. 2003, Kranz et al. 2009). These different modes of CCMs and their regulation with pCO_2 have increased our understanding about species-specific responses toward OA in diatoms, coccolithophores and cyanobacteria. Little is yet known about other taxa, such as dinoflagellates.

Earlier work suggested severe CO_2 limitation in photosynthesis of dinoflagellates (Colman et al. 2002, Dason et al. 2004). This was attributed to their type II RubisCO, which has the lowest affinity for CO_2 of all eukaryotic phytoplankton (Morse et al. 1995, Badger et al. 1998), as well as limited ability to use HCO_3^-. Recent studies have, however, demonstrated high HCO_3^- uptake rates in the dinoflagellates species *Ceratium lineatum*, *Heterocapsa triquetra*, *Prorocentrum minimum* (Rost et al. 2006, Fu et al. 2008) and *Protoceratium reticulatum* (Ratti and Giordano 2007), indicating rather efficient modes of CCMs that may make them relatively independent from changes in CO_2 availability. In some dinoflagellates, CCMs have been shown to respond to changes in carbonate chemistry, e.g. by lowered photosynthetic affinities for CO_2 and DIC (Rost et al. 2006, Ratti and Giordano 2007), or by downregulation of CA transcripts (Van de Waal et al. 2013) with increasing pCO_2. Such apparent differences in the regulation of CCMs may explain the observed variability in responses to OA in growth and primary production of different dinoflagellate species (Fu et al. 2007, 2010) or strains (Brading et al. 2011, 2013).

To improve our understanding about growth responses and the functioning of CCMs in dinoflagellates under OA, this study investigated the eco-physiology of two distinct dinoflagellate species, the calcareous *Scrippsiella trochoidea* and the toxic *Alexandrium tamarense* over a range of pCO_2. Both are bloom-forming species that co-occur in the North Sea (Fistarol et al. 2004, McCollin et al. 2011). As one has the potential to calcify and the other is a potent toxin producer, different ecological strategies can be expected, which may also be reflected in the functioning of their CCM. Hence, measurements on growth and biomass production were accompanied by measurements on inorganic carbon fluxes and CA activities using membrane-inlet mass spectrometry (MIMS).

Materials and methods

Species and growth conditions

Scrippsiella trochoidea GeoB267 (culture collection of the University of Bremen) and *Alexandrium tamarense* Alex5 (Tillmann et al. 2009), both isolates from the North Sea, were cultured at 15°C in 0.2 µm filtered North Sea water (salinity 34). Vitamins and trace metals were added according to f/2 medium (Guillard and Ryther 1962), except for $FeCl_3$ (1.9 µmol l^{-1}), H_2SeO_3 (10 nmol l^{-1}) and $NiCl_2$ (6.3 nmol l^{-1}). Nitrate and

phosphate were added to final concentrations of 100 and 6.25 µmol l^{-1}, respectively. Culture medium was pre-aerated with air containing pCO_2 of 180 µatm (Last Glacial Maximum), 380 µatm (present-day), 800 µatm and 1200 µatm (scenarios of the year 2100 and beyond). These concentrations were obtained by mixing CO_2-free air (<0.1 µatm pCO_2; Domnick Hunter, Willich, Germany) with pure CO_2 (Air Liquide Deutschland, Düsseldorf, Germany) using mass flow controllers (CGM 2000 MCZ Umwelttechnik, Bad Nauheim, Germany). CO_2 concentrations were regularly verified by a non-dispersive infrared analyzer system (LI6252, LI-COR Biosciences, Bad Homburg, Germany).

Cultures were grown in 2.4 l borosilicate bottles and placed on a roller table to allow homogenous mixing. Light was provided by OSRAM daylight tubes (18 W/965 Biolux) at a light : dark cycle of 16:8 h. Light was adjusted to an incident photon flux density (PFD) of 250 ± 25 µmol photons m^{-2} s^{-1} using a spherical micro quantum sensor (Walz, Effeltrich, Germany). Prior to the onset of the experiments, cells were acclimated to the respective CO_2 concentrations for at least 14 days. To ensure dilute batch conditions with minor changes in carbonate chemistry, cultures were diluted about once a week and population densities were kept <400 cells ml^{-1}. Experiments were run in triplicates (n = 3) over at least 5 days.

Sampling and analyses

Samples were always taken 5–7 h after the start of the light period. Every other day, pH was measured with a 2-point calibrated WTW pH meter 3110 (Wissenschaftlich-Technische Werkstätten GmbH, Weilheim, Germany). Samples for total alkalinity (TA) were analyzed by a fully automated titration system (SI Analytics, Mainz, Germany) with a mean accuracy of 13 µmol l^{-1}. DIC samples were analyzed in a QuAAtro high performance microflow analyzer (Seal, Mequon, WI) with a mean accuracy of 8 µmol l^{-1}. Changes in TA and DIC over the course of the incubations were <2 and <3.4%, respectively. Owing to the decreasing buffer capacity with increasing pCO_2 (Egleston et al. 2010), DIC consumption caused higher variability in pH and pCO_2 in the high CO_2 treatments (Table 1). Carbonate chemistry was calculated with CO2sys (Pierrot et al. 2006) using pH_{NBS} (National Bureau of Standards) and TA of each incubation. Equilibrium constants of Mehrbach et al. (1973), refitted by Dickson and Millero (1987) were chosen.

To determine population densities, 20–60 ml culture suspension was fixed with Lugol's solution (2% final concentration). Each day, triplicate cell counts were performed with an Axiovert 40C inverted microscope (Carl Zeiss MicroImaging GmbH, Hamburg, Germany). Specific growth rates (μ) were calculated by an exponential fit through cell counts over at least 4 days for each biological replicate (n = 3).

Table 1. Carbonate chemistry for the different CO_2 treatments. Values for TA, DIC and pH indicate the mean of triplicate incubations (n = 3; ± sd). pCO_2 was calculated based on pH and TA of each incubation, using equilibrium constants by Mehrbach et al. (1973), refitted by Dickson and Millero (1987)

CO_2 treatment	TA (µmol l^{-1})	DIC (µmol l^{-1})	pH_{NBS}	pCO_2 (µatm)
S. trochoidea				
180	2386 ± 1	1972 ± 16	8.45 ± 0.01	180 ± 6
380	2388 ± 2	2096 ± 10	8.21 ± 0.02	358 ± 15
800	2385 ± 1	2223 ± 11	7.91 ± 0.03	785 ± 55
1200	2386 ± 4	2268 ± 18	7.77 ± 0.04	1133 ± 97
A. tamarense				
180	2434 ± 3	1992 ± 33	8.50 ± 0.06	162 ± 24
380	2439 ± 1	2117 ± 41	8.27 ± 0.07	315 ± 57
800	2434 ± 2	2245 ± 37	7.97 ± 0.10	706 ± 154
1200	2418 ± 1	2283 ± 34	7.83 ± 0.12	995 ± 248

At the end of each experiment, samples were taken to assess particulate organic carbon and nitrogen (POC and PON), particulate inorganic carbon (PIC, as difference between total particulate carbon and POC), as well as chlorophyll *a* (Chl *a*). For analyses of POC and PON, 300–400 ml culture suspension was filtered in duplicate on pre-combusted GF/F filters (500°C, 6 h). Prior to POC measurements, 200 ml of HCl (0.1 mol l^{-1}) was added to the filters to remove all PIC, and filters were dried overnight. Filters were wrapped in tin foil cups and analyzed by an ANCA-SL 20–20 mass spectrometer (SerCon Ltd., Crewe, UK). To determine Chl *a*, 100–200 ml culture suspension was filtered in duplicate on cellulose-nitrate filters (Whatman, Maidstone, UK), rapidly frozen in liquid nitrogen and subsequently stored at −80°C. Extraction and fluorometric determination of Chl *a* were done according to Knap et al. (1996), using a TD-700 Fluorometer (Turner Designs, Sunnyvale, CA).

Oxygen and inorganic carbon flux measurements

O_2 and CO_2 fluxes were measured by means of MIMS (Isoprime, GV Instruments, Manchester, UK) to determine photosynthetic O_2 evolution and respiratory O_2 uptake, as well as CO_2 and HCO_3^- fluxes. Net O_2 fluxes were converted to inorganic carbon (C_i) fluxes by applying a photosynthetic quotient of 1.4 (as nitrate was the only nitrogen source in the growth medium) and a respiratory quotient of 1.0 (Williams and Robertson 1991). The applied approach by Badger et al. (1994) depends on a chemical disequilibrium between CO_2

and HCO_3^-, which is induced by photosynthetic C_i uptake in the absence of eCA activity. O_2 and CO_2 fluxes were measured simultaneously during steady-state photosynthesis in consecutive light–dark intervals with increasing amounts of DIC. Maximum rates (V_{max}) and half-saturation concentrations ($K_{1/2}$) for respective C_i species (CO_2 and HCO_3^-) and DIC were determined by applying a Michaelis–Menten fit. Negative estimates of HCO_3^- concentrations, which were occasionally calculated for the lowest DIC concentrations, were omitted from the Michaelis–Menten fit. Measurements were performed in a 4-(2-hydroxylethyl)-1-piperazine-ethanesulfonic acid (HEPES, 50 mmol l^{-1}) buffer in f/2 medium with a pH of 8.0 ± 0.1 at 15 ± 0.3°C. The applied pH in the MIMS assay represents an intermediate value of the pH values of the acclimations. Provided that these differences in pH have minor effects on C_i uptake kinetics, rates in the assays are also representative for the acclimation. For more details on the method see Badger et al. (1994) and Rost et al. (2007).

Prior to the experimental series, the shape and speed of the stirrer in the MIMS-cuvette were tested on both species to eliminate biases from mechanical and physiological stress for the dinoflagellate species. In test runs, photosynthetic O_2 and respiration evolution was measured in intervals for about 1 h, confirming that rates remained unaffected over the duration of the assay. Light and dark intervals were adjusted to 4.5 and 3.5 min, respectively, to allow the CO_2 and O_2 traces to reach steady-state conditions (i.e. a linear slope; see Rost et al. 2006). The light intensity in the cuvette was set to the light intensity of the experiments (tested with the same light meter) with very comparable light spectra as similar daylight tubes have been used. Prior to the measurements, acclimated dinoflagellate cells were concentrated by gentle vacuum filtration (<200 mbar) over a 10 µm membrane filter (Millipore, Billerica, MA). Culture medium was exchanged with DIC-free assay medium and 8 ml of this concentrated cell suspension was transferred into the MIMS cuvette. During the first dark phase, membrane-impermeable dextran-bound sulphonamide (DBS; Synthelec AB, Lund, Sweden) was added to a final concentration of 50 µmol to inhibit any potential eCA activity. In order to normalize rates, duplicate Chl *a* samples were taken after each measurement.

Extracellular carbonic anhydrase activities

The determination of eCA activity was monitored by the ^{18}O depletion rate of doubly labeled $^{13}C^{18}O_2$ in sea water via alternating hydration and dehydration steps (Silverman 1982). As CA catalyzes the interconversion between HCO_3^- and CO_2, it concomitantly enhances the exchange of ^{18}O in $^{13}C^{18}O^{18}O$ (m/z = 49) with ^{16}O from water molecules, forming $^{13}C^{18}O^{16}O$ (m/z = 47) and subsequently $^{13}C^{16}O^{16}O$ (m/z = 45). In the dark, $NaH^{13}C^{18}O_3$ label was injected into the cuvette containing 8 ml HEPES-buffered culture medium with a pH of 8.0 ± 0.1 at 15 ± 0.3°C. After recording the steady-state depletion in ^{18}O enrichment for approximately 8 min (S_1), 400 µl of the concentrated cell suspension was injected, and the ^{18}O depletion was followed for another 10 min (S_2). Units of eCA activity (U) were calculated using the catalyzed and non-catalyzed rates S_2 and S_1, respectively, and subsequently normalized to Chl *a* (Badger and Price 1989). As a consequence, U corresponds to the enhancement in the interconversion between CO_2 and HCO_3^-, expressed as % µg Chl a^{-1}. For more details on the method see Palmqvist et al. (1994) and Rost et al. (2007).

Statistics

Normality of data was confirmed using the Shapiro-Wilk test. Variables were log-transformed if this improved the homogeneity of variances, as tested by Levene's test. Significant differences between treatments were tested using one way ANOVA, followed by post hoc comparison of the means using Tukey's HSD ($\alpha = 0.05$; Quinn and Keough 2002); significant differences between species, i.e. comparing the respective treatments, were tested using *t*-test; significances of relationships between HCO_3^- to net C fixation and CO_2 concentrations were tested by means of linear regression.

Results

Growth characteristics

In both species, growth remained largely unaffected by changes in pCO_2 (Table 2), but *S. trochoidea* grew significantly faster than *A. tamarense* ($P < 0.001$) with average growth rates of 0.60 ± 0.05 day^{-1} compared to 0.47 ± 0.02 day^{-1}, respectively. *Scrippsiella trochoidea* displayed a decrease in POC quota in response to elevated pCO_2 (Table 2), which was in line with a reduction in cell size (data not shown). In *A. tamarense*, POC quota remained unaltered over the applied pCO_2 range (Table 2), and were about twofold higher compared to *S. trochoidea*. Chl *a* quota in *S. trochoidea* showed maximum values in the 380 and 800 µatm CO_2 treatments, whereas in *A. tamarense*, they remained largely constant over the pCO_2 range (Table 2). Average Chl *a* quota were about sixfold higher in *A. tamarense* as compared to *S. trochoidea*. As a consequence of the

Table 2. Growth characteristics of *Scrippsiella trochoidea* and *Alexandrium tamarense* in the different CO_2 treatments. A significant difference between treatments is denoted by different letters. Values represent the mean ± sd of triplicate incubations (n = 3).

pCO_2 (µatm)	Growth rate (day^{-1})	POC production (ng $cell^{-1}$ day^{-1})	POC production (pg (pg Chl *a*)$^{-1}$ day)	Chl *a* (pg $cell^{-1}$)	POC (ng $cell^{-1}$)	POC:PON (molar)	POC:Chl *a* (mass)
S. trochoidea							
180	0.61 ± 0.03	1.21 ± 0.04^{a}	283 ± 38^{a}	4.3 ± 0.71^{a}	1.99 ± 0.04^{a}	7.6 ± 0.2^{ac}	469 ± 81^{a}
380	0.61 ± 0.05	1.08 ± 0.08^{ab}	143 ± 13^{b}	7.6 ± 1.19^{ab}	1.76 ± 0.02^{ab}	8.1 ± 0.3^{ab}	236 ± 42^{b}
800	0.61 ± 0.04	1.10 ± 1.14^{a}	127 ± 20^{b}	8.7 ± 0.52^{b}	1.79 ± 0.22^{ab}	8.4 ± 0.3^{b}	206 ± 28^{b}
1200	0.58 ± 0.02	0.87 ± 0.02^{b}	188 ± 52^{b}	4.9 ± 1.25^{a}	1.50 ± 0.09^{b}	7.4 ± 0.1^{c}	321 ± 77^{ab}
A. tamarense							
180	0.46 ± 0.02^{ab}	1.47 ± 0.08	40.5 ± 3.9	36.3 ± 1.52	3.17 ± 0.25	5.8 ± 0.1	88 ± 11
380	0.46 ± 0.02^{ab}	1.68 ± 0.12	42.0 ± 4.6	40.1 ± 2.75	3.62 ± 0.31	5.8 ± 0.3	91 ± 9
800	0.48 ± 0.01^{a}	1.67 ± 0.06	42.4 ± 3.1	39.5 ± 3.34	3.46 ± 0.15	5.7 ± 0.1	88 ± 6
1200	0.45 ± 0.01^{b}	1.55 ± 0.06	43.2 ± 7.7	36.4 ± 5.82	3.46 ± 0.17	5.6 ± 0.1	97 ± 15

differences in growth and POC quota, POC production rates of *S. trochoidea* decreased from 180 to 1200 µatm pCO_2 ($P = 0.005$; Table 2). *Alexandrium tamarense* displayed no changes in POC production rates toward elevated pCO_2 (Table 2), which were on average twice as high as in *S. trochoidea*.

The POC:PON ratio of *S. trochoidea* ranged between 7.4 and 8.4 with highest values in the 380 and 800 µatm CO_2 treatments, whereas the POC:Chl *a* ratio were highest in the 180 and 1200 µatm CO_2 treatments with 469 ± 81 and 321 ± 77, respectively (Table 2). In *A. tamarense*, POC:PON and POC:Chl *a* ratios remained unaffected by elevated pCO_2 with average values of 5.7 ± 0.2 and 90 ± 10, respectively. Calcification in *S. trochoidea* was very low with PIC:POC ratios <0.1 in all CO_2 treatments (data not shown), suggesting that calcite cyst formation in exponentially growing cells remains low (Wang et al. 2007).

Oxygen and carbon fluxes

In *S. trochoidea*, net photosynthesis (V_{max}) and dark respiration remained largely unaltered between the different CO_2 treatments (Fig. 1). With mean values of 323 ± 68 and 173 ± 21 µmol O_2 (mg Chl *a*)$^{-1}$ h^{-1}, respectively, net photosynthetic rates were about twofold higher than dark respiration rates. In *A. tamarense*, net photosynthetic rates decreased from 142 ± 4 to 86 ± 11 µmol O_2 (mg Chl *a*)$^{-1}$ h^{-1} ($P = 0.034$), while dark respiration rates increased from 88 ± 5 to 116 ± 9 µmol O_2 (mg Chl *a*)$^{-1}$ h^{-1} from the lowest to the highest CO_2 treatment ($P = 0.009$).

Scrippsiella trochoidea preferentially took up HCO_3^- with high affinities [i.e. low $K_{1/2}$ (HCO_3^-); Table 3]. In contrast, *A. tamarense* exhibited a high CO_2 uptake with high affinities [i.e. low $K_{1/2}$ (CO_2); Table 3]. Hence, the relative contribution of CO_2 and HCO_3^- to net C fixation differed between the investigated species and

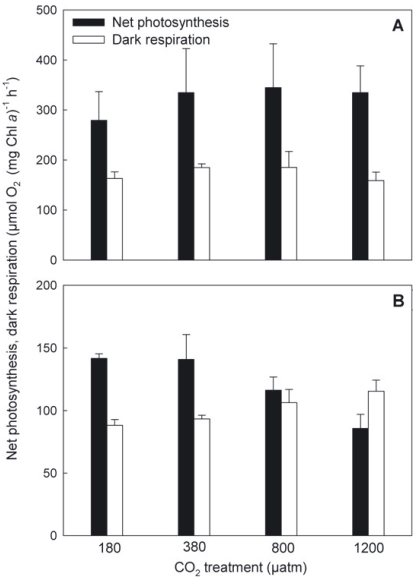

Fig. 1. Chl *a*-specific rates of net photosynthesis and dark respiration of *Scrippsiella trochoidea* (A) and *Alexandrium tamarense* (B) acclimated to different CO_2 concentrations. Bars represent mean ± sd (n = 3).

furthermore changed under elevated pCO_2. *Scrippsiella trochoidea* showed a decrease in the HCO_3^- to net C fixation ratio from 0.99 ± 0.17 at the lowest to 0.70 ± 0.14 at the highest CO_2 treatment ($f = 1.065 - 0.0009x$; $R^2 = 0.48$; $P = 0.0128$; Fig. 2). *Alexandrium tamarense* used both HCO_3^- and CO_2 as carbon source, with an increase in the HCO_3^- to net C fixation ratio from 0.36 ± 0.06 at the lowest to 0.64 ± 0.27 at the highest CO_2 treatment ($f = 0.29 + 0.0003x$; $R^2 = 0.40$; $P = 0.0280$; Fig. 2).

Table 3. Net C fixation, net CO_2 uptake, HCO_3^- uptake, eCA activity and leakage of *Scrippsiella trochoidea* and *Alexandrium tamarense* in the different CO_2 treatments. Values for V_{max} and $K_{1/2}$ are given in μmol mg^{-1} Chl *a* h^{-1} and μmol l^{-1}, respectively. A dash indicates that values could not be determined. If not stated otherwise, values represent the mean ± SD of triplicate incubations (n = 3). A significant difference between treatments is denoted by different letters.

	Net C fixation			Net CO_2 uptake		HCO_3^- uptake		eCA activity	Leakage
pCO_2 (μatm)	V_{max}	$K_{1/2}$ (CO_2)	$K_{1/2}$ (DIC)	V_{max}	$K_{1/2}$ (CO_2)	V_{max}	$K_{1/2}$ (HCO_3^-)	U (μg Chl *a*)$^{-1}$	CO_2 efflux: total C_i uptake
S. trochoidea									
180	199 ± 41	3.8 ± 0.5	94 ± 50	−13 ± 37^{a}	–	194 ± 5	7.2 ± 12.4	1573 ± 108	0.56 ± 0.06
380	239 ± 62	4.7 ± 1.1	160 ± 40	−7 ± 29^{a}	–	225 ± 40	17 ± 1.4	1416 ± 22	0.53 ± 0.06
800	246 ± 62	5.5 ± 0.9	263 ± 51	−3 ± 40^{ab}	–	202 ± 32	3.7 ± 5.5	1232 ± 144	0.54 ± 0.01
1200	239 ± 38	5.1 ± 0.4	269 ± 78	89 ± 22^{b}	20.1 ± 0.6	165 ± 26	10.3 ± 17	1301 ± 99	0.48 ± 0.04
A. tamarense									
180	101 ± 2^{a}	2.4 ± 0.1	267 ± 43	66 ± 9^{a}	3.3 ± 0.2	36 ± 5	105 ± 45	19 ± 48 (n = 2)	0.44 ± 0.01^{a}
380	101 ± 14^{ab}	2.8 ± 0.2	309 ± 67	60 ± 16^{ab}	3.3 ± 0.3	38 ± 7	220 ± 96	86 ± 2 (n = 2)	0.46 ± 0.02^{a}
800	83 ± 7^{ab}	2.0 ± 0.9	206 ± 65	42 ± 8^{ab}	3.1 ± 1.0	42 ± 10	158 ± 143	156 ± 12 (n = 2)	0.53 ± 0.02^{b}
1200	61 ± 8^{c}	2.5 ± 0.2	173 ± 15	23 ± 26^{b}	4.5 ± 0.8	38 ± 13	148 ± 28	124 (n = 1)	0.63 ± 0.05^{c}

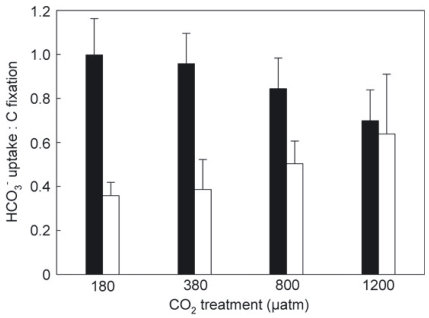

Fig. 2. Contribution of HCO_3^- uptake relative to net C fixation of *Scrippsiella trochoidea* (black bars) and *Alexandrium tamarense* (white bars) acclimated to different CO_2 concentrations. Ratios were calculated using the Michaelis–Menten kinetics (Table 3) and the corresponding carbonate chemistry of the respective CO_2 treatments (Table 1). Bars represent mean ± SD (n = 3).

Carbonic anhydrase activity

Scrippsiella trochoidea displayed exceptionally high eCA activities with up to 1600 U (μg Chl *a*)$^{-1}$ irrespective of the CO_2 treatments (Table 3). In contrast, *A. tamarense* contained relatively low eCA activities with mean values of 95 U (μg Chl *a*)$^{-1}$.

Discussion

In this study, two bloom-forming dinoflagellate species with different traits, the calcifying *S. trochoidea* and the toxic *A. tamarense*, were exposed to a range of pCO_2 to investigate the effects of OA. While growth rates remained largely unaltered, elemental composition and production rates were responsive to OA. Both species also strongly regulated their underlying physiology with surprisingly different strategies to deal with changes in CO_2 supply.

Growth and biomass production

Both species showed relatively small effects in terms of growth rates, yet we observed CO_2-dependent differences in POC production rates between species. In *S. trochoidea*, POC production rates decreased by almost 30%, which is reflected by a reduced cell size (data not shown) as well as lowered POC quota under elevated pCO_2 (Table 2). On the contrary, in *A. tamarense*, POC production rates and POC quotas remained largely unaltered (Table 2), the latter being similar to Leong et al. (2010). Average Chl *a* quota in *S. trochoidea* was largely comparable with earlier findings (Haardt and Maske 1987), whereas for *A. tamarense*, the average Chl *a* quota was about twice as high as earlier reported values (Carreto et al. 2001, Hu et al. 2006). Note that in none of the mentioned studies carbonate chemistry was controlled.

Regarding elemental composition, *S. trochoidea* showed highest POC:PON ratios under intermediate CO_2 concentrations (Table 2), with average ratios being lower than previously observed (approximately 9.3 in Burkhardt et al. 1999). These changes in POC:PON ratios are the result of disproportionally decreasing POC and PON quota under elevated pCO_2. In *A. tamarense*, POC:PON ratios were unaltered by the applied CO_2 treatments, and values were comparable with results of Leong et al. (2010). The significantly lower POC:PON ratio of *A. tamarense*, compared to *S. trochoidea*, may partly be attributed to the fact that it produces nitrogen-rich paralytic shellfish poisoning toxins (PST; Bates et al. 1978). However, the overall contribution of PST to

total cellular nitrogen for this strain of *A. tamarense* accounts for less than 4% (Van de Waal et al. 2014), and thus cannot alone explain the observed differences in POC:PON between both species.

In contrast to our expectations, processes like growth and elemental ratios were not strongly affected by OA. With respect to POC production, however, species differed in their responses, which could be attributed to CO_2-dependent changes in photosynthesis, in particular in their mode of C_i acquisition. We therefore performed MIMS measurements targeting those underlying processes.

Photosynthesis and respiration

In *S. trochoidea*, rates of O_2 evolution (i.e. net photosynthesis) were more than twofold higher than in *A. tamarense*, which is in line with higher growth rates as well as higher POC:Chl *a* ratios (Table 2). Both species exhibited high dark respiration rates compared to net photosynthetic rates (Fig. 1). Provided that measured respiration during darkness is representative also for the light phase, respiration was approximately 50% of net photosynthesis in *S. trochoidea*, whereas in *A. tamarense* both rates were equally high. Comparable high dark respiration rates have since long also been shown for other dinoflagellate species, including zooxanthellae (e.g. Burris 1977). In *A. tamarense*, net photosynthesis and respiration furthermore showed opposing trends in response to elevated pCO_2. The decrease in net photosynthesis in *A. tamarense* may be largely caused by the increased dark respiration under elevated pCO_2. Other processes affecting O_2 uptake in the light, such as Mehler Reaction and photorespiration, can however not be excluded here and may potentially alter the trends. Brading et al. (2013), for example, observed significant light-dependent O_2 uptake in four *Symbiodinium* strains, which remained unaltered under OA. Other studies showed that OA effects can be modulated under different light levels and may enhance mitochondrial respiration, photorespiration and ultimately reduce growth and biomass production under high light (Gao et al. 2012, Rokitta and Rost 2012, Li and Campbell 2013). Interestingly, the increase in respiration with pCO_2 observed in *A. tamarense* was found to have no effect on growth or POC production rates. Overall, it can be concluded that the sum of net photosynthesis and respiration, i.e. gross photosynthesis, remained largely unaffected in both tested species.

Previous studies on *Protoceratium reticulatum* and four strains of *Symbiodinium* showed basically no CO_2 effect on photosynthesis and respiration (Ratti and Giordano 2007, Brading et al. 2011), with the exception of one *Symbiodinium* strain that showed higher rates of net photosynthesis under OA (Brading et al. 2011). Interestingly, in *Protoceratium reticulatum* and another *Symbiodinium* strain, growth nonetheless increased with elevated pCO_2 (Ratti and Giordano 2007, Brading et al. 2011). These findings, together with our current results, demonstrate that responses in growth and biomass production toward OA cannot always be explained by changes in O_2 fluxes, but instead may be attributed to the mode of C_i acquisition. High sensitivities in growth and biomass production toward OA, for instance, have often been associated with a strong dependency on CO_2 as a C_i source for photosynthesis (Colman et al. 2002, Fu et al. 2008), whereas when HCO_3^- is the dominant C_i source, much less sensitivity toward changes in CO_2 is expected (Burkhardt et al. 1999, Rost et al. 2008). Therefore, we assessed various key components of the CCM and their potential CO_2-dependent regulation to understand the responses of *S. trochoidea* and *A. tamarense* toward OA.

Carbon source and carbonic anhydrase

Among the various studies on carbon acquisition in dinoflagellates, either CO_2 (Colman et al. 2002, Dason et al. 2004, Fu et al. 2008, Lapointe et al. 2008, Brading et al. 2013) or HCO_3^- (Rost et al. 2006, Ratti and Giordano 2007, Fu et al. 2008) was estimated to be the dominant C_i source. Here we show that *S. trochoidea* and *A. tamarense* used CO_2 as well as HCO_3^- for photosynthesis, though their contribution to net C fixation and response to elevated pCO_2 were very different. As one would expect, *S. trochoidea* displayed an increase in relative CO_2 uptake, or in other words, a decrease in relative HCO_3^- uptake to net fixation under elevated pCO_2 (Fig. 2). Such a trend has also been observed in other functional groups, e.g. diatoms (Burkhardt et al. 2001, Trimborn et al. 2009, 2013), coccolithophores (Rost et al. 2003) or cyanobacteria (Kranz et al. 2009). The response in *A. tamarense*, however, was surprising as it showed the reverse trend, i.e. an increase of HCO_3^- uptake in response to elevated pCO_2 (Fig. 2). This could be associated with the generally high and increasing rates of respiration and CO_2 efflux observed in this species (Fig. 1, Table 3). HCO_3^- uptake may therefore be simply upregulated to compensate for the increasing CO_2 efflux. Even though respiration can partly cause the high loss of C_i from the cell, it could be speculated that the increase in respiration may also provide the required ATP to fuel the higher HCO_3^- uptake. Why mitochondrial activity, in the first place, is stimulated under OA scenarios remains elusive, but it could be associated to altered proton gradients across the mitochondrial membrane or to pH-dependent

changes in the functioning of respiratory enzymes (Amthor 1991).

According to the common notion, eCA functions to replenish the CO_2 pool in the CO_2 depleted boundary layer of a cell, thereby fuelling the CO_2 uptake systems (Badger and Price 1989, Sültemeyer 1998, Elzenga et al. 2000). Such mechanism would obviously be most effective when a cell predominantly uses CO_2 as its C_i source. For dinoflagellates, a major role of eCA activity in CCM functioning was only indicated for the CO_2 user *Lingulodinium polyedrum* and *Symbiodinium* A20 (Lapointe et al. 2008, Brading et al. 2013). Activities of eCA in most other tested dinoflagellates, including *A. tamarense* in this study, were close to detection limits and therefore likely play only a minor role, if any, in C_i acquisition (Table 3; Colman et al. 2002, Rost et al. 2006, Ratti and Giordano 2007). In *S. trochoidea*, however, we observed exceptionally high eCA activities of up to 1600 U (μg Chl *a*)$^{-1}$ over the entire pCO_2 range (Table 3). Why would a predominant HCO_3^- user have such high eCA activities? Comparable high eCA activities in concert with high HCO_3^- contribution have been observed previously (Martin and Tortell 2008, Trimborn et al. 2008, 2013), and our observation that eCA and HCO_3^- uptake are both upregulated at high pH casts further doubts on an universal role of eCA.

Trimborn et al. (2008) proposed that in HCO_3^- users, eCA may convert effluxing CO_2 to HCO_3^-, which is subsequently taken up again by the cell. Such a 'CO_2 recycling mechanism' would be particularly advantageous for species with high respiration rates, which was indeed the case for *S. trochoidea* (Fig. 1). For *Thalassiosira* spp., however, the effectiveness of such a mechanism was recently questioned as it would increase the C_i uptake rate by less than 1% only (Hopkinson et al. 2013). This situation may, however, strongly differ between species as model estimates depend on the net CO_2 uptake, which is large for *Thalassiosira* spp. (Hopkinson et al. 2013) but not for *S. trochoidea* (Table 3). In fact, net CO_2 uptake in *S. trochoidea* was close to zero or even negative and there was a high leakage, i.e. about 50% of the C_i taken up by the cell was leaking out as CO_2 (Table 3), which is not accounted for in the model calculations (Hopkinson et al. 2013). Particular high leakage has also been measured in other dinoflagellates (Rost et al. 2006). It should be noted, however, that C_i fluxes are typically determined using disequilibrium approaches and thus require the inhibition of potential eCA activity (Badger et al. 1994). If eCA activity would indeed be involved in minimizing the CO_2 efflux, this approach may overestimate leakage for *S. trochoidea*, while estimates in *A. tamarense*, which lacks eCA activity, would not be biased by the approach. In any case, although eCA presumably contributes to the CCM, its role and correlation with high HCO_3^- uptake remains puzzling and requires further investigations.

CCMs and trade-offs within

With respect to net C fixation, both *S. trochoidea* and *A. tamarense* displayed half-saturation concentrations ($K_{1/2}$) of <6 μmol CO_2 l^{-1} at all applied CO_2 levels (Table 3). These results were consistent with previously published $K_{1/2}$ values of other dinoflagellates (Rost et al. 2006, Ratti and Giordano 2007) and fall in the same range as those measured for temperate diatoms (Burkhardt et al. 2001, Trimborn et al. 2008, 2009, Yang and Gao 2012), which are known to feature very effective CCMs (Reinfelder 2011 for review). Interestingly, the K_m value of the type II RubisCO employed in dinoflagellates (80–250 μmol CO_2 l^{-1}) is much higher than the K_m of type I in diatoms (31–41 μmol CO_2 l^{-1}; Badger et al. 1998). In other words, the CCM in these dinoflagellates increased not only their CO_2 affinities by more than one order of magnitude relative to their RubisCO kinetics, but also demonstrates that the activity of the CCM in dinoflagellates must be up to sixfold higher than that of diatoms. Additionally, dinoflagellate cells are typically larger than diatoms, which automatically reduces the surface to volume ratio and hence the specific reaction diffusion-supply rate of CO_2 to the cell surface (Reinfelder 2011). The correspondingly higher energy expenditure for running their CCM could thus, to a large degree, explain why dinoflagellates grow generally much slower than diatoms and thrive under different environmental conditions (Smayda 1997).

Next to the $K_{1/2}$ value, also the maximum rate (V_{max}) plays an important role in determining the competitive success of a species (Healey 1980). Interestingly, our data indicate a trade-off between V_{max} and $K_{1/2}$ values between both species. *Scrippsiella trochoidea* displayed relatively high V_{max} and high $K_{1/2}$ values, while *A. tamarense* showed the inverse pattern, i.e. relatively low V_{max} and low $K_{1/2}$ (Fig. 3). The observed trade-off within the kinetic properties of C_i acquisition is also present between the different CO_2 treatments, especially for *S. trochoidea* showing a relative decrease in affinities with increasing maximum rates. This correlation may reflect fundamental characteristics of nutrient uptake in microalgae (Raven 1980, Aksnes and Egges 1991, Lichtman et al. 2007). Given the limited area of the cell's surface available for nutrient uptake, the number of transporters with small active area per transporter (leading to higher V_{max} and higher $K_{1/2}$) 'compete' with the number of uptake sites with relatively large active areas (leading to lower V_{max} and lower $K_{1/2}$).

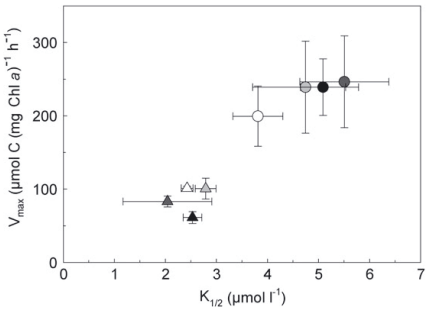

Fig. 3. V_{max} vs $K_{1/2}$ of photosynthetic carbon fixation of *Scrippsiella trochoidea* (circles), *Alexandrium tamarense* (triangles) acclimated to different CO_2 concentrations. Color of symbols indicates CO_2 treatments from low (white) to high (black). Symbols represent mean ± SD (n = 3).

The fact that cells do not come up with transporters being characterized by high V_{max} as well as low $K_{1/2}$ is probably dictated by biochemical constraints, i.e. transporters can be faster only at the expense of lower affinities or vice versa (Fersht 1974). Our findings on the trade-off between V_{max} and $K_{1/2}$ in C_i acquisition are in line with previously observed characteristics on N acquisition in the major eukaryotic phytoplankton groups (Lichtman et al. 2007) as well as different strains of two N_2 fixing cyanobacteria species (Hutchins et al. 2013). However, whether this trade-off in C_i acquisition is a general feature holding true also for other species and strains (Brading et al. 2013 show V_{max} and $K_{1/2}$ values of two *Symbiodinium* strains being similar to *S. trochoidea*) and even taxa needs to be further investigated.

Ecological implications

To compensate potential limitations in the carboxylation reaction of RubisCO, *S. trochoidea* and *A. tamarense* operate effective CCMs, allowing both species to grow unaltered over the applied range of pCO_2. More specifically, both species substantially increased their overall affinities for photosynthesis, relative to what would be predicted by RubisCO, and were also able to use HCO_3^- as C_i source. However, the high levels of C_i accumulation required for the low affine RubisCO, the predominant HCO_3^- uptake, as well as the high CO_2 leakage cause C_i acquisition to be very costly, which may have profound ecological consequences. For instance, it could partly explain why dinoflagellates display generally lower growth rates compared to other major groups of marine phytoplankton, which employ a more affine type I RubisCO (Smayda 1997). Reasons why dinoflagellates yet thrive well in many environments can partly be attributed to their mixotrophic behavior (Jeong et al. 2005), the potential of some species to produce allelopathic compounds (Cembella 2003) and the ability to migrate within the water column to circumvent nutrient and light limitation (MacIntyre et al. 1997). Active swimming may as well lower diffusion limitation (Pahlow et al. 1997), in particular for nutrients like nitrate or trace elements, but it could also enhance the CO_2 supply to the cell surface and thereby possibly reduce the costs of CCMs in dinoflagellates.

The observed trade-off between maximum uptake rates and affinities for CO_2 may also play a role in optimizing the competitive success of both species at different CO_2 levels. More specifically, having a higher V_{max} and higher growth rate, *S. trochoidea* exhibits the 'velocity' strategy (Sommer 1984), which will be favored under high and dynamic C_i availabilities. With a lower $K_{1/2}$, on the other hand, *A. tamarense* exhibits an 'affinity' strategy (Sommer 1984) that will have a competitive advantage under low C_i concentrations (Fig. 3, Table 3). During phytoplankton blooms, carbonate chemistry may substantially change and drift toward high pH and low CO_2 concentrations (Hansen 2002). As a consequence, species with a low $K_{1/2}$ for CO_2, such as *A. tamarense*, may be favored. At the same time, however, carbonate chemistry may also exhibit strong daily fluctuations as results of day-time photosynthesis and night-time respiration. Under these conditions, species with a high V_{max} and growth rate, like *S. trochoidea*, are likely to be favored. On top of that, the high preference of *S. trochoidea* for HCO_3^- may further support its growth during blooms. It thus seems that *A. tamarense* and *S. trochoidea* exhibit different strategies allowing them to cope with dense bloom conditions. Such differences in competitive strategies, induced by physiological characteristics, may furthermore allow coexistence of multiple species.

Species being able to regulate their CCM in response toward high pCO_2 and low pH conditions will have advantages in a future ocean. Even though both tested species were regulating their CCM, *S. trochoidea* showed strongest changes in response to OA. Modes of CCMs and thus CO_2 sensitivities in growth and biomass production may, however, change strongly under resource limitation, i.e. nutrient depleted or low light conditions, and therefore alter the outcome of competition under OA. For bloom-forming species like *S. trochoidea* and *A. tamarense*, which tend to flourish late in the succession, investigations on the interactive effects of nutrient limitation and OA as well as dynamic changes therein are crucial to improve our understanding of the response of this important group of phytoplankton in a future, high CO_2 world.

Acknowledgements – Grant support was provided by European Community's Seventh Framework Programme (FP7/2007-2013)/ERC No. 205150, EPOCA No. 211384 and BIOACID programme, financed by the German Ministry of Education and Research. We thank Karin Zonneveld (University of Bremen, Germany) for providing *Scrippsiella trochoidea* strain 267 and Urban Tillmann (Alfred Wegener Institute for Polar and Marine Research, Bremerhaven, Germany) for providing *Alexandrium tamarense* strain Alex5. We thank Klaus-Uwe Richter, Ulrike Richter and Yvette Bublitz for assistance during the work and Sebastian Rokitta for having a critical view on the manuscript.

References

Aksnes DL, Egge JK (1991) A theoretical model for nutrient uptake in phytoplankton. Mar Ecol Prog Ser 70: 65–72

Amthor JS (1991) Respiration in a future, higher-CO_2 world. Plant Cell Environ 14: 13–20

Badger MR, Price GD (1989) Carbonic anhydrase activity associated with the cyanobacterium *Synechococcus* PCC7942. Plant Physiol 89: 51–60

Badger MR, Palmqvist K, Jian-Wei Y (1994) Measurement of CO_2 and HCO_3^- fluxes in cyanobacteria and microalgae during steady-state photosynthesis. Physiol Plant 90: 529–536

Badger MR, Andrews TJ, Whitney SM, Ludwig M, Yellowlees DC, Leggat W, Price GD (1998) The diversity and coevolution of Rubisco, plastids, pyrenoids, and chloroplast-based CO_2-concentrating mechanisms in algae. Can J Bot 76: 1052–1071

Bates HA, Kostriken R, Rapoport H (1978) The occurrence of saxitoxin and other toxins in various dinoflagellates. Toxicon 16: 595–601

Brading P, Warner ME, Davey P, Smith DJ, Achterberg EP, Suggett DJ (2011) Differential effects of ocean acidification on growth and photosynthesis among phylotypes of *Symbiodinium* (Dinophyceae). Limnol Oceanogr 56: 927–938

Brading P, Warner ME, Smith DJ, Suggett DJ (2013) Contrasting modes of inorganic carbon acquisition amongst *Symbiodinium* (Dinophyceae) phylotypes. New Phytol 200: 432–442

Burkhardt S, Zondervan I, Riebesell U (1999) Effect of CO_2 concentration on C:N:P ratio in marine phytoplankton: a species comparison. Limnol Oceanogr 44: 683–690

Burkhardt S, Amoroso S, Riebesell U, Sültemeyer D (2001) CO_2 and HCO_3^- uptake in marine diatoms acclimated to different CO_2 concentrations. Limnol Oceanogr 46: 1378–1391

Caldeira K, Wickett ME (2003) Anthropogenic carbon and ocean pH. Nature 425: 365

Carreto JI, Carignan MO, Montoya NG (2001) Comparative studies on mycosporine-like amino acids, paralytic shellfish toxins and pigment profiles of the toxic dinoflagellates *Alexandrium tamarense, A. catenella* and *A. minutum*. Mar Ecol Prog Ser 223: 49–60

Cembella AD (2003) Chemical ecology of eukaryotic microalgae in marine ecosystems. Phycologia 42: 420–447

Colman B, Huertas IE, Bhatti S, Dason JS (2002) The diversity of inorganic carbon acquisition mechanisms in eukaryotic microalgae. Funct Plant Biol 29: 261–270

Dason JS, Huertas IE, Colman B (2004) Source of inorganic carbon for photosynthesis in two marine dinoflagellates. J Phycol 40: 229–434

Dickson AG, Millero FJ (1987) A comparison of the equilibrium constants for the dissociation of carbonic acid in seawater media. Deep-Sea Res 34: 1733–1743

Doney SC, Fabry VJ, Feely RA, Kleypas JA (2009) Ocean acidification: the other CO_2 problem. Annu Rev Mar Sci 1: 169–192

Egleston ES, Sabine CL, Morel FMM (2010) Revelle revisited: buffer factors that quantify the response of ocean chemistry to changes in DIC and alkalinity. Global Biogeochem Cycles 24: GB1002

Elzenga JTM, Prins HBA, Stefels J (2000) The role of extracellular carbonic anhydrase activity in inorganic carbon utilization of *Phaeocystis globosa* (Prymnesiophyceae): a comparison with other marine algae using the isotope disequilibrium technique. Limnol Oceanogr 45: 372–380

Fabry JV, Seibel AB, Feely RA, Orr JC (2008) Impacts of ocean acidification on marine fauna and ecosystem processes. ICES J Mar Sci 65: 414–432

Falkowski PG, Barber RT, Smetacek V (1998) Biogeochemical controls and feedbacks on ocean primary production. Science 281: 200–206

Fersht AR (1974) Catalysis, binding and enzyme-substrate complementarity. Proc R Soc Lond B Biol Sci 187: 397–407

Fistarol GO, Legrand C, Rengefors K, Granéli E (2004) Temporary cyst formation in phytoplankton: a response to allelopathic competitors? Environ Microbiol 6: 791–798

Fu FX, Warner ME, Zhang Y, Feng Y, Hutchins DA (2007) Effects of increased temperature and CO_2 on photosynthesis, growth, and elemental ratios in marine *Synechococcus* and *Prochlorcoccus* (Cyanobacteria). J Phycol 43: 485–496

Fu FX, Zhang Y, Warner ME, Feng Y, Sun J, Hutchins DA (2008) A comparison of future increased CO_2 and temperature effects on sympatric *Heterosigma akashiwo* and *Prorocentrum minimum*. Harmful Algae 7: 76–90

Fu FX, Place AR, Garcia NS, Hutchins DA (2010) CO_2 and phosphate availability control the toxicity of the harmful bloom dinoflagellate *Karlodinium veneficum*. Aquat Microb Ecol 59: 55–56

Gao K, Xu J, Gao G, Li Y, Hutchins DA, Huang B, Wang L, Zheng Y, Jin P, Cai X, Häder D-P, Li W, Xu K, Liu N,

Riebesell U (2012) Rising CO_2 and increased light exposure synergistically reduce marine primary productivity. Nat Clim Change 2: 519–523
Giordano M, Beardall J, Raven JA (2005) CO_2 concentrating mechanisms in algae: mechanisms, environmental modulation, and evolution. Annu Rev Plant Biol 56: 99–131
Guillard RRL, Ryther JH (1962) Studies of marine planktonic diatoms: I. *Cyclotella nana* Hustedt, and *Detonula confervacea* Cleve. Can J Microbiol 8: 229–239
Haardt H, Maske H (1987) Specific in vivo absorption coefficient of chlorophyll *a* at 675 nm. Limnol Oceanogr 32: 608–619
Hansen PJ (2002) Effect of high pH on the growth and survival of marine phytoplankton: implications for species succession. Aquat Microb Ecol 28: 279–288
Healey FP (1980) Slope of the Monod equation as an indicator of advantage in nutrient competition. Microb Ecol 5: 281–286
Hopkinson BM, Meile C, Chen S (2013) Quantification of extracellular carbonic anhydrase activity in two marine diatoms and investigation of its role. Plant Physiol 162: 1142–1152
Hu H, Shi Y, Cong W (2006) Improvement in growth and toxin production of *Alexandrium tamarense* by two-step culture method. J Appl Phycol 18: 119–126
Hutchins DA, Fei-Xue F, Webb EA, Walworth N, Tagliabue A (2013) Taxon-specific response of marine nitrogen fixers to elevated carbon dioxide concentrations. Nat Geosci 6: 790–795
IPCC (2007) Global Climate Projections. In: Solomon S, Qin D, Manning M, Chen Z, Marquis M, Averyt KB, Tignor M, Miller HL (eds) Climate Change 2007: The Physical Science Basis. Contribution of Working Group I to the Fourth Assessment Report of the Intergovernmental Panel on Climate Change. Cambridge University Press, Cambridge; New York
Jeong HJ, Yoo YD, Park JY, Song JY, Kim ST, Lee SH, Kim KY, Yih WH (2005) Feeding by phototrophic red-tide dinoflagellates: five species newly revealed and six species previously known to be mixotrophic. Aquat Microb Ecol 40: 133–150
Knap A, Michaells A, Close A, Ducklow H, Dickson A (eds) (1996) Protocols for the Joint Global Ocean Flux Study (JGOFS) Core Measurements. JGOFS Report No. 19, vi+170 pp. Reprint of the IOC Manuals and Guides No. 29, UNESCO 1994
Kranz SA, Sültemeyer D, Richter K-U, Rost B (2009) Carbon acquisition by *Trichodesmium*: the effect of pCO_2 and diurnal changes. Limnol Oceanogr 54: 548–559
Lapointe M, MacKenzie TBD, Morse D (2008) An external δ-carbonic anhydrase in a free-living marine dinoflagellate may circumvent diffusion-limited carbon acquisition. Plant Physiol 147: 1427–1436
Leong SCY, Maekawa M, Taguchi S (2010) Carbon and nitrogen acquisition by the toxic dinoflagellate *Alexandrium tamarense* in response to different nitrogen sources and supply modes. Harmful Algae 9: 48–58
Li G, Campbell DA (2013) Rising CO_2 interacts with growth light and growth rate to alter photosystem II photoinactivation of the coastal diatom *Thalassiosira pseudonana*. PLoS ONE 8: e55562
Lichtman E, Klausmeier CA, Schofield OM, Falkowski PG (2007) The role of functional traits and trade-offs in structuring phytoplankton communities: scaling from cellular to ecosystem level. Ecol Lett 10: 1170–1181
MacIntyre JG, Cullen JJ, Cembella AD (1997) Vertical migration, nutrition and toxicity in the dinoflagellate *Alexandrium tamarense*. Mar Ecol Prog Ser 148: 201–216
Martin CL, Tortell PD (2008) Bicarbonate transport and extracellular carbonic anhydrase in marine diatoms. Physiol Plant 133: 106–116
McCollin T, Lichtman D, Bresnan E, Berx B (2011) A study of phytoplankton communities along a hydrographic transect on the north east coast of Scotland. Marine Scotland Science Report 04/11
Mehrbach C, Culberson CH, Hawley JE, Pytkowicz RM (1973) Measurement of the apparent dissociation constants of carbonic acid in seawater at atmospheric pressure. Limnol Oceanogr 18: 897–907
Morse D, Salois P, Markovic P, Hastings JW (1995) A nuclear-encoded form II RuBisCO in dinoflagellates. Science 268: 1622–1624
Pahlow M, Riebesell U, Wolf-Gladrow DA (1997) Impact of cell shape and chain formation on nutrient acquisition by marine diatoms. Limnol Oceanogr 42: 1660–1672
Palmqvist K, Yu J-W, Badger MR (1994) Carbonic anhydrase activity and inorganic carbon fluxes in low- and high-C_i cells of *Clamydomonas reinhardtii* and *Scenedesmus obliquus*. Physiol Plant 90: 537–547
Pierrot DE, Lewis E, Wallace DWR (2006) Program Developed for CO_2 System Calculations. Carbon Dioxide Information Analysis Center, Oak Ridge National Laboratory. Available at: http://cdiac.ornl.gov/oceans/co2rprt.html (accessed 1 March 1997)
Quinn GP, Keough MJ (2002) Experimental Design and Data Analysis for Biologists. Cambridge University Press, Cambridge
Ratti S, Giordano M (2007) CO_2-concentrating mechanisms of the potentially toxic dinoflagellate *Protoceratium reticulatum* (Dinophyceae, Gonyaulacales). J Phycol 43: 693–701
Raven JA (1980) Nutrient transport in microalgae. Adv Microb Physiol 21: 47–226

Reinfelder JR (2011) Carbon concentrating mechanisms in eukaryotic marine phytoplankton. Annu Rev Mar Sci 3: 291–315

Rokitta SD, Rost B (2012) Effects of CO_2 and their modulation by light in the life-cycle stages of the coccolithophore *Emiliania huxleyi*. Limnol Oceanogr 57: 607–618

Rost B, Riebesell U, Burkhardt S, Sültemeyer D (2003) Carbon acquisition of bloom-forming marine phytoplankton. Limnol Oceanogr 48: 55–67

Rost B, Richter K-U, Riebesell U, Hansen PJ (2006) Inorganic carbon acquisition in red tide dinoflagellates. Plant Cell Environ 29: 810–822

Rost B, Kranz S, Richter K-U, Tortell P (2007) Isotope disequilibrium and mass spectrometric studies of inorganic carbon acquisition by phytoplankton. Limnol Oceanogr Methods 5: 328–337

Rost B, Zondervan I, Wolf-Gladrow DA (2008) Sensitivity of phytoplankton to future changes in ocean carbonate chemistry: current knowledge, contradictions and research directions. Mar Ecol Prog Ser 373: 227–237

Silverman DN (1982) Carbonic anhydrase. Oxygen-18 exchange catalyzed by an enzyme with rate-contributing proton-transfer steps. Methods Enzymol 87: 732–752

Smayda TJ (1997) Harmful algal blooms: their ecophysiology and general relevance to phytoplankton blooms in the sea. Limnol Oceanogr 42: 1137–1153

Sommer U (1984) The paradox of the plankton: fluctuations of phosphorus availability maintain diversity of phytoplankton in flow-through cultures. Limnol Oceanogr 29: 633–636

Sültemeyer D (1998) Carbonic anhydrase in eukaryotic algae: characterization, regulation, and possible function during photosynthesis. Can J Bot 76: 962–972

Tillmann U, Alpermann TL, da Purificação RC, Krock B, Cembella A (2009) Intra-population clonal variability in allelochemical potency of the toxigenic dinoflagellate *Alexandrium tamarense*. Harmful Algae 8: 759–769

Trimborn S, Lundholm N, Thoms S, Richter K-U, Krock B, Hansen PJ, Rost B (2008) Inorganic carbon acquisition in potentially toxic and non-toxic diatoms: the effect of pH-induced changes in seawater carbonate chemistry. Physiol Plant 133: 92–105

Trimborn S, Wolf-Gladrow DA, Richter K-U, Rost B (2009) The effect of pCO_2 on carbon acquisition and intracellular assimilation in four marine diatoms. J Exp Mar Biol Ecol 376: 26–36

Trimborn S, Brenneis T, Sweet E, Rost B (2013) Sensitivity of Antarctic phytoplankton species to ocean acidification: growth, carbon acquisition, and species interaction. Limnol Oceanogr 58: 997–1007

Van de Waal DB, John U, Ziveri P, Reichart G-J, Hoins M, Sluijs A, Rost B (2013) Ocean acidification reduces growth and calcification in a marine dinoflagellate. PLoS ONE 8: e65987

Van de Waal DB, Eberlein T, John U, Wohlrab S, Rost B (2014) Impact of elevated pCO_2 on paralytic shellfish poisoning toxin content and composition in *Alexandrium tamarense*. Toxicon 78: 58–67

Wang ZH, Qi YZ, Yang YF (2007) Cyst formation: an important mechanism for the termination of *Scrippsiella trochoidea* (Dinophyceae) bloom. J Plankton Res 29: 209–218

Williams PJL, Robertson JE (1991) Overall planktonic oxygen and carbon dioxide metabolisms: the problem of reconciling observations and calculations of photosynthetic quotients. J Plankton Res 13: 153–169

Wolf-Gladrow DA, Riebesell U, Burkhardt S, Bijma J (1999) Direct effects of CO_2 concentration on growth and isotopic composition of marine plankton. Tellus B51: 461–476

Yang G, Gao K (2012) Physiological responses of the marine diatom *Thalassiosira pseudonana* to increased pCO_2 and seawater acidity. Mar Environ Res 79: 142–151

Edited by D. Campbell

2.3 Publication II

Interactive effects of ocean acidification and nitrogen limitation on two bloom-forming dinoflagellate species.

Vol. 543: 127–140, 2016
doi: 10.3354/meps11568

MARINE ECOLOGY PROGRESS SERIES
Mar Ecol Prog Ser

Published February 3

Interactive effects of ocean acidification and nitrogen limitation on two bloom-forming dinoflagellate species

Tim Eberlein[1], Dedmer B. Van de Waal[1,2,*], Karen M. Brandenburg[1,2], Uwe John[1], Maren Voss[3], Eric P. Achterberg[4], Björn Rost[1]

[1]Alfred Wegener Institute, Helmholtz Centre for Polar and Marine Research, Am Handelshafen 12, 27570 Bremerhaven, Germany
[2]Netherlands Institute of Ecology (NIOO-KNAW), PO Box 50, 6700 AB, Wageningen, The Netherlands
[3]Leibniz Institute for Baltic Sea Research Warnemünde, Seestrasse 15, 18119 Rostock, Germany
[4]GEOMAR Helmholtz Centre for Ocean Research, Wischhofstraße 1–3, 24148 Kiel, Germany

ABSTRACT: Global climate change involves an increase in oceanic CO_2 concentrations as well as thermal stratification of the water column, thereby reducing nutrient supply from deep to surface waters. Changes in inorganic carbon (C) or nitrogen (N) availability have been shown to affect marine primary production, yet little is known about their interactive effects. To test for these effects, we conducted continuous culture experiments under N limitation and exposed the bloom-forming dinoflagellate species *Scrippsiella trochoidea* and *Alexandrium fundyense* (formerly *A. tamarense*) to CO_2 partial pressures (pCO_2) ranging between 250 and 1000 µatm. Ratios of particulate organic carbon (POC) to organic nitrogen (PON) were elevated under N limitation, but also showed a decreasing trend with increasing pCO_2. PON production rates were highest and affinities for dissolved inorganic N were lowest under elevated pCO_2, and our data thus demonstrate a CO_2-dependent trade-off in N assimilation. In *A. fundyense*, quotas of paralytic shellfish poisoning toxins were lowered under N limitation, but the offset to those obtained under N-replete conditions became smaller with increasing pCO_2. Consequently, cellular toxicity under N limitation was highest under elevated pCO_2. All in all, our observations imply reduced N stress under elevated pCO_2, which we attribute to a reallocation of energy from C to N assimilation as a consequence of lowered costs in C acquisition. Such interactive effects of ocean acidification and nutrient limitation may favor species with adjustable carbon concentrating mechanisms and have consequences for their competitive success in a future ocean.

KEY WORDS: Dinoflagellates · Ocean acidification · Nitrogen limitation · Paralytic shellfish poisoning · PSP toxins

INTRODUCTION

Anthropogenic activities such as fossil fuel burning and changes in land use have caused atmospheric CO_2 levels to rise at an unprecedented rate and concentrations are expected to approximately double from 400 µatm at present to 900 µatm by the year 2100 (RCP8.5 scenario; IPCC 2013). CO_2 is taken up by the oceans and will shift the speciation of dissolved inorganic carbon, resulting in higher CO_2 and HCO_3^- concentrations, lower CO_3^{2-} concentrations, and an associated drop in pH by as much as 0.3 units for 2100 (i.e. ocean acidification; Caldeira & Wickett 2003). Being a major greenhouse gas, CO_2 also contributes to global warming, and sea surface temperatures are expected to rise by up to 4°C over the course of this century (RCP8.5 scenario; IPCC 2013). Consequently, thermal stratification of the water col-

*Corresponding author: d.vandewaal@nioo.knaw.nl

Publisher: Inter-Research · www.int-res.com

umn may be enhanced, reducing the supply of nutrients from deep waters to the surface mixed layer, with likely consequences for primary production (Behrenfeld et al. 2006). Moreover, increasing temperatures may cause a shoaling of the surface mixed layer and thus enhance the mean irradiance phytoplankton experience over the day (Rost & Riebesell 2004, Sarmiento et al. 2004).

In the past decades, numerous studies have described the effects of elevated CO_2 partial pressure (pCO_2) on phytoplankton (Rost et al. 2008), but very few have investigated the combined effect with other variables such as temperature (e.g. Fu et al. 2007, 2008, Feng et al. 2008) or irradiance (e.g. Rokitta & Rost 2012, Gao et al. 2013). This is surprising because nutrients, particularly nitrogen (N), are considered key elements that limit primary production in large parts of the present-day ocean (Elser et al. 2007, Moore et al. 2013). The projected decrease in N supply to the upper mixed layer may be accompanied by lowered nitrification rates under ocean acidification, both leading to lower nitrate-supported primary production (Hutchins et al. 2009, Beman et al. 2011). In view of this and the fact that assimilation of carbon (C) and N are closely linked (Flynn 1991, Turpin 1991), it is particularly relevant to study the effects of elevated pCO_2 under N-limiting conditions.

While the combined effects of elevated pCO_2 and N limitation have been assessed in diatoms (Li et al. 2012, Hennon et al. 2014) and coccolithophores (Sciandra et al. 2003, Rouco et al. 2013), dinoflagellates have so far been largely overlooked. Yet, they are expected to be highly sensitive to changes in CO_2 availability due to their type II ribulose 1,5-bisphosphate carboxylase/oxygenase (RuBisCO), which features low affinities for its substrate CO_2 (Morse et al. 1995, Badger et al. 1998). Some dinoflagellate species express effective and adjustable carbon concentrating mechanisms (CCMs), which can prevent CO_2 limitation in growth and primary production (Rost et al. 2006, Eberlein et al. 2014). In those studies, CCMs were shown to be down-regulated under elevated pCO_2. Such a down-regulation could, in contrast to constitutively expressed CCMs, allow for a reallocation of energy to other cellular processes, e.g. the acquisition of limiting resources, an aspect that may be especially relevant under nutrient limitation.

Estuaries may promote coastal acidification even beyond the calculated CO_2 projections for pelagic systems (Melzner et al. 2013, Wallace et al. 2014) and likely suffer from N limitation due to unbalanced nutrient loads. Dinoflagellates often proliferate in these eutrophic coastal waters, forming dense harmful algal blooms (HABs). HABs may not only have adverse effects on the ecosystem as result of high population densities, but their toxins also pose a direct threat to birds, fish, whales, and humans (Anderson et al. 2002, Granéli & Turner 2006). The genus *Alexandrium* consists of many species that produce paralytic shellfish poisoning (PSP) toxins, which are potent neurotoxins that can accumulate in shellfish (Anderson et al. 2012a). PSP toxins are N-rich alkaloids with several analogues (Shimizu 1996, Cembella 1998, Anderson et al. 2012b), and their synthesis has been shown to depend on N availability (e.g. Boyer et al. 1987, Van de Waal et al. 2013, 2014b), but also on changes in pCO_2 (Tatters et al. 2013, Van de Waal et al. 2014a, Hattenrath-Lehmann et al. 2015). Little is yet known about the combined effects of N limitation and elevated pCO_2.

In order to improve our estimates about the responses of bloom-forming dinoflagellates to future changes, we investigated the combined effect of elevated pCO_2 and N limitation on 2 dinoflagellate species, *Scrippsiella trochoidea* and *Alexandrium fundyense* (formerly *A. tamarense*; John et al. 2014). Both dinoflagellate species co-occur in the North Sea (Fistarol et al. 2004, McCollin et al. 2011) and while *S. trochoidea* has the ability to calcify, *A. fundyense* is a notorious PSP toxin producer, which may imply different strategies for N assimilation. By using a continuous culture system especially designed for dinoflagellates (Van de Waal et al. 2014c), we maintained both species under N limitation and studied the effects of increasing CO_2 concentrations on growth, elemental composition and toxin content.

MATERIALS AND METHODS

Experimental setup

Scrippsiella trochoidea GeoB267 (culture collection of the University of Bremen) and *Alexandrium fundyense* (formerly *A. tamarense* strain Alex5; Tillmann et al. 2009), both originating from the North Sea, were cultured at 15°C in sterile-filtered North Sea water (0.2 µm, salinity 34). Vitamins and trace metals were added according to f/2 medium (Guillard & Ryther 1962), except for $FeCl_3$ (1.9 µmol l^{-1}), H_2SeO_3 (10 nmol l^{-1}) and $NiCl_2$ (6.3 nmol l^{-1}). Phosphate was added to yield a final concentration of 6.25 µmol l^{-1}, whereas additions of nitrate differed between species, yielding final concentrations of 8 and 16 µmol l^{-1} for *S. trochoidea* and *A. fundyense*,

respectively. Light was provided by daylight tubes (18W/965 Biolux, OSRAM) at a 16 h light:8 h dark cycle and adjusted to an incident photon flux density (PFD) of 250 ± 30 µmol photons m^{-2} s^{-1} using a spherical micro quantum sensor (Heinz Walz).

To maintain species under N-limiting conditions, a continuous culture system was applied (also referred to as chemostats). The advantage of this method is that at steady-state conditions, the consumption of N equals the supply rate of N, and the growth rate is fixed by the dilution rate. Thus, continuous cultures allow controlled growth under N-limited conditions. In classical batch cultures, cells experience changing growth phases with an initial N-replete phase followed by N-limited and N-starved phases, which are accompanied by a decrease in growth rate. Growth characteristics (e.g. elemental quotas) thus consist of both N-replete and N-limited growth periods. In this study, we therefore applied a continuous culture system. This furthermore allowed comparison with previous studies that applied a dilute batch system (i.e. Eberlein et al. 2014, Van de Waal et al. 2014a) to obtain information on the responses under N-replete conditions with minimal changes in growth phases due to low population densities.

Species were grown in 2.1 l continuous culture systems specially designed for dinoflagellates (for more details, see Van de Waal et al. 2014c). Homogeneous mixing was ensured by placing these vessels on a 3-dimensional orbital shaker (TL10, Edmund Bühler), set at an angle of 9° with a shaking speed of 16 rpm, allowing a headspace and a polyoxymethylene ball to mix the system gently. Prior to the onset of the experiments, cells were acclimated for at least 1 wk to the mixing system at ambient and elevated pCO_2. High pCO_2 was obtained by mixing CO_2-free air (<0.1 µatm pCO_2; Domnick Hunter) with pure CO_2 (Air Liquide Deutschland) using mass flow controllers (CGM 2000, MCZ Umwelttechnik). pCO_2 mixtures were regularly verified by measurements with a nondispersive infrared analyzer system (LI6252, LI-COR Biosciences). Initial pCO_2 were achieved by aeration of the culture medium in the reservoir tanks, yielding values (mean ± SD) of between 428 ± 96 and 1224 ± 90 µatm for *S. trochoidea*, and 444 ± 85 and 829 ± 96 µatm for *A. fundyense*. Owing to dilution-dependent exchange of culture medium, and dissolved inorganic carbon (DIC) drawdown during biomass build-up in the transition phase, steady-state pCO_2 ranged from 300 to 800 µatm for *S. trochoidea*, and from 250 to 1000 µatm for *A. fundyense*, which were grouped into 3 CO_2 treatments per species (Table 1).

To obtain steady-state population densities similar to those observed in dinoflagellate blooms (i.e. remaining below 1000 cells ml^{-1}; Wyatt & Jenkinson 1997, Anderson et al. 2012b), the tested species required different dilution rates as well as different dissolved inorganic nitrogen (DIN) concentrations in the medium reservoir. Applied dilution rates yielded comparable growth limitation for the 2 species, i.e. ~33 % of their maximum growth rate. More specifically, *S. trochoidea* was grown at 0.2 ± 0.01 d^{-1} and 8 µmol l^{-1} DIN, while *A. fundyense* was set to 0.15 ± 0.01 d^{-1} and 16 µmol l^{-1} DIN. These differences in initial DIN concentrations have no effect on pH or pCO_2. Every 2 to 3 d and 5 to 7 h after the start of the light period, samples were taken to determine population densities, carbonate chemistry and residual DIN concentrations. Continuous culture systems that were exposed to elevated pCO_2 generally required a longer time period to establish a steady state than those under ambient pCO_2. For this reason, transition phases ranged from 22 to 42 d. The carbonate chemistry parameters presented in Table 1 relate to the steady-state conditions after the transition phase of 6 individual continuous culture experiments per species, grouped into the 3 CO_2 treatments. Values in Table 1 thus represent means and data ranges based

Table 1. Carbonate chemistry for the different continuous culture experiments. Mean values of pCO_2 and respective data range (minimum and maximum) were calculated based on dissolved inorganic carbon (DIC) and pH values during steady state using CO_2Sys (Pierrot et al. 2006). pH values are given on the NBS scale (pH_{NBS}). Total alkalinity (TA) values indicate the mean of values obtained at the beginning and the end of each continuous culture experiment

CO_2 treatment (µatm)	pCO_2 (µatm)	TA (µmol l^{-1})	DIC (µmol l^{-1})	pH_{NBS}
Scrippsiella trochoidea				
300	298 (259–337)	2349 (2305–2385)	2148 (2141–2161)	8.31 (8.25–8.36)
600	601 (572–650)	2389 (2367–2405)	2230 (2205–2235)	8.03 (8.00–8.06)
800	793 (742–855)	2365 (2357–2373)	2252 (2241–2265)	7.92 (7.89–7.95)
Alexandrium fundyense				
250	237 (220–258)	2372 (2336–2392)	2097 (2077–2122)	8.39 (8.36–8.41)
800	813 (727–937)	2398 (2392–2405)	2252 (2240–2271)	7.91 (7.90–7.96)
1000	1018 (918–1154)	2397 (2392–2407)	2272 (2263–2291)	7.82 (7.77–7.86)

Table 2. Responses of *Scrippsiella trochoidea* and *Alexandrium fundyense* grown under N-limited conditions and different pCO_2 (CO_2 treatment). Values for particulate organic carbon (POC):particulate organic nitrogen (PON) ratios, POC, PON, and chl *a* show the biological mean of replicates (n = 2) and data range (minimum and maximum)

CO_2 treatment (µatm)	POC:PON (molar)	POC (ng cell $^{-1}$)	PON (ng cell $^{-1}$)	Chl *a* (pg cell $^{-1}$)	POC:chl *a* (mass)	Volume (µm^3 cell $^{-1}$)
S. trochoidea						
300	21.34 (20.33–22.34)	4.29 (4.15–4.43)	0.24 (0.23–0.24)	8.99 (7.84–10.14)	489 (419–558)	9204 (8933–9475)
600	24.71 (24.26–25.15)	4.24 (4.07–4.4)	0.20 (0.19–0.21)	9.20 (8.77–9.63)	464 (454–474)	7959 (7690–8227)
800	18.01 (17.27–18.74)	4.07 (3.84–4.29)	0.27 (0.26–0.27)	11.18 (10.59–11.76)	369 (330–407)	12 046 (11 780–12 311)
A. fundyense						
250	9.53 (9.23–9.82)	3.93 (3.9–3.96)	0.48 (0.46–0.5)	22.92 (21.22–24.62)	173 (161–184)	17 496 (16 699–18 293)
800	6.75 (6.68–6.82)	2.71 (2.68–2.74)	0.47 (0.47–0.47)	24.66 (24.6–24.71)	106 (100–111)	15 591 (14 533–16 649)
1000	5.77 (5.5–6.04)	3.55 (3.43–3.66)	0.72 (0.71–0.73)	33.05 (31.34–34.75)	108 (99–117)	17 658 (16 279–19 036)

on 4 consecutive sampling points during steady state, while values in Table 2 represent means and data ranges based on mean steady-state values of 2 biological replicates for each treatment.

Sampling and analysis

To determine population densities, cell samples were fixed with Lugol's solution (1% final concentration) and counted in duplicates (during the experiment) or triplicates (at the end of each experiment) with an Axiovert 40C inverted microscope (Carl Zeiss MicroImaging GmbH). Size measurements (i.e. for calculating biovolume) were performed with the same microscope using the AxioCam MRc5 (software SE64 Rel. 4.8, Carl Zeiss MicroImaging GmbH), and all values represent the mean ± SD of at least 50 cells.

The pH was measured with a 3-point calibrated pH meter (826 pH mobile, Metrohm). Duplicate DIC samples were analyzed in a QuAAtro high performance microflow analyzer (Seal Analytical) with a mean precision of 8 µmol l^{-1}. Samples for total alkalinity (TA) were taken at the beginning and the end of each experiment (n = 2) and analyzed by a fully automated titration system (SI Analytics) with a mean precision of 13 µmol l^{-1}. Certified Reference Materials supplied by A. G. Dickson (Scripps Institution of Oceanography) were used to correct for inaccuracies in TA and DIC measurements. Subsequently, carbonate chemistry was calculated with CO_2Sys (Pierrot et al. 2006) using pH_{NBS} (National Bureau of Standards) and DIC with equilibrium constants of Mehrbach et al. (1973), refitted by Dickson & Millero (1987).

The residual DIN concentrations, i.e. nitrate (NO_3^-) and nitrite (NO_2^-), in the continuous culture systems were determined in sterile-filtered culture medium (0.2 µm), which was stored at –20°C in acid-washed tubes prior to analysis. Samples were analyzed through a custom-made nanomolar nutrient system (Ocean Optics). The system comprised a 2 m liquid waveguide capillary cell (World Precision Instruments) with a tungsten halogen light source (LS1-LL, Ocean Optics) and a miniaturized spectrophotometer (USB2000 VIS-NIR, Ocean Optics). Samples were introduced to the system via a conventional segmented-flow autoanalyzer. Prior to determination of DIN, NO_3^- was reduced to NO_2^- using a copperized cadmium column and all NO_2^- was spectrophotometrically detected at 540 nm following the sulphanilamide and N-(1-Naphthyl)-ethylenediamine (NED) reaction. For more details on the method see Patey et al. (2008).

Cultures were kept for >5 d in steady-state conditions (also referred to as equilibrium-state), during which population densities and carbonate chemistry remained largely constant (Table 1). Therefore, potential carry-over effects from the initial conditions are assumed to be negligible. At the end of this steady-state period, experiments were stopped and samples were taken to assess particulate organic carbon (POC) and nitrogen (PON), chlorophyll *a* (chl *a*); and for PSP toxins, in the case of *A. fundyense*.

For determination of POC and PON, culture suspension was filtered in triplicate on pre-combusted GF/F filters (500°C, 6 h; Whatman). To remove potential inorganic carbon retained on the filter, 200 µl HCl (0.2 mol l^{-1}) was added to each sample. Filters were dried at 60°C in a drying oven for at least 24 h. The filters were then packed into tin cups, pressed into pellets and measured with a Delta S isotopic ratio mass spectrometer (Thermo) connected to an elemental analyzer CE1108 via an open split interface (Conflow II, Thermo). The reference gases were ultra-high purity N_2 and CO_2 from a gas cylinder calibrated against standards from the International Atomic Energy Agency (IAEA N1, N2, N3, C3, C6, and NBS 22). Acetanilid and Peptone (Merck Millipore) served as lab-internal elemental and isotope standards for daily calibration.

To determine chl *a*, culture medium was filtered in duplicate on 0.45 µm cellulose-nitrate membrane filters (Whatman), rapidly frozen in liquid nitrogen and subsequently stored at –80°C. Extraction and fluorometric determination of chl *a* were performed in accordance with Knap et al. (1996) using a TD-700 Fluorometer (Turner Designs).

To determine the predominant PSP toxin analogues of *A. fundyense*, including the non-sulfated saxitoxin (STX) and neosaxitoxin (NEO), the mono-sulfated gonyautoxins (GTX 1–4), and the di-sulfated C-toxins (C1 + C2), culture samples were filtered in duplicate over polycarbonate filters (1.0 µm pore size; Whatman) and stored in Eppendorf tubes at –20°C. Toxins were extracted following the method of Van de Waal et al. (2014a) and analyzed in accordance with Krock et al. (2007). Cellular toxicity was estimated from the cellular PSP content and the relative toxicity of each PSP toxin analogue (Wiese et al. 2010).

Statistics and error propagation

For every parameter, various statistical models were applied (linear and exponential regression, Gaussian peak) to test for correlations with pCO_2, using the 6 biological replicates for the continuous culture experiments (this study), and 12 biological replicates of the dilute batch experiments (Eberlein et al. 2014, Van de Waal et al. 2014a). The 3-parameter models were tested against 2-parameter models using the Akaike information criterion (AIC; Rawlings et al. 1998). The 2-parameter models were tested against each other on the basis of the coefficient of determination (R^2). The best fit is quoted in the text.

Linear regression model:

$$y(x) = y_0 + ax \quad (1)$$

where y_0 is the *y*-intercept and *a* represents the slope.

The 2-parameter exponential regression model:

$$y(t) = y_0 e^{bt} \quad (2)$$

where y_0 is the initial quantity, *b* represents the growth rate and *t* is time in days. When applying an exponential decay model, *b* is negative.

Gaussian peak regression model:

$$y(x) = a^{\left(-\frac{(x-b)^2}{2c^2}\right)} \quad (3)$$

where *a* is the height, *b* is the location of the centroid and *c* represents the width.

As our results suggested a non-linear relationship between PSP toxin content and POC:PON ratios, we applied a 3-parameter exponential decay model and determined the minimum cellular toxin content:

$$PSP_{min} = PSP - y_0 e^{-b(POC:PON)} \quad (4)$$

where PSP and PSP_{min} are the measured and minimum PSP toxin content, respectively.

Half-saturation concentrations ($K_{1/2}$) for growth were calculated based on Monod (1949), according to:

$$K_{1/2} = \frac{R\,\mu_{max}}{\mu_{limited}} - R \quad (5)$$

where μ_{max} was taken from N-replete experiments (Eberlein et al. 2014), $\mu_{limited}$ represents growth rates in the continuous culture system (equal to the dilution rate), and *R* is the residual DIN concentration (often referred to as the lowest resource requirement, i.e. R^*). Propagation of uncertainties was calculated using the law of combination of errors (e.g. Barlow 1989).

For testing interactive effects of CO_2 and N availability on PSP toxin content, toxicity, and toxin composition, we applied analysis of covariance (ANCOVA). In case the assumption of homogeneity of regression slopes was violated, we performed the Johnson-Neyman technique (Johnson & Neyman 1936). We defined the range of significant differences using the software IBM SPSS Statistics, version 12 (Hayes & Matthes 2009). Normality and homogeneity of PSP toxin content, toxicity, and composition were confirmed by applying the Shapiro-Wilks and Levene's test, respectively. Variables were log-transformed if this improved the equality of variables. The threshold significance level (α) in all tests was set at 0.05.

RESULTS

Growth characteristics

For both tested species, population densities at the start of the continuous culture experiments ranged from 10 to 70 cells ml^{-1}. These low initial population densities and the initially high DIN concentrations allowed for maximum growth rates, which were 0.48 ± 0.05 and 0.41 ± 0.03 d^{-1} for *Scrippsiella trochoidea* and *Alexandrium fundyense*, respectively. In the course of biomass build-up, DIN concentrations decreased and cultures grew into N limitation. Here, growth rates were lowered and population densities in the continuous culture experiments stabilized, reaching a steady-state. Under these conditions, growth rates resembled the dilution rates of 0.2 ± 0.01 and 0.15 ± 0.01 d^{-1} for *S. trochoidea* and *A. fundyense*, respectively. Steady-state pCO_2 ranged from about 300 to 800 µatm for *S. trochoidea* and 250 to 1000 µatm for *A. fundyense*, which were grouped into 3 CO_2 treatments per species (Table 1).

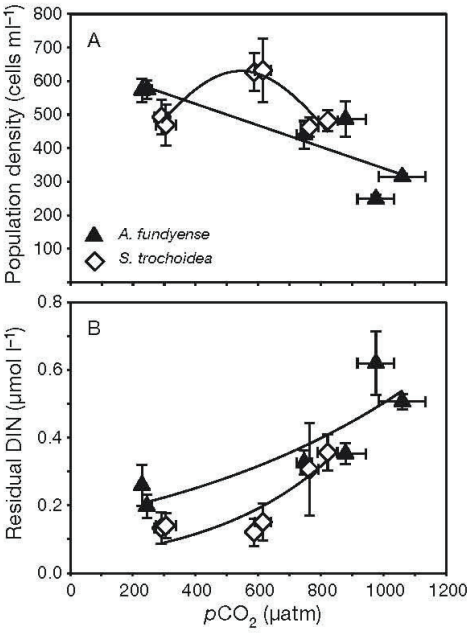

Fig. 1. Effects of elevated pCO_2 under N limitation on (A) population densities and (B) residual dissolved inorganic nitrogen (DIN) concentrations for *Scrippsiella trochoidea* (◇) and *Alexandrium fundyense* (▲). Symbols indicate the mean ± SD of replicates over time from each steady state (n ≥4). Solid lines indicate significant trends and the best fits from the tested regression models: (A) *S. trochoidea*, Gaussian peak regression model: R^2 = 0.87, n = 6, p = 0.049; *A. fundyense*, linear regression model: R^2 = 0.76, n = 6, p = 0.024. (B) *S. trochoidea*, exponential regression model: R^2 = 0.78, n = 6, p = 0.020; *A. fundyense*, exponential regression model: R^2 = 0.75, n = 6, p = 0.025

Population densities during steady state differed between pCO_2 treatments of both species (Fig. 1A). Densities of *S. trochoidea* showed a bell-shaped pattern, being highest at intermediate pCO_2 with ~630 cells ml^{-1}, and similarly low in the low and high pCO_2 treatments with ~475 cells ml^{-1} (Fig. 1A). In *A. fundyense*, cell densities decreased with increasing pCO_2 from ~570 cells ml^{-1} at low pCO_2 towards 280 cells ml^{-} at the highest pCO_2 (Fig. 1A). The observed decrease in densities was stronger between intermediate and high, than between low and intermediate pCO_2.

Residual DIN concentrations during steady state were reduced to values below 1 µmol l^{-1} for both species. In *S. trochoidea*, lowest DIN concentrations of 137 ± 46 nmol l^{-1} were observed at low and intermediate pCO_2, while they increased to 330 ± 105 nmol l^{-1} in the high pCO_2 treatment (Fig. 1B). Increasing residual DIN concentrations under elevated pCO_2 were also observed for *A. fundyense*, as they increased from 227 ± 62 nmol l^{-1} at low pCO_2 towards 549 ± 79 nmol l^{-1} at high pCO_2 (Fig. 1B).

Elemental composition

Here we present elemental composition and PSP toxin data of N-limited *S. trochoidea* and *A. fundyense* cultures exposed to a range of pCO_2 (this study), which are compared with data obtained under N-replete conditions (Eberlein et al. 2014, Van de Waal et al. 2014a). Consequently, we can assess the effect of N availability on CO_2 responses.

Under N limitation, the cellular POC:PON ratios of *S. trochoidea* were generally high and ranged between 17 and 25, showing maximum values in the intermediate, and lowest values in the high pCO_2 treatment (Table 2; Gaussian peak model: R^2 = 0.92, n = 6, p = 0.022). In comparison to N-replete conditions, the observed ratios were more than 2-fold higher (Table 2; cf. Eberlein et al. 2014). In *A. fundyense*, POC:PON ratios under N limitation decreased from about 10 to 6 in the low to the high pCO_2 treatment (Table 2; linear regression model: R^2 = 0.94, n = 6, p = 0.001), and thereby reached values similar to N-replete conditions (Table 2; cf. Eberlein et al. 2014).

For both species, the decrease in POC:PON ratios under elevated pCO_2 was accompanied by an in-

crease in residual DIN concentrations, resulting in lowest POC:PON ratios at highest residual DIN concentrations (Table 2). The high POC:PON ratios in *S. trochoidea* reflected 2-fold increased POC quotas under N limitation, while PON quotas remained largely unaltered (Table 2; cf. Eberlein et al. 2014). The changes in POC:PON ratios under elevated pCO_2, however, resulted from alterations in PON quotas, which were highest in the high pCO_2 treatment (Table 2). In *A. fundyense*, POC:PON ratios decreased with increasing pCO_2, reflecting both a change in POC as well as in PON quotas. More specifically, PON quotas were highest in the high pCO_2 treatment and POC quotas were lowest in the intermediate pCO_2 treatment (Table 2). POC quotas largely resembled those under N-replete conditions, while PON quotas were generally lower, except for the highest pCO_2 treatment where PON quotas were similar (Table 2; cf. Eberlein et al. 2014).

In both tested species, chl *a* quotas increased under elevated pCO_2 (Table 2). In *S. trochoidea*, values under N limitation were generally higher as compared to those under N-replete conditions, whereas in *A. fundyense* values were lower and approximated those under N-replete conditions at high pCO_2 (Table 2; cf. Eberlein et al. 2014). Cell volumes of *S. trochoidea* and *A. fundyense* remained largely unaffected by elevated pCO_2 (Table 2). For *S. trochoidea*, however, cell volumes were higher under N limitation compared to those under N-replete conditions (~5000 µm^3 cell^{-1}). Calcification in *S. trochoidea* was very low with PIC:POC ratios <0.1 in all pCO_2 treatments, irrespective of N availability (data not shown).

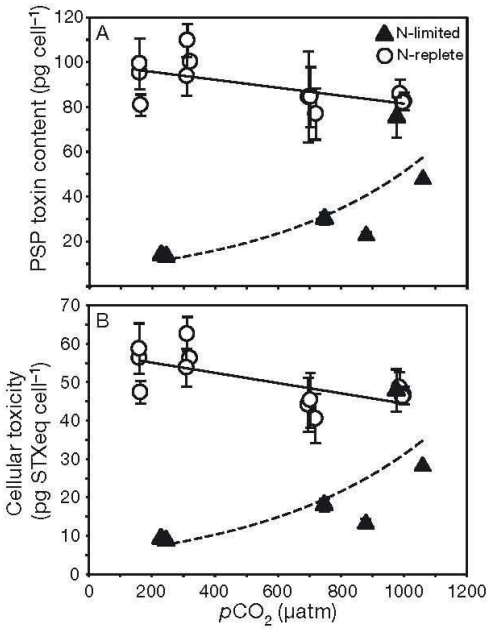

Fig. 2. Effect of elevated pCO_2 on (A) paralytic shellfish poisoning (PSP) toxin content and (B) cellular toxicity in saxitoxin equivalents (STXeq) for *Alexandrium fundyense* under N-limiting (▲, this study) and N-replete (○, Van de Waal et al. 2014a) conditions. Symbols indicate the mean ± SD of technical replicates (n = 2). Solid (significant trend) and dashed (non-significant trend) lines indicate the best fits of tested regression models. (A) N-limited, exponential regression model: $R^2 = 0.61$, n = 6, p = 0.242; N-replete, linear regression model: $R^2 = 0.37$, n = 12, p = 0.036. (B) N-limited, exponential regression model: $R^2 = 0.55$, n = 6, p = 0.303; N-replete, linear regression model: $R^2 = 0.45$, n = 12, p = 0.018

PSP toxin content and composition in *A. fundyense*

Under N limitation, cellular PSP toxin content increased over the applied range of pCO_2 (Fig. 2A), which can be attributed to a general increase in all PSP toxin analogues. In the high pCO_2 treatment, total PSP toxin content was close to values observed under N-replete conditions, reaching above 70 pg cell^{-1} compared to about 80 pg cell^{-1}, respectively. Cellular toxicity largely followed these changes in toxin content and increased with elevated pCO_2 towards 48 pg STX equivalents (STXeq) cell^{-1} compared to 47 pg STXeq cell^{-1} under N-replete conditions (Fig. 2B).

The contribution of STX relative to total PSP toxin content increased under elevated pCO_2 (Fig. 3A), while the relative contribution of GTX1+4 decreased (Fig. 3B), displaying opposite patterns as observed under N-replete conditions (Fig. 3A,B). Significantly higher contributions of GTX1+4 under N-limited compared to N-replete conditions were recorded over almost the entire range of applied pCO_2, while contributions of STX were lower under N-limited compared to N-replete conditions (Johnson-Neyman: $p < 0.05$). The relative contribution of C1+C2 to total PSP toxin content increased under elevated pCO_2 (Fig. 3C), displaying a similar trend as under N-replete conditions (Fig. 3C). Contributions of C1+C2 were, however, significantly lower under N-limited conditions at a pCO_2 higher than 200 µatm (Johnson-Neyman: $p < 0.05$). Relative contributions of NEO and GTX2+3 remained largely unaltered over the applied range of pCO_2 and were comparable to those under N-replete conditions (Fig. 3D,E). The CO_2-

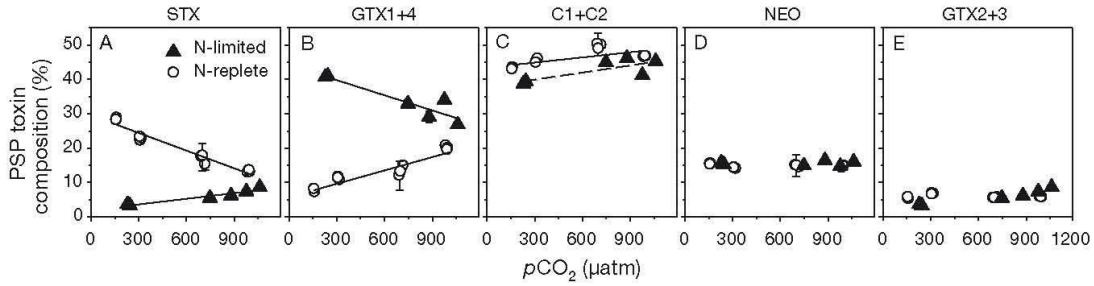

Fig. 3. (A–E) Effect of elevated pCO_2 on PSP toxin composition in *Alexandrium fundyense* under N-limiting (▲, this study) and N-replete (○, Van de Waal et al. 2014a) conditions. STX: saxitoxins; GTX: gonyautoxins; C1+C2: C-toxins; NEO: neosaxitoxins. Symbols indicate the mean ± SD of technical replicates (n = 2). Solid (significant trend) and dashed (non-significant trend) lines indicate the best fits of tested regression models. (A) N-limited, linear regression model: $R^2 = 0.92$, n = 6, p = 0.002; N-replete, linear regression model: $R^2 = 0.95$, n = 12, $p < 0.001$. (B) N-limited, linear regression model: $R^2 = 0.85$, n = 6, p = 0.009; N-replete, linear regression model: $R^2 = 0.90$, n = 12, $p < 0.001$; (C) N-limited, linear regression model: $R^2 = 0.60$, n = 6, p = 0.069; N-replete, linear regression model: $R^2 = 0.46$, n = 12, p = 0.015

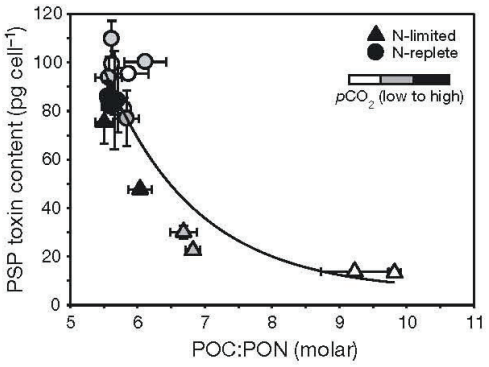

Fig. 4. Effect of elevated pCO_2 on PSP toxin content versus particulate organic carbon (POC): particulate organic nitrogen (PON) ratios in *Alexandrium fundyense* under N-limited (▲, this study) and N-replete conditions (●, Van de Waal et al. 2014a). Symbols indicate the mean ± SD of technical replicates (n = 2). Solid line indicates the significant trend and best fit from a 3-parameter exponential decay model ($R^2 = 0.77$, n = 18, $p < 0.001$)

dependent increase in toxin content under N-limited conditions was accompanied by a decrease in the POC:PON ratio (Fig. 4), so that both PSP toxin content and POC:PON ratios were comparable to the N-replete conditions under elevated pCO_2.

DISCUSSION

Although various experiments have investigated the responses of dinoflagellates under elevated pCO_2 (e.g. Rost et al. 2006, Fu et al. 2008, Brading et al. 2013) or N limitation (e.g. Leong & Taguchi 2004, Collos et al. 2005, Van de Waal et al. 2013), this study is, to our knowledge, the first to look at the combined effects in this phytoplankton group. Using a continuous culturing system especially designed for dinoflagellates (Van de Waal et al. 2014c) allowed us to maintain cultures of *Scrippsiella trochoidea* and *Alexandrium fundyense* under N limitation while studying their responses to elevated pCO_2. By comparing our results with recent work on the same strains under N-replete conditions (Eberlein et al. 2014, Van de Waal et al. 2014a), we were then able to describe the effect of N availability on CO_2 responses.

Effects of N limitation and elevated pCO_2 on elemental stoichiometry

Under N limitation, species showed different trends in population densities and residual DIN concentrations in response to increasing pCO_2. Population densities of *S. trochoidea* followed a bell-shaped pattern, indicating that intermediate pCO_2 supported highest population densities in these N-limited systems (Fig. 1A). Residual DIN concentrations showed highest values under elevated pCO_2, suggesting highest efficiencies of DIN uptake under intermediate and low pCO_2 (Fig. 1B). Cultures of *A. fundyense* were also sensitive to changes in pCO_2 and became less dense under elevated pCO_2, while residual DIN concentrations showed the inverse pattern with highest values under elevated pCO_2 (Fig. 1). The observed CO_2-dependent changes in POC:PON ratios (Table 2) were driven by species-

specific alterations in either PON quotas alone (*S. trochoidea*) or both POC and PON quotas (*A. fundyense*).

Previous studies on dinoflagellates, including *A. fundyense*, have shown up to 2-fold higher POC quotas under N limitation (Leong & Taguchi 2004, Fuentes-Grünewald et al. 2012). In our study, *A. fundyense* displayed no such effect (Table 2; Eberlein et al. 2014), which may be due to differences in culture conditions or species- and strain-specific regulation of enzymes involved in C storage under N limitation (Dagenais-Bellefeuille & Morse 2013). The few studies on combined effects of N limitation and elevated pCO_2 on marine phytoplankton do indeed show a high variety with respect to elemental quotas. In the coccolithophore *Emiliania huxleyi*, for instance, POC:PON ratios were higher under N limitation as compared to N-replete conditions, but remained similarly high (Müller et al. 2012, Rouco et al. 2013) or even decreased under elevated pCO_2 (Sciandra et al. 2003), the latter reflecting a reduction in POC quotas. Besides strain-specific growth characteristics, these different responses may also have resulted from dissimilar growth conditions. In N-limited cultures of the diatom *Phaeodactylum tricornutum*, POC:PON ratios increased with increasing pCO_2 as a result of a relatively stronger increase in POC compared to PON quotas (Li et al. 2012).

According to our data, POC:PON ratios are particularly responsive to increasing pCO_2 when limited by N, which is in line with theory (Verspagen et al. 2014). Although the underlying responses in elemental composition were species-specific, we were able to link the CO_2-dependent changes in PON quotas to shifts in N assimilation properties (see below), which may also apply to some of the observed responses in previous studies. In turn, changes in N assimilation properties can explain the observed shifts in residual DIN concentrations and population densities.

Elevated pCO_2 alleviates stress of N limitation

For both species, PON quotas and residual DIN concentrations increased under elevated pCO_2 (Fig. 1, Table 2). Irrespective of the CO_2-dependent changes of these 2 measures, the relationship between the amount of N that can be incorporated by the cell and the amount of N that will remain in the medium reflects fundamental biochemical constrains of nutrient uptake in microalgae (Fersht 1974). It has been argued that under severe N limitation, the optimal strategy for a phytoplankton species is to reduce the number of uptake sites and to increase the number of active uptake areas per site, which will result in relatively low maximum uptake rates (V_{max}) with high substrate affinities (i.e. low half-saturation concentrations, $K_{1/2}$) (Litchman et al. 2007).

Using our residual DIN concentrations at the given growth rates (i.e. dilution rates) together with maximum growth rates under N-replete conditions (Eq. 5), we estimated $K_{1/2}$ values (DIN) for growth and compared them with PON production rates from each experiment. The low pCO_2 treatments showed low PON production rates combined with a low $K_{1/2}$ and confirmed the N-limitation strategy described by Litchman et al. (2007). Interestingly, under elevated pCO_2, PON production rates and $K_{1/2}$ values simultaneously increased and showed a linear relationship (Fig. 5; *S. trochoidea*: $R^2 = 0.701$, n = 6, p = 0.038; *A. fundyense*: $R^2 = 0.837$, n = 6, p = 0.011). It thus seems that high pCO_2 shifts N assimilation towards higher PON production rates and lower affinities, which could indicate that species suffer less from N limitation. Such CO_2-dependent changes in N assimilation characteristics may also apply to other phytoplankton species. The coccolithophore *E. huxleyi*, for instance, also expressed higher PON production rates and residual DIN concentrations (which scale with a higher $K_{1/2}$) under elevated pCO_2 (Müller et al. 2012). More experiments are needed, however, to verify whether this concept may be a general strategy and whether it can be attributed to CO_2-dependent regulation in physiological key processes.

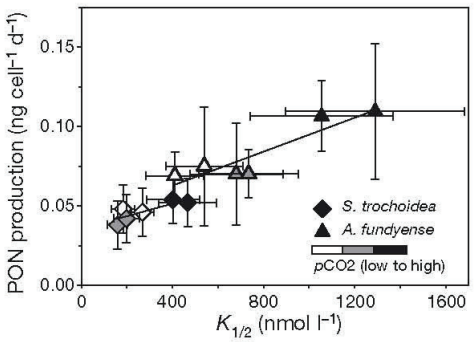

Fig. 5. Effect of elevated pCO_2 on PON production rates versus half-saturation concentrations ($K_{1/2}$) of growth for *Scrippsiella trochoidea* (◆) and *Alexandrium fundyense* (▲) under N limitation. Solid lines indicate significant trends and best fits from linear regression models (*S. trochoidea*: $R^2 = 0.701$, n = 6, p = 0.038; *A. fundyense*: $R^2 = 0.837$, n = 6, p = 0.011)

Reallocation of energy from CCM down-regulation

The observed shifts in N-uptake characteristics towards higher PON production rates and lower affinities with elevated pCO_2 could partly be explained by the reallocation of energy from down-regulating CCMs. The majority of marine phytoplankton exhibit effective CCMs, which allow them to grow rather independently from CO_2 availability (e.g. Rost et al. 2006, Fu et al. 2007, Ratti et al. 2007). This does not mean, however, that species do not benefit from increasing CO_2 concentrations. In fact, increasing CO_2 concentrations often lead to a down-regulation of phytoplankton CCMs, thereby reducing the costs for acquiring inorganic C (Giordano et al. 2005).

In an earlier study, we showed that both dinoflagellate species *S. trochoidea* and *A. fundyense* possess an effective and adjustable CCM (Eberlein et al. 2014). Specifically, their overall CO_2 affinity was 10-fold higher than would be expected from RuBisCO kinetics, and cells were able to take up HCO_3^- as their major C source. With respect to elevated pCO_2, the relative HCO_3^- uptake decreased for *S. trochoidea*, which may liberate energy for other processes (Eberlein et al. 2014). In *A. fundyense*, elevated pCO_2 also caused a down-regulation of genes expressing carbonic anhydrase (CA) homologues (Van de Waal et al. 2014a), which is in line with frequently observed down-regulated CA activity under elevated pCO_2.

It is conceivable that under N limitation, 'extra' energy resulting from the down-regulated CCM, as well as the shift in photosynthesis and respiration, may be reallocated to the uptake and assimilation of N, especially since N assimilation also occurs mainly during the photoperiod (Paasche et al. 1984, Leong et al. 2010). Higher PON production rates under elevated pCO_2 were also accompanied by higher quotas of N-rich compounds, such as chl *a* and PSP toxins (Fig. 2, Table 2). Despite the apparent beneficial effect of elevated pCO_2, the increased assimilation of N per cell was accompanied by a lowering of the affinity for DIN. Although we predicted the opposite pattern, i.e. increasing affinities for DIN under elevated pCO_2, these results demonstrate a trade-off in N uptake between maximum PON production rates and affinities (Fig. 5). In a continuous culture system with a fixed dilution rate (i.e. a fixed supply rate of nutrients), such physiological changes may directly feed back on cellular growth as shown by the lower population densities under elevated pCO_2 (Fig. 1A). These changes may affect the competitive success of both species, but aspects such as altered toxicity may also need to be considered when making predictions for the future ocean.

PSP toxin content and composition in *A. fundyense*

N limitation led to a strong change in PSP toxin content in *A. fundyense*. More specifically, under low pCO_2, values were 4-fold lower compared to those obtained under N-replete conditions (Fig. 2A). This observation reflects the dependency of N-rich PSP toxins on N availability and is in line with previous findings that show decreased PSP toxin contents under N limitation in various *Alexandrium* species (e.g. Boyer et al. 1987, Van de Waal et al. 2013). Interestingly, PSP toxin contents and the associated cellular toxicity increased with elevated pCO_2 (Fig. 2). Starting from a minimum PSP toxin content of ~5.5 pg cell^{-1}, values increased more than 8-fold and closely resembled the PSP toxin contents observed under N-replete and high pCO_2 conditions. The associated increase in toxicity showed the same CO_2 dependency and was no longer different to N-replete conditions above a pCO_2 of 1000 µatm (Johnson-Neyman: $p > 0.05$). The CO_2-dependent increase in PSP toxin contents correlated with the decrease in POC:PON ratios and was accompanied by an increase in PON quotas and PON production rates (Fig. 4, Table 2). Thus, the relatively higher N availability in the cells, as a result of down-regulated CCM, may explain the increased cellular PSP toxin content. Therefore, elevated pCO_2 seems to not only alleviate the negative effects of N limitation on elemental quotas in general, but also to facilitate the synthesis of N-rich compounds such as PSP toxins (Fig. 4).

While there are, to our knowledge, no studies that have investigated the combined effects of elevated pCO_2 and N limitation on PSP toxin production in the genus *Alexandrium*, there are several that have tested the effects of elevated pCO_2. In 2 *A. fundyense* strains, for instance, PSP toxin content decreased under elevated pCO_2 (Van de Waal et al. 2014a), whereas it remained relatively unaltered in some *A. ostenfeldii* strains (Kremp et al. 2012). In contrast, PSP toxin content in *A. catenella* increased under elevated pCO_2 and further increased 10-fold when phosphorus (P) was limiting (Tatters et al. 2013). The relative availabilities of N and P have been shown to exert strong control on PSP toxin synthesis, which generally decreases under N limitation and increases under P limitation (e.g. Boyer et al. 1987, Cembella

1998, Van de Waal et al. 2014b). Here, we demonstrate that the negative impact of N limitation on PSP toxin production is reduced under elevated pCO_2.

Regarding toxin profiles of *A. fundyense*, contributions of the analogues C1+C2, GTX2+3, and NEO to total PSP toxin content remained largely unaltered in response to elevated pCO_2 and N limitation (Fig. 3C–E). Interestingly, STX increased and GTX1+4 decreased with elevated pCO_2, showing opposite trends than those observed under N-replete conditions (Fig. 3A,B). Van de Waal et al. (2014a) argued that the observed down-regulation in sulfatases and up-regulation of sulfotransferases under elevated pCO_2 could be a reason for the decrease in nonsulfated STX and the increase in mono-sulfated GTX1+4 under N-replete conditions. In view of our data, one could argue that N limitation may modulate the sulfur metabolism in the opposite direction. CO_2-dependent changes have also been reported for other *Alexandrium* species. For instance, *A. ostenfeldii* showed increased STX under elevated pCO_2 (Kremp et al. 2012), whereas *A. catenella* and *A. fundyense* (NPB8) displayed an increase in both STX and GTX1+4 under elevated pCO_2 (Tatters et al. 2013, Hattenrath-Lehmann et al. 2015). Thus, PSP toxin composition by *Alexandrium* species lacks an unambiguous response to elevated pCO_2. Further studies are required to understand the potential role of sulfur metabolism in synthesis of sulfonated PSP analogues.

These findings demonstrate that *Alexandrium* responds to elevated pCO_2, and that these responses may be influenced by other co-occurring environmental changes. With an increasing number of reports on HAB events, there is a great need to improve our understanding of the impacts of global change on toxin synthesis (Fu et al. 2012). However, the increase in HAB reports may reflect, in part at least, a greater awareness of such blooms due to the increase in shellfish farming and the requirement for greater monitoring effort, as opposed to a major increase in such blooms per se (Hallegraeff 2010). With our data, we can clearly show that N availability may strongly modulate the responses in PSP toxin content to elevated pCO_2. At the same time, however, the increase in toxin content under N limitation and elevated pCO_2 was accompanied by a reduction in population densities (Fig. 1A). This implies that, under global change, the increase in PSP toxin quota or relative toxicity (Fig. 2) may be counteracted by a reduction in population densities. Obviously, the toxicity of natural *Alexandrium* blooms in a high-CO_2 and nutrient-depleted ocean is also determined by other factors, including light and temperature. Multifactorial experiments are therefore needed to fully elucidate the impacts of global change on the quota and composition of PSP toxins.

Ecological consequences

The observed combined effects of elevated pCO_2 and N limitation on cellular composition were accompanied by CO_2-dependent changes in N assimilation. Together with other trade-offs (e.g. in C assimilation; Eberlein et al. 2014), these changes reflect important strategies of nutrient utilization and may ultimately have contributed to niche development. The potential of producing allelopathic compounds (Cembella 2003, John et al. 2015), being mixotrophic (Jeong et al. 2005), and motile (MacIntyre et al. 1997) further represents characteristic traits, which could explain why dinoflagellates thrive well in various environments. These traits may also allow species to temporarily avoid N limitation and prevent direct relationships between biomass build-up and inorganic nutrient availability, as assessed in this study. However, the presented insights into N and C assimilation under ocean acidification combined with N limitation demonstrate that interactions therein may influence, or even improve, certain trait values. The ability of both species to invest in 'biomass quality' under elevated pCO_2 in combination with N limitation (i.e. lowered POC:PON ratios, higher chl *a*, and higher PSP toxin content in *A. fundyense*) may potentially optimize their persistence. Yet, the increase in biomass quality came at the expense of lower affinities for DIN (i.e. higher residual DIN concentrations) and subsequent lower population densities. According to theory, the residual amount of DIN in continuous culture experiments represents R^*, which is the lowest resource requirement for a species to maintain a stable population density at a given mortality or dilution rate (Tilman et al. 1982, Grover 1997). While elevated pCO_2 may optimize species persistence under N limitation, the CO_2-dependent increase in R^* hints towards a lowered competitive ability for N assimilation. Whether ocean acidification turns out to be beneficial or detrimental under N limitation therefore depends on the ecological significance of the anticipated changes in species persistence and resource requirement. The interplay with additional traits such as allelopathy, mixotrophy, and vertical migration will further influence the success of the tested dinoflagellate species, with possible consequences for the viability and toxicity of their blooms.

Acknowledgements. We thank Joaquin Baro (GEOMAR) for help with nutrient measurements and subsequent data analysis. We further acknowledge Nancy Kühne (Alfred Wegener Institute) for the assistance with toxin extraction and analysis. The work was funded by the European Community's Seventh Framework Programme (FP7/2007-2013)/ERC No. 205150 and the BIOACID II programme from the German Ministry of Education and Research.

LITERATURE CITED

Anderson DM, Glibert PM, Burkholder JM (2002) Harmful algal blooms and eutrophication: nutrient sources, composition, and consequences. Estuaries 25:704–726

Anderson DM, Alpermann TJ, Cembella AD, Collos Y, Masseret E, Montresor M (2012a) The globally distributed genus *Alexandrium*: multifaceted roles in marine ecosystems and impacts on human health. Harmful Algae 14:10–35

Anderson DM, Cembella AD, Hallegraeff GM (2012b) Progress in understanding harmful algal blooms: paradigm shifts and new technologies for research, monitoring, and management. Annu Rev Mar Sci 4:143–176

Badger MR, Andrews TJ, Whitney SM, Ludwig M, Yellowlees DC, Leggat W, Price GD (1998) The diversity and coevolution of RuBisCO, plastids, pyrenoids, and chloroplast-based CO_2-concentrating mechanisms in algae. Can J Bot 76:1052–1071

Barlow RJ (1989) Statistics: a guide to the use of statistical methods in the physical sciences, Vol 29. John Wiley & Sons, Chichester

Behrenfeld MJ, O'Malley TR, Siegel DA, McClain CR and others (2006) Climate-driven trends in contemporary ocean productivity. Nature 444:752–755

Beman JM, Chow CE, King AL, Feng Y and others (2011) Global declines in oceanic nitrification rates as a consequence of ocean acidification. Proc Natl Acad Sci USA 108:208–213

Boyer GL, Sullivan JJ, Anderson RJ, Harrison PJ, Taylor FJR (1987) Effects of nutrient limitation on toxin production and composition in the marine dinoflagellate *Protogonyaulax tamarensis*. Mar Biol 96:123–128

Brading P, Warner ME, Smith DJ, Suggett DJ (2013) Contrasting modes of inorganic carbon acquisition amongst *Symbiodinium* (Dinophyceae) phylotypes. New Phytol 200:432–442

Caldeira K, Wickett ME (2003) Anthropogenic carbon and ocean pH. Nature 425:365

Cembella AD (1998) Ecophysiology and metabolism of paralytic shellfish toxins in marine microalgae. In: Anderson DM, Cembella AD, Hallegraeff GM (eds) Physiological ecology of harmful algal blooms, Book G41. Springer-Verlag, Berlin, p 281–403

Cembella AD (2003) Chemical ecology of eukaryotic microalgae in marine ecosystems. Phycologia 42:420–447

Collos Y, Vaquer A, Souchu P (2005) Acclimation of nitrate uptake by phytoplankton to high substrate levels. J Phycol 41:466–478

Dagenais-Bellefeuille S, Morse D (2013) Putting the N in dinoflagellates. Front Microbiol 4:369

Dickson AG, Millero FJ (1987) A comparison of the equilibrium constants for the dissociation of carbonic acid in seawater media. Deep-Sea Res 34:1733–1743

Eberlein T, Van de Waal DB, Rost B (2014) Differential effects of ocean acidification on carbon acquisition in two bloom-forming dinoflagellate species. Physiol Plant 151: 468–479

Elser JJ, Bracken MES, Cleland EE, Gruner DS and others (2007) Global analysis of nitrogen and phosphorus limitation of primary producers in freshwater, marine and terrestrial ecosystems. Ecol Lett 10:1135–1142

Feng Y, Warner ME, Zhang Y, Sun J, Fu FX, Hutchins DA (2008) Interactive effects of increased pCO_2, temperature and irradiance on the marine coccolithophore *Emiliania huxleyi* (Prymnesiophyceae). Eur J Phycol 43: 87–98

Fersht AR (1974) Catalysis, binding and enzyme-substrate complementarity. Proc R Soc Lond B 187:397–407

Fistarol GO, Legrand C, Rengefors K, Granéli E (2004) Temporary cyst formation in phytoplankton: a response to allelopathic competitors? Environ Microbiol 6:791–798

Flynn KJ (1991) Algal carbon-nitrogen metabolism: a biochemical basis for modelling the interactions between nitrate and ammonium uptake. J Plankton Res 13: 373–387

Fu FX, Warner ME, Zhang Y, Feng Y, Hutchins DA (2007) Effects of increased temperature and CO_2 on photosynthesis, growth, and elemental ratios in marine *Synechococcus* and *Prochlorococcus* (cyanobacteria). J Phycol 43:485–496

Fu FX, Zhang Y, Warner ME, Feng Y, Sun J, Hutchins DA (2008) A comparison of future increased CO_2 and temperature effects on sympatric *Heterosigma akashiwo* and *Prorocentrum minimum*. Harmful Algae 7:76–90

Fu FX, Tatters AO, Hutchins DA (2012) Global change and the future of harmful algal blooms in the ocean. Mar Ecol Prog Ser 470:207–233

Fuentes-Grünewald C, Garcés E, Alacid E, Sampedro E, Rossi S, Camp J (2012) Improvement of lipid production in the marine strains *Alexandrium minutum* and *Heterosigma akashiwo* by utilizing abiotic parameters. J Ind Microbiol Biot 39:207–216

Gao K, Xu J, Gao G, Li Y and others (2013) Rising CO_2 and increased light exposure synergistically reduce marine primary productivity. Nat Clim Change 2:519–523

Giordano M, Beardall J, Raven JA (2005) CO_2 concentrating mechanisms in algae: mechanisms, environmental modulation, and evolution. Annu Rev Plant Biol 56:99–131

Granéli E, Turner JT (2006) Ecology of harmful algae. Springer Verlag, Berlin

Grover JP (1997) Resource competition. Chapman & Hall, London

Guillard RRL, Ryther JH (1962) Studies of marine planktonic diatoms: I. *Cyclotella nana* Hustedt, and *Detonula confervacea* Cleve. Can J Microbiol 8:229–239

Hallegraeff GM (2010) Ocean climate change, phytoplankton community responses, and harmful algal blooms: a formidable predictive challenge. J Phycol 46:220–235

Hattenrath-Lehmann TK, Smith JL, Wallace RB, Merlo LR and others (2015) The effects of elevated CO_2 on the growth and toxicity of field populations and cultures of the saxitoxin-producing dinoflagellate, *Alexandrium fundyense*. Limnol Oceanogr 60:198–214

Hayes AF, Matthes J (2009) Computational procedures for probing interactions in OLS and logistic regression: SPSS and SAS implementations. Behav Res Meth 41:924–936

Hennon GMM, Quay P, Morales RL, Swanson LM, Armbrust EV (2014) Acclimation conditions modify physiological response of the diatom *Thalassiosira pseudonana* to ele-

vated CO_2 concentrations in a nitrate-limited chemostat. J Phycol 50:243–253

Hutchins DA, Mulholland MR, Fu FX (2009) Nutrient cycles and marine microbes in a CO_2-enriched ocean. Oceanography 22:128–145

IPCC (Intergovernmental Panel on Climate Change) (2013) Climate change 2013: the physical science basis. In: Stocker TF, Qin D, Plattner GK, Tignor M and others (eds) Working Group 1 contribution to the Fifth Assessment Report of the Intergovernmental Panel on Climate Change. Cambridge University Press, Cambridge

Jeong HJ, Yoo YD, Park JY, Song JY and others (2005) Feeding by phototrophic red-tide dinoflagellates: five species newly revealed and six species previously known to be mixotrophic. Aquat Microb Ecol 40:133–150

John U, Litaker RW, Montresor M, Murray S, Brosnahan ML, Anderson DM (2014) Formal revision of the *Alexandrium tamarense* species complex (Dinophyceae) taxonomy: the introduction of five species with emphasis on molecular-based (rDNA) classification. Protist 165:779–804

John U, Tillmann U, Hülskötter J, Alpermann TJ, Wohlrab S, Van de Waal DB (2015) Intraspecific facilitation by allelochemical mediated grazing protection within a toxigenic dinoflagellate population. Proc R Soc Lond B 282: 20141268

Johnson PO, Neyman J (1936) Tests of certain linear hypotheses and their application to some educational problems. Stat Res Mem 1:57–93

Knap A, Michaels A, Close A, Ducklow H, Dickson AG (eds) (1996) Protocols for the Joint Global Ocean Flux Study (JGOFS) core measurements. JGOFS Report No. 19, IOC Manuals and Guides, UNESCO, Bergen

Kremp A, Godhe A, Egardt J, Dupont S, Suikkanen S, Casabianca S, Penna A (2012) Intraspecific variability in the response of bloom-forming marine microalgae to changed climate conditions. Ecol Evol 2:1195–1207

Krock B, Seguel CG, Cembella AD (2007) Toxin profile of *Alexandrium catenella* from the Chilean coast as determined by liquid chromatography with fluorescence detection and liquid chromatography coupled with tandem mass spectrometry. Harmful Algae 6:734–744

Leong SCY, Taguchi S (2004) Response of the dinoflagellate *Alexandrium tamarense* to a range of nitrogen sources and concentrations: growth rate, chemical carbon and nitrogen, and pigments. Hydrobiologia 515:215–224

Leong SCY, Maekawa M, Taguchi S (2010) Carbon and nitrogen acquisition by the toxic dinoflagellate *Alexandrium tamarense* in response to different nitrogen sources and supply modes. Harmful Algae 9:48–58

Li W, Gao K, Beardall J (2012) Interactive effects of ocean acidification and nitrogen-limitation on the diatom *Phaeodactylum tricornutum*. PLoS ONE 7:e51590

Litchman E, Klausmeier CA, Schofield OM, Falkowski PG (2007) The role of functional traits and trade-offs in structuring phytoplankton communities: scaling from cellular to ecosystem level. Ecol Lett 10:1170–1181

MacIntyre JG, Cullen JJ, Cembella AD (1997) Vertical migration, nutrition and toxicity in the dinoflagellate *Alexandrium tamarense*. Mar Ecol Prog Ser 148:201–216

McCollin T, Lichtman D, Bresnan E, Berx B (2011) A study of phytoplankton communities along a hydrographic transect on the north east coast of Scotland. Marine Scotland Science Report 04/11, Marine Scotland, Aberdeen

Mehrbach C, Culberson CH, Hawley JE, Pytkowicz RM (1973) Measurement of the apparent dissociation constants of carbonic acid in seawater at atmospheric pressure. Limnol Oceanogr 18:897–907

Melzner F, Thomsen J, Koeve W, Oschlies A and others (2013) Future ocean acidification will be amplified by hypoxia in coastal habitats. Mar Biol 160:1875–1888

Monod J (1949) The growth of bacterial cultures. Annu Rev Microbiol 3:371–394

Moore CM, Mills MM, Arrigo KR, Berman-Frank I and others (2013) Processes and patterns of oceanic nutrient limitation. Nat Geosci 6:701–710

Morse D, Salois P, Markovic P, Hastings JW (1995) A nuclear-encoded form II RuBisCO in dinoflagellates. Science 268:1622–1624

Müller MN, Beaufort L, Bernard O, Pedrotti ML, Talec A, Sciandra A (2012) Influence of CO_2 and nitrogen limitation on the coccolith volume of *Emiliania huxleyi* (Haptophyta). Biogeosciences 9:4155–4167

Paasche E, Bryceson I, Tangen K (1984) Interspecific variation in dark nitrogen uptake by dinoflagellates. J Phycol 20:394–401

Patey MD, Rijkenberg MJA, Statham PJ, Mowlem M, Stinchcombe MC, Achterberg EP (2008) Determination of nitrate and phosphate in seawater at nanomolar concentrations. Trends Anal Chem 27:169–182

Pierrot DE, Lewis E, Wallace DWR (2006) MS Excel program developed for CO_2 system calculations. Carbon Dioxide Information Analysis Center, Oak Ridge National Laboratory, Oak Ridge, TN. http://cdiac.ornl.gov/oceans/co2rprt.html

Ratti S, Giordano M, Morse D (2007) CO_2-concentrating mechanisms of the potentially toxic dinoflagellate *Protoceratium reticulatum* (Dinophyceae, Gonyaulacales). J Phycol 43:693–701

Rawlings JO, Pantula SG, Dickey DA (1998) Applied regression analysis, 2nd edn. Springer-Verlag, New York, NY

Rokitta SD, Rost B (2012) Effects of CO_2 and their modulation by light in the life-cycle stages of the coccolithophore *Emiliania huxleyi*. Limnol Oceanogr 57:607–618

Rost B, Riebesell U (2004) Coccolithophores and the biological pump: responses to environmental changes. In: Thierstein HR, Young JR (eds) Coccolithophores: from molecular processes to global impact. Springer, Berlin, p 99–125

Rost B, Richter KU, Riebesell U, Hansen PJ (2006) Inorganic carbon acquisition in red tide dinoflagellates. Plant Cell Environ 29:810–822

Rost B, Zondervan I, Wolf-Gladrow D (2008) Sensitivity of phytoplankton to future changes in ocean carbonate chemistry: current knowledge, contradictions and research directions. Mar Ecol Prog Ser 373:227–237

Rouco M, Branson O, Lebrato M, Iglesias-Rodríguez MD (2013) The effect of nitrate and phosphate availability on *Emiliania huxleyi* (NZEH) physiology under different CO_2 scenarios. Front Microbiol 4:155

Sarmiento JL, Slater R, Barber R, Bopp L and others (2004) Response of ocean ecosystems to climate warming. Global Biogeochem Cycles 18:GB3003, doi:10.1029/2003GB002134

Sciandra A, Harlay J, Lefèvre D, Lemée R, Rimmelin P, Denis M, Gattuso JP (2003) Response of coccolithophorid *Emiliania huxleyi* to elevated partial pressure of CO_2 under nitrogen limitation. Mar Ecol Prog Ser 261: 111–122

Shimizu Y (1996) Microalgal metabolites: a new perspective. Annu Rev Microbiol 50:431–465

Tatters AO, Flewelling LJ, Fu FX, Granholm AA, Hutchins DA (2013) High CO_2 promotes the production of paralytic shellfish poisoning toxins by *Alexandrium catenella* from southern California waters. Harmful Algae 30: 37–43

Tillmann U, Alpermann TL, da Purificacao RC, Krock B, Cembella AD (2009) Intra-population clonal variability in allelochemical potency of the toxigenic dinoflagellate *Alexandrium tamarense*. Harmful Algae 8:759–769

Tilman D, Kilham SS, Kilham P (1982) Phytoplankton community ecology: the role of limiting nutrients. Annu Rev Ecol Syst 13:349–372

Turpin DH (1991) Effects of inorganic N availability on algal photosynthesis and carbon metabolism. J Phycol 27: 14–20

Van de Waal DB, Tillmann U, Zhu M, Koch BP, Rost B, John U (2013) Nutrient pulse induces dynamic changes in cellular C:N:P, amino acids, and paralytic shellfish poisoning toxins in *Alexandrium tamarense*. Mar Ecol Prog Ser 493:57–69

Van de Waal DB, Eberlein T, John U, Wohlrab S, Rost B (2014a) Impact of elevated pCO_2 on paralytic shellfish poisoning toxin content and composition in *Alexandrium tamarense*. Toxicon 78:58–67

Van de Waal DB, Smith VH, Declerck SAJ, Stam ECM, Elser JJ (2014b) Stoichiometric regulation of phytoplankton toxins. Ecol Lett 17:736–742

Van de Waal DB, Eberlein T, Bublitz Y, John U, Rost B (2014c) Shake it easy: a gently mixed continuous culture system for dinoflagellates. J Plankton Res 36:889–894

Verspagen JMH, Van de Waal DB, Finke JF, Visser PM, Huisman J (2014) Contrasting effects of rising CO_2 on primary production and ecological stoichiometry at different nutrient levels. Ecol Lett 17:951–960

Wallace RB, Baumann H, Grear JS, Aller RC, Gobler CJ (2014) Coastal ocean acidification: the other eutrophication problem. Estuar Coast Shelf Sci 148:1–13

Wiese M, D'Agostino PM, Mihali TK, Moffitt MC, Neilan BA (2010) Neurotoxic alkaloids: saxitoxin and its analogs. Mar Drugs 8:2185–2211

Wyatt T, Jenkinson IR (1997) Notes on *Alexandrium* population dynamics. J Plankton Res 19:551–575

Editorial responsibility: Graham Savidge, Portaferry, UK

Submitted: June 24, 2015; Accepted: November 20, 2015
Proofs received from author(s): January 12, 2016

2.4 Publication III

Effects of ocean acidification on primary production in a coastal North Sea phytoplankton community *(accepted for PLoS ONE)*

T. Eberlein [1,*], S. Wohlrab[1], B. Rost[1], U. John[1,2], L. T. Bach[3], U. Riebesell[3], and D. B. Van de Waal[1,4].

[1]Alfred Wegener Institute, Helmholtz Centre for Polar and Marine Research, Am Handelshafen 12, 27570 Bremerhaven, Germany

[2]Helmholtz Institute for Functional Marine Biodiversity Oldenburg (HIFMB), Carl von Ossietzky Straße, D-26129 Oldenburg Germany

[3]GEOMAR Helmholtz Centre for Ocean Research Kiel, Düsternbrooker Weg 20, 24105 Kiel, Germany

[4]Netherlands Institute of Ecology (NIOO-KNAW), PO Box 50, 6700 AB, Wageningen, The Netherlands

* Corresponding author: tim.eberlein@rub.de

Keywords: Phytoplankton succession, nutrient limitation, photoacclimation

Abstract

We studied the effect of ocean acidification (OA) on a coastal North Sea plankton community in a long-term mesocosm CO_2-enrichment experiment. This BIOACID II long-term mesocosm study was conducted from March to July 2013, for which 10 mesocosms of 19 m length with a volume of 47.5 to 55.9 m^3 were deployed in the Gullmar Fjord, Sweden. CO_2 concentrations were enriched in five mesocosms to reach average CO_2 partial pressures (pCO_2) of 760 µatm. The remaining five mesocosms were used as control at ambient pCO_2 of 380 µatm. Our paper is part of a PLOS collection about this experiment. Here, we tested the effect of OA on total primary production (PP_T) by performing ^{14}C-based bottle incubations for 24 h. Furthermore, photoacclimation was assessed by conducting ^{14}C-based photosynthesis-irradiance response (P/I) curves. Changes in chlorophyll *a* concentrations over time were reflected in the development of PP_T, and showed higher phytoplankton biomass build-up under OA. We observed two subsequent phytoplankton blooms in all mesocosms, with peaks in PP_T around day 33 and day 56. OA had no significant effect on PP_T, except for a marginal increase during the second phytoplankton bloom when inorganic nutrients were already depleted. Maximum light use efficiencies and light saturation indices calculated from the P/I curves changed simultaneously in all mesocosms, and suggest that OA did not alter phytoplankton photoacclimation. Despite large variability in time-integrated productivity estimates among replicates, our overall results indicate that coastal phytoplankton communities can be affected by OA at certain times of the seasonal succession with potential consequences for ecosystem functioning.

Introduction

Atmospheric CO_2 partial pressure (pCO_2) is currently rising at an unprecedented rate due to anthropogenic activities. This leads to enhanced CO_2 uptake by the oceans and a decrease in ocean surface water pH, referred to as ocean acidification (OA) [1,2]. From 1765 until 1994, pH values were calculated to have already decreased by 0.08 units. Present-day CO_2 concentrations of around 400 µatm are predicted to more than double by the year 2100, which will result in a further acidification of the ocean [3]. After the Polar Oceans, the North Atlantic is expected to show strongest changes in response to rising pCO_2 [3,4]. As a major sink of anthropogenic CO_2, the North Atlantic Ocean basin stores almost a quarter of the global oceanic anthropogenic CO_2, although covering only 15% of the global ocean area [5]. The projected changes in ocean carbonate chemistry may thus not only have strong effects on the marine biota, but also on the oceanic carbon cycling.

Phytoplankton take up inorganic carbon (C_i) in the photic zone and fix it into organic compounds, thereby providing a carbon and energy source for higher trophic levels. The key enzyme of carbon fixation, the CO_2-binding enzyme Ribulose 1,5-bisphosphate Carboxylase/Oxygenase (RubisCO), exhibits a generally low affinity for its substrate CO_2 [6-8]. To avoid C_i limitation, many phytoplankton species operate carbon concentrating mechanisms (CCMs) [9,10]. The efficiency in CO_2 fixation depends on both the type of RubisCO as well as the mode of CCMs so that the response of phytoplankton to OA cannot be generalized across taxa [11-13]. Various studies have provided mechanistic insights into the CO_2-dependent regulation of CCMs and thus CO_2 fixation over a range of phytoplankton species [e.g. 14-16]. Besides species-specific differences, also strains of the same species may respond differently [e.g. 17-19], which further complicates predictions on OA-driven changes in primary production.

To test these effects directly, numerous studies have exposed natural phytoplankton communities to high pCO_2, either in bottle incubations or mesocosms, often finding higher rates of CO_2 fixation under OA [20]. In these experiments, which lasted only a couple of days up to a month, the effects were yet relatively small. Here, we investigated the impact of OA on primary production by a natural phytoplankton community over an entire winter-to-summer succession. Experiments were performed in large scale mesocosms, deployed in the Gullmar Fjord located in Southwest Sweden at the Skagerrak coast in 2013 [21]. Depending on the wind direction and tides, the fjord consists of high saline bottom water from the North Atlantic, a low salinity thin surface layer fed with water from the river Örekil, and in between a layer fed by the Baltic current. Monitoring data from over 100 years have shown that the phytoplankton spring community in the Gullmar Fjord is typically dominated by diatoms, whereas summer blooms often comprise dinoflagellates [22,23]. We assessed primary production of the phytoplankton community from the mesocosms as well as the fjord by applying ^{14}C incubations over 24 h [24]. We furthermore assessed the light dependency of CO_2 fixation by performing photosynthesis-irradiance response curves in short incubations (80 min.).

Material and methods

The KOSMOS 2013 mesocosm experiment was performed in the Gullmar Fjord (Kristineberg, Sweden) from March until July 2013 as part of the project BIOACID (Biological Impacts of Ocean ACIDification) phase II. Ten mesocosms were deployed near Kristineberg, with permission from the Sven Lovén Centre for Marine Infrastructure. The mesocosms were cylindrical polyurethane bags with a 2 m diameter mounted in a floatation frame [25]. The bags reached a depth of 17 m and were closed at the bottom with a 2 m long conical sediment trap [26]. Two days prior to the experiment (i.e. t-2), a water body was enclosed inside the mesocosms by lifting the upper end about one meter above the surface.

All mesocosms had a salinity of about 29, and nitrate, phosphate and silicate concentrations of about 7, 0.8, and 10 µmol L^{-1}, respectively. CO_2 enrichment was conducted on t-1 and t0, for which sterile-filtered and CO_2-saturated seawater from the Gullmar Fjord was added to five mesocosms (M2, M4, M6, M7, M8). The remaining five mesocosms (M1, M3, M5, M9, M10) were treated as controls and received no CO_2-enriched seawater. Average pCO_2 (based on dissolved inorganic carbon (DIC) and spectrophotometric pH_T measurements) in the 'low' and 'high' CO_2 treatments were about 380 and 760 µatm, respectively. The systems were open and allowed a gas exchange at the sea surface. To account for CO_2 losses to the atmosphere by outgassing and for CO_2 consumption by primary production, CO_2 was added on a regular basis to the 'high' CO_2 treatments. As a consequence, CO_2 concentrations remained above the control treatment at all times (for more details see [21]). Sampling of seawater from each mesocosm was done with a depth-integrated water sampler (Hydro-Bios). After initial sampling on t0 and t1, samples were taken every other day until t109 (i.e. t3, t5, t7 etc.). For further information on the

design and set-up of the experiment, as well as the CO_2 perturbation and sampling techniques, we refer to [21].

Sampling for primary production

For our measurements, integrated water samples from 0–17 m depth were taken in a four day interval (i.e. t1, t5, t9, etc.) from each of the ten mesocosms, and an additional sample was taken from the fjord. Sampling usually took place between 9 and 12 a.m. and aliquots from well mixed water samples were filled in gas-tight and headspace-free bottles (Schott) of 250 mL (for the 24 h incubations) and 500 mL (for the photosynthesis-irradiance response (P/I) curves). Samples were brought directly to the laboratory, where they were gently filtered over a 500 µm mesh-size filter to remove larger zooplankton from the samples, and were kept at the *in situ* water temperature until incubations started. Over the course of the entire experiment, the temperature in the fjord increased from 1.5 °C at t1 towards 15.5 °C at t109, and we adjusted the incubation temperatures accordingly (Fig. 1A). Only at the beginning of the experiment, when productivity and biomass was still low, we could not fully match the temperature from the fjord as our incubator was not able to maintain temperatures below 4 °C. Light was provided by daylight tubes (OSRAM) from the side in a 16:8 h light-dark cycle. To account for the increase in light intensities over the course of the experiment in the mesocosms, the light intensity was stepwise increased in the incubator (Fig. 1B). Using a spherical micro quantum sensor (Walz), we increased the photon flux density (PFD) every 16 days (i.e. after 4 sampling days) by about 20 µmol photons m^{-2} s^{-1}, starting with around 100 µmol photons m^{-2} s^{-1} at t1 and ending with 240 µmol photons m^{-2} s^{-1} at t109.

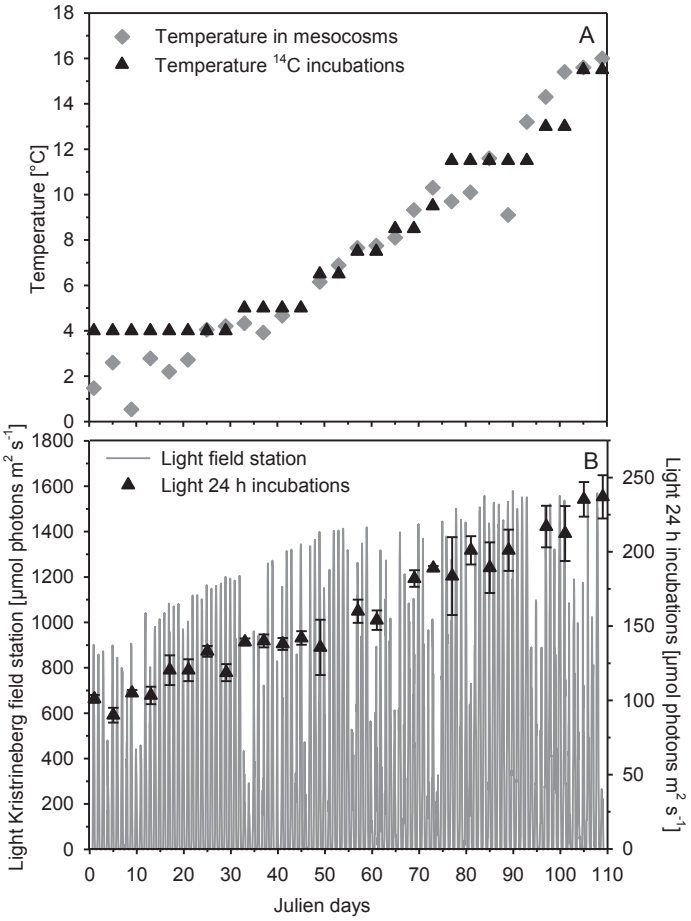

Fig. 1. Mean temperature in mesocosms (grey diamonds) and during ^{14}C incubations (black triangles) (A), and incoming light (PAR) at the Kristineberg field station around midday (http://www.weather.loven.gu.se/kristineberg/en; grey lines) and during ^{14}C-based 24 h incubations (black triangles) (B). Triangles indicate the mean ± SD of three light measurements from the bottom, middle and top of a representative incubation vial.

Primary production measurements

Primary production experiments did not involve endangered or protected species. Primary productivity was measured according to Steeman Nielsen [24]. Despite limitations [27], this approach has remained the method of choice, especially for field work, as it allows assessing rates even at times of low productivity. One has to keep in mind, however, that measured rates have different meanings depending on the incubation time [27]. In our 80 min. incubations for

^{14}C-based photosynthesis-irradiance response (P/I) curves, we obtained rates of gross primary production because there is only little loss of incorporated ^{14}C via respiration and exudation over such short timescales. In our 24 h incubations for the ^{14}C-based primary production measurements, respiration lowers the ^{14}C incorporation and thus net rates of primary production are obtained. To account for fixed ^{14}C ending up in the dissolved phase, which can be a significant proportion under nutrient deplete conditions, we included values of the filtrate in our PP_T estimates.

^{14}C-based primary production measurements

For the 24 h incubations, 40 mL sample volumes were spiked with 20 µL of ^{14}C-labeled sodium bicarbonate ($NaH^{14}CO_3$; from a 1 mCi mL^{-1} = 37 MBq mL^{-1} stock solution; PerkinElmer). Two incubation vials for each mesocosm, and the fjord water, were prepared accordingly (i.e. 22 vials in total, of which 11 were used for the light and the remaining 11 for the dark incubations). Determination of total ^{14}C-spike addition was done from an extra 40 mL ^{14}C-spiked water sample. For this purpose, 1 mL was directly transferred into a 20 mL scintillation vial (PerkinElmer) containing 10 mL scintillation cocktail (Ultima Gold AB; PerkinElmer) and counted in a liquid scintillation analyzer (Beckman LS6500). Blank determination was done by transferring 1 mL from the extra ^{14}C-spiked water sample into 6 mL of 6 M HCl, which degassed for 48 h and was then counted after adding 10 mL scintillation cocktail. All incubations were placed on an orbital shaker in a temperature-controlled incubator.

Incubations were stopped after 24 h by vacuum filtration onto GF/F filters (Whatman). To estimate the amount of C_i fixation into particulate organic carbon (POC), filters were rinsed twice with 20 mL of sterile filtered seawater (0.2 µm), and subsequently placed in scintillation vials containing 300 µL of 3 M HCl to remove ^{14}C-labeled DIC. To estimate the amount of C_i fixation

ending up in the pool of dissolved organic carbon (DOC), 6 mL of filtrate was transferred into a scintillation vial, acidified with 1 mL 6 M HCl, and placed under a fume hood for 48 hours for degassing DI^{14}C. Prior to measurements, 10 mL of scintillation cocktail was added to each vial and filter, thoroughly mixed, and counted in a liquid scintillation analyzer. Primary production (PP) was calculated according to:

$$PP = \frac{DIC \cdot (DPM_{sample} - DPM_{blank}) \cdot 1.05}{(DPM_{100\%} \cdot t)} \quad \text{eq. 1}$$

where *DPM* represents the decays per minute and *t* represents time. Correction for non-specific ^{14}C fixation in the dark was done by subtracting dark incubations from light incubations. Dark ^{14}C fixation accounted for about 1 to 6 % of the light incubations during times of high and low productivity, respectively. Based on the phytoplankton community composition [21], some primary producers were smaller than the pore size of our filters (i.e. <0.7 µm). We therefore reported total primary production (PP_T; µmol C L^{-1} h^{-1}) from the 24 h incubations as the sum of CO_2 fixation into POC and DOC.

^{14}C-based photosynthesis-irradiance response curves

For the photosynthesis-irradiance response (P/I) curves, 300 mL sample volume from each mesocosm was spiked with 100 µCi of $NaH^{14}CO_3^-$ (PerkinElmer) and subdivided into seven 40 mL glass vials. From the remaining ^{14}C-spiked seawater, 200 µL aliquots were transferred into a 10 mL scintillation cocktail to determine total spike addition for each P/I curve. While one vial was incubated in the dark, the six remaining vials were exposed to increased light intensities ranging from about 10 to 700 µmol photons m^{-2} s^{-1} in a custom-made photosynthetron. Light was supplied from below and the PFD was assessed prior to each experimental day. The photosynthetron was placed in the same incubator as the 24 h incubations. Additional

temperature control was achieved via a water bath connected to the sample holder. After an incubation time of 80 min. at the respective light conditions, samples were filtered on GF/F filters (Whatman). Analysis of $PO^{14}C$ was determined following the same procedure as for the 24 h incubations and data was fitted according to:

$$PP_{P/I} = P_{max} \cdot (1 - e^{-\alpha \cdot (I - I_k)}) \quad \text{eq. 2}$$

where P_{max} is the light-saturated rate of photosynthesis, α is the light-limited (i.e. initial) slope of the P/I curve representing the maximum light-use efficiency, I is the irradiance, and I_k is the light saturation index. Rates of $PP_{P/I}$ were normalized to chlorophyll *a* (Chl *a*) concentrations in the samples from the particular day and mesocosm [21].

Statistics

Differences in PP_T, Chl *a*, P_{max}, I_k and α between the CO_2 treatments were tested over time by a two-way repeated measures Analysis of Variance (rmANOVA), and the association between PP_T and Chl *a* was tested by Pearson product-moment correlations. Variables were log+1 or square root transformed if this improved normality or homogeneity of variances, as tested by the Shapiro-Wilk test or Levene's test, respectively. All statistics were performed with Sigmaplot 12.5 (Systat).

Results

Total primary production

For the first three weeks of the experiment, estimates on PP_T were lower in the mesocosms than in the fjord (Fig. 2A). All mesocosms showed comparable development in PP_T, with an initial period of low productivity (phase I, t1-t16), a first spring bloom of highest productivity around

t33 (phase II, t17-t40), followed by a second bloom of highest productivity around t57 (phase III, t41-77), and a subsequent period of low productivity until the end of the experiment (phase IV, t78-t109; Fig. 2A, Table 1). Dynamics in primary production in the mesocosms differed from that in the fjord. For example, PP_T was higher in the fjord during phase I, while PP_T was higher in the mesocosms during phase II. Also, a small increase in PP_T present in the fjord at the start of phase IV was lacking in the mesocosms (Fig. 2A).

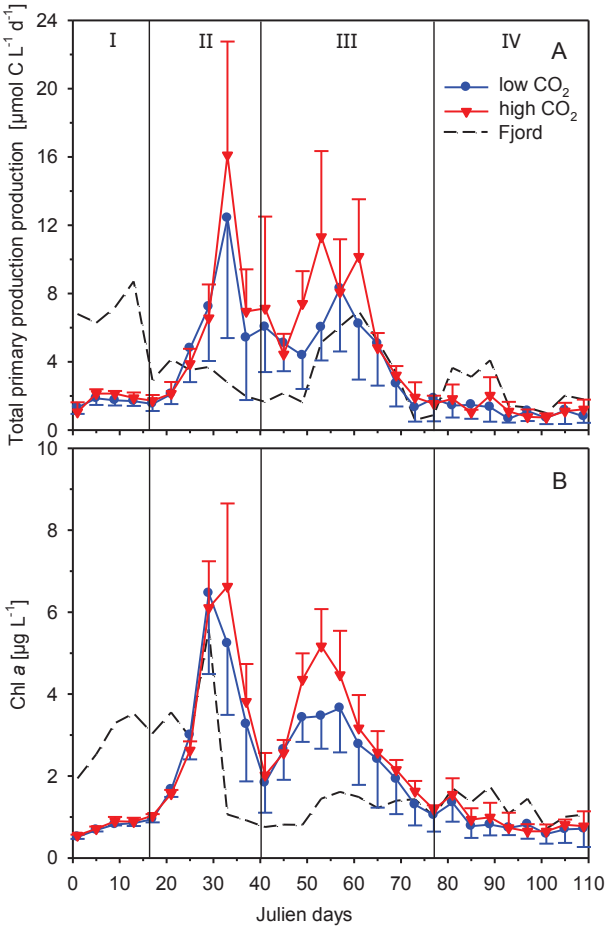

Fig. 2. Mean values of total primary production (from ^{14}C-based 24 h incubations; A) and chlorophyll *a* concentrations (B) from mesocosm and fjord samples. Triangles (red; high pCO_2) and circles (blue; low pCO_2) represent the mean ± SD of five biological replicates. Roman numbers denote the different phases of the experiment.

Table 1. Total primary production (µmol C L^{-1} d^{-1}) in the mesocosms derived from 24 h incubations. Values at high pCO_2 are indicated in bold letters (M2, M4, M6-8). Grey shading indicates the peak of the two bloom phases.

Julien day	M1	**M2**	M3	**M4**	M5	**M6**	**M7**	**M8**	M9	M10
1	1.88	**1.34**	0.85	**1.42**	1.44	**1.46**	**0.95**	**0.08**	1.16	1.28
5	1.75	**1.97**	1.29	**2.04**	2.15	**2.58**	**2.12**	**1.96**	1.82	2.26
9	1.96	**2.16**	1.25	**2.30**	1.93	**2.27**	**1.96**	**2.01**	1.93	1.65
13	1.69	**1.60**	1.26	**2.22**	2.02	**2.22**	**1.81**	**1.57**	1.80	1.68
17	1.48	**1.53**	1.83	**1.48**	0.85	**1.43**	**2.13**	**2.03**	1.88	1.61
21	2.63	**2.15**	2.04	**2.46**	1.77	**3.07**	**1.34**	**1.66**	1.34	2.72
25	6.08	**4.60**	2.81	**4.22**	2.65	**2.92**	**4.70**	**2.98**	5.34	7.05
29	9.48	**6.88**	4.68	**8.39**	3.27	**6.45**	**7.77**	**3.30**	7.88	10.79
33	15.94	**5.04**	4.92	**22.40**	13.20	**15.47**	**18.89**	**18.73**	6.16	21.83
37	7.70	**3.40**	3.29	**9.70**	4.05	**7.62**	**8.37**	**5.65**	1.45	10.47
41	8.91	**3.08**	5.25	**16.59**	2.02	**5.11**	**5.17**	**5.68**	6.32	7.65
45	5.10	**2.73**	6.98	**5.25**	2.50	**5.48**	**5.07**	**3.66**	5.14	5.70
49	5.65	**8.65**	2.45	**8.10**	3.43	**8.60**	**4.10**	**7.59**	3.16	7.15
53	9.01	**4.90**	4.93	**14.08**	5.80	**12.51**	**17.43**	**7.65**	3.89	6.41
57	9.69	**6.15**	3.91	**9.96**	9.95	**10.87**	**9.84**	**3.59**	12.80	5.10
61	6.77	**7.60**	2.78	**13.59**	3.42	**6.64**	**13.83**	**9.15**	7.24	10.85
65	5.77	**4.71**	1.24	**4.10**	4.49	**6.21**	**4.98**	**4.08**	5.90	7.90
69	3.13	**2.54**	1.06	**3.80**	1.85	**2.83**	**3.69**	**3.17**	4.55	2.97
73	1.05	**1.75**	0.69	**1.71**	0.65	**1.84**	**3.36**	**0.92**	1.58	2.62
77	3.68	**0.90**	0.85	**1.94**	0.53	**1.97**	**1.70**	**1.22**	1.41	2.77
81	2.40	**0.39**	0.72	**2.05**	0.86	**1.93**	**2.41**	**2.40**	1.36	1.79
85	2.16	**1.28**	1.35	**0.88**	0.75	**0.98**	**1.07**	**1.01**	0.65	2.49
89	1.10	**1.13**	1.02	**1.52**	1.08	**1.40**	**3.74**	**2.37**	0.67	2.83
93	0.29	**0.52**	0.73	**1.23**	0.81	**0.80**	**1.98**	**0.94**	0.83	0.65
97	1.29	**0.57**	1.01	**0.43**	0.19	**0.47**	**1.44**	**0.98**	1.27	1.79
101	0.83	**0.63**	0.41	**1.02**	1.30	**0.64**	**0.44**	**0.95**	0.50	0.52
105	0.78	**0.85**	1.91	**0.99**	2.11	**1.98**	**0.86**	**0.85**	0.35	0.62
109	1.05	**1.65**	0.48	**0.65**	1.34	**0.54**	**1.63**	**1.60**	0.48	0.66

High pCO_2 yielded higher mean estimates on PP_T during both blooms, although differences during both blooms were not significant (Table 2). Highest PP_T was observed during the first bloom at t33, with up to 16.1 ± 6.7 µmol C L^{-1} d^{-1} at high pCO_2 and 12.4 ± 7.0 µmol C L^{-1} d^{-1} at low pCO_2. During the second bloom, PP_T amounted to highest values of 11.3 ± 5.0 µmol C L^{-1}

d^{-1} at t53 for high pCO_2, and 6.0 ± 1.9 µmol C L^{-1} d^{-1} at day t57 for low pCO_2. At the peak of the second bloom, PP_T appeared to be higher at high pCO_2, though this difference was marginally significant and dependent on time (Table 2; rmANOVA, Time x CO_2 treatment, P=0.098). During both blooms phases, Chl *a* remained unaltered in response to OA (Table 2), though at times showed higher concentrations at high pCO_2 [21]. Furthermore, Chl *a* was strongly correlated to PP_T ($\sigma = 0.87$, $P < 0.0001$).

Table 2. Output of the repeated measures ANOVA for phase II, phase III, peak of bloom 1 and peak of bloom 2, with degrees of freedom (df), the *F*-value and the *P*-value. Significant outcomes are indicated with P < 0.001 (***), P < 0.01 (**), P < 0.05 (*) and P < 0.1 (·).

	Parameter	Effect	df	*F*	*P*
Phase II (incl. bloom 1; t17-t40)	PP_T (µmol C L^{-1} d^{-1})	CO_2 treatment	1	0.278	0.612
		Time	5	38.060	<0.001***
		Time x CO_2 treatment	5	0.814	0.547
	Chl *a* (µg Chl *a* L^{-1})	CO_2 treatment	1	0.228	0.646
		Time	5	13.818	<0.001***
		Time x CO_2 treatment	5	0.245	0.940
	P_{max} (µg C (µg Chl *a*)$^{-1}$ h^{-1})	CO_2 treatment	1	0.845	0.383
		Time	5	15.796	<0.001***
		Time x CO_2 treatment	5	0.497	0.776
	I_K (µmol photons m^{-2} s^{-1})	CO_2 treatment	1	0.651	0.443
		Time	5	2.647	0.037*
		Time x CO_2 treatment	5	0.712	0.618
	Alpha	CO_2 treatment	1	0.023	0.883
		Time	5	10.814	<0.001***
		Time x CO_2 treatment	5	0.633	0.676
Phase III (incl. bloom 2; t41-t77)	PP_T (µmol C L^{-1} d^{-1})	CO_2 treatment	1	1.481	0.258
		Time	9	26.124	<0.001***
		Time x CO_2 treatment	9	1.566	0.142
	Chl *a* (µg Chl *a* L^{-1})	CO_2 treatment	1	0.395	0.547
		Time	9	9.258	<0.001***
		Time x CO_2 treatment	9	0.915	0.517
	P_{max} (µg C (µg Chl *a*)$^{-1}$ h^{-1})	CO_2 treatment	1	1.538	0.250
		Time	9	4.126	<0.001***
		Time x CO_2 treatment	9	0.565	0.821
	I_K (µmol photons m^{-2} s^{-1})	CO_2 treatment	1	0.181	0.681
		Time	9	4.544	<0.001***
		Time x CO_2 treatment	9	0.422	0.919
	Alpha	CO_2 treatment	1	0.767	0.407
		Time	9	6.914	<0.001***
		Time x CO_2 treatment	9	1.338	0.233
Peak of bloom 1 (t29-t33)	PP_T (µmol C L^{-1} d^{-1})	CO_2 treatment	1	0.340	0.576
		Time	1	13.682	0.006**
		Time x CO_2 treatment	1	1.194	0.306
	Chl *a* (µg Chl *a* L^{-1})	CO_2 treatment	1	0.092	0.769
		Time	1	50.114	<0.001***
		Time x CO_2 treatment	1	0.152	0.707
	P_{max} (µg C (µg Chl *a*)$^{-1}$ h^{-1})	CO_2 treatment	1	0.372	0.559
		Time	1	38.768	<0.001***
		Time x CO_2 treatment	1	0.017	0.899
	I_K (µmol photons m^{-2} s^{-1})	CO_2 treatment	1	0.858	0.381
		Time	1	0.590	0.465

		Time x CO_2 treatment	1	0.581	0.468
	Alpha	CO_2 treatment	1	0.360	0.565
		Time	1	33.248	<0.001***
		Time x CO_2 treatment	1	0.653	0.442
Peak of bloom 2 (t53-t61)	PP_T (µmol C L^{-1} d^{-1})	CO_2 treatment	1	3.134	0.115
		Time	2	0.099	0.907
		Time x CO_2 treatment	2	2.701	0.098·
	Chl *a* (µg Chl *a* L^{-1})	CO_2 treatment	1	1.200	0.305
		Time	2	2.168	0.147
		Time x CO_2 treatment	2	2.278	0.135
	P_{max} (µg C (µg Chl *a*)$^{-1}$ h^{-1})	CO_2 treatment	1	0.506	0.497
		Time	2	9.666	0.002**
		Time x CO_2 treatment	2	0.029	0.972
	I_K (µmol photons m^{-2} s^{-1})	CO_2 treatment	1	0.120	0.738
		Time	2	5.210	0.018**
		Time x CO_2 treatment	2	1.874	0.186
	Alpha	CO_2 treatment	1	0.072	0.795
		Time	2	1.366	0.283
		Time x CO_2 treatment	2	0.311	0.737

When cumulated over the experimental period of 109 days, the PP_T data yielded a total of 92 ± 29.21 and 110 ± 25.79 µmol C L^{-1} at low and high pCO_2, respectively. In the fjord, cumulative PP_T yielded 95 µmol C L^{-1} (Fig. 3A), being more comparable to PP_T in the mesocosms at low pCO_2. The difference in cumulative PP_T between low and high pCO_2 was about 20% and closely matched the observed difference in Chl *a* concentration of about 15%. Consequently, no differences in the yields were observed when normalizing cumulated PP_T to Chl *a* (as to account for changes in phytoplankton biomass). In both treatments, we observed a cumulative PP_T of around 600 µg C (µg Chl *a*)$^{-1}$ (Fig. 3B). Chl *a*-normalized cumulative PP_T in the fjord was higher than in the mesocosms and amounted to a total of about 700 µg C (µg Chl *a*)$^{-1}$ (Fig. 3B).

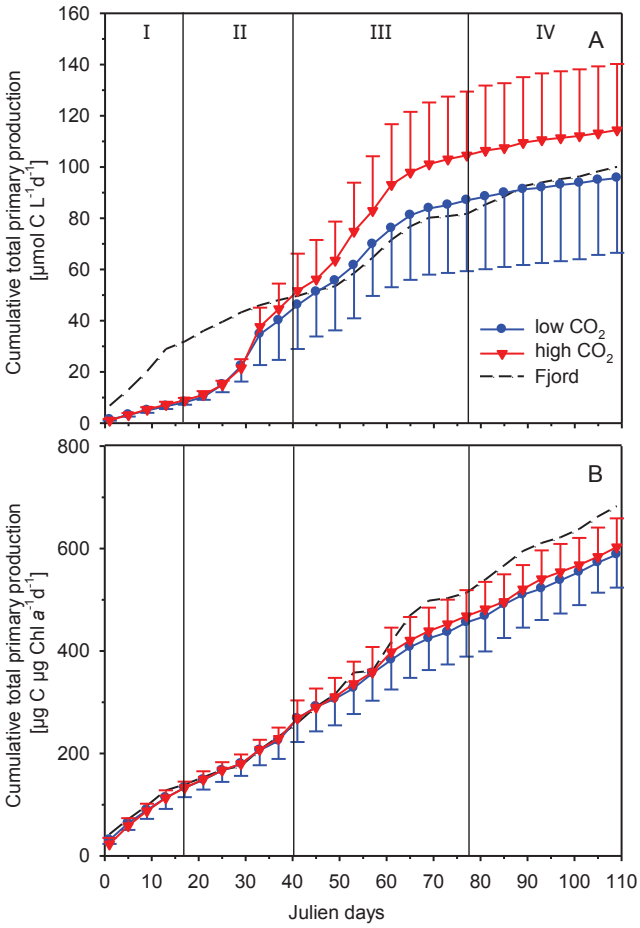

Fig. 3. Cumulative total primary production (from ^{14}C-based 24 h incubations; A) and normalized to chlorophyll *a* concentrations (B) from mesocosm and fjord samples. Triangles (red; high pCO_2) and circles (blue; low pCO_2) represent the mean ± SD of five biological replicates. Roman numbers denote the different phases of the experiment.

Photoacclimation

P/I curves provided information on the photoacclimation of the phytoplankton communities in the mesocosms and the fjord. P_{max} was on average 3.17 ± 0.54 and 3.38 ± 0.26 µg C (µg Chl *a*)$^{-1}$ h^{-1} at low and high pCO_2, respectively. There was no apparent CO_2 effect on P_{max} during both blooms (Table 2), which furthermore strongly varied between mesocosms and sampling days (Fig. 4A). I_k, indicating the light intensity at which phytoplankton shifts from light limitation to light saturation, changed over the course of the experiment (Fig. 4B). More specifically, in the

period prior to the first bloom (phase I), I_k remained around 100 µmol photons m^{-2} s^{-1} and increased towards the end of the first bloom phase reaching mean values of approximately 160 and 250 µmol photons m^{-2} s^{-1} at high and low pCO_2, respectively. In the course of the second bloom, I_k decreased resulting in lowest values of 50 µmol photons m^{-2} s^{-1} around t61 (Fig. 4), after which it increased again to values of around 150 µmol photons m^{-2} s^{-1} (Fig. 4B). Besides these general changes over the season, we did not observe a significant CO_2 effect on I_k values during both blooms (Table 2). The maximum light-use efficiency also changed in the course of the phytoplankton succession. Highest α values coincided with the phytoplankton blooms during phases II and III and were observed around t30 and t56 in all mesocosms (Fig. 4C). Similar to the other parameters, there was no significant CO_2 effect on α values during both blooms (Table 2).

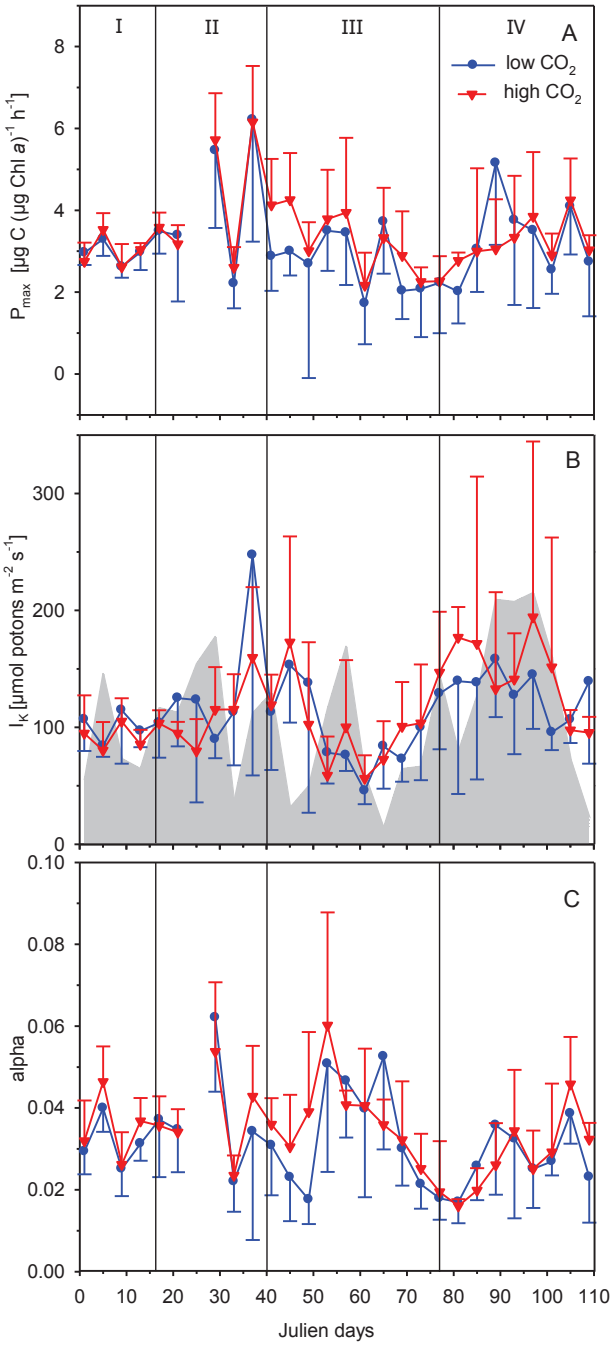

Fig. 4. Light-saturated maximum rates (P_{max}; A), light saturation index (I_k; B), and light-limited slope (alpha; C) of the photosynthesis-response irradiance curves. Triangles (high pCO_2) and circles (low pCO_2) represent the mean ± SD of five biological replicates. The grey area in Fig. B indicates average water column light intensities (0-19 m depth) during midday for all ten mesocosms. Roman numbers denote the different phases of the experiment.

Discussion

We did not observe a sustained effect of OA on primary production during the investigated winter-to-summer plankton succession. When focusing on the peak of the second spring bloom in phase III, however, PP_T showed a marginally significant increase under high pCO_2 (Table 2). During this distinct phase, the availability of inorganic nutrients was low and primary production was fueled by *in situ* remineralization [21]. Integrated over the entire experimental period, OA yielded about 20% more CO_2 fixation. Such enhanced primary production is in line with the higher Chl *a* concentration under these conditions.

At the onset of the experiment, concentrations of major nutrients in the mesocosms were higher than in the fjord (for more details, see Bach et al. [21]). The lower concentrations in the fjord were the result of higher primary production compared to the mesocosms right after closure of the mesocosms (beginning at t-2, Fig. 2). Although initial conditions in the mesocosms were largely comparable to the situation in the fjord, perturbations induced during the set-up of the mesocosms [21], e.g. the water column mixing (t0) or the establishment of CO_2 treatments (t-1 and t0), may have contributed to the delay in primary production.

In the mesocosms, PP_T as well as Chl *a* concentrations remained relatively low during phase I and started to increase more pronounced around t20, leading to a first phytoplankton bloom with highest PP_T around t33 (Fig. 2). During this phase II, major nutrients such as inorganic phosphate and nitrogen were depleted to very low values (for more details, see Bach et al. [21]). This nutrient depletion, particularly for nitrogen, together with grazing presumably caused the collapse of the phytoplankton bloom and the decrease in PP_T as well as Chl *a* concentrations (Fig. 2). At the same time at the Kristineberg field station (~3 km distance to mesocosm deployment site), a sudden drop in the *in situ* light intensity was detected (Fig. 1B), coinciding with the peak of the

first bloom (Fig. 2A). In fact, the average water column light intensities (0–19 m depth) during midday for all ten mesocosms were reduced to about 35 µmol photons m^{-2} s^{-1} for several days (Fig. 4B), and dropped below the I_k values (about 115 µmol photons m^{-2} s^{-1}). Such lower light levels may possibly have, at least temporally, limited photosynthesis and thereby affected the response of phytoplankton to low nutrient levels. While there were dynamic changes in P_{max}, I_k, and α over the course of the phytoplankton succession (Fig. 4), there was no effect of OA on photoacclimation.

Dissolved phosphate and inorganic nitrogen concentrations remained low during phase III, while PP_T and Chl *a* concentrations increased again, causing the second bloom (Fig. 2). An earlier study in the Gullmar Fjord also showed a relatively high primary production during summer months, despite low nutrient concentrations [28,29]. According to this long-term Gullmar Fjord time-series study, nutrients were not only derived from recycled production, but also from local precipitation, run-off, and input from the Kattegat [29]. As the mesocosms were isolated from the surrounding water, nutrient input for primary production should have derived from regeneration only. In fact, dissolved organic nitrogen and NH_4^+ concentrations in the mesocosms remained low, indicating a rapid cycling of nutrients in the food web [21]. Interestingly, it is under these conditions of recycled production and low concentrations of inorganic nutrients that we observed the strongest response in PP_T towards OA (Fig. 2A). Under nutrient-limited conditions, effects of elevated pCO_2 on phytoplankton productivity, standing stock and community composition were often found to be stronger [30-32] and comparable findings were also reported with respect to iron limitation [33]. Since nitrogen, phosphorus and iron predominantly limit phytoplankton growth in the global surface oceans [34,35], more studies investigating the combined effects of elevated pCO_2 and resource limitation are required to provide a mechanistic understanding on the impacts of OA on future primary production.

Even though we did not find a consistent CO_2 response over the entire winter-to-summer plankton succession, the stimulation in primary production under elevated pCO_2 at the peak of the second bloom was also observed in earlier studies looking at mixed natural assemblages as well as monoclonal laboratory cultures. During a mesocosm study in Bergen (Norway), for instance, DIC uptake increased under a comparable OA scenario by about 40 % [30,36]. Moreover, a mesocosm study in Kongsfjorden (Svalbard, Norway) showed an OA-induced increase in primary production of 10 to 60% over the experimental period [37]. Such increases in primary production may derive from physiological changes in predominant species and/or shifts in community composition both leading to higher phytoplankton biomass buildup. At a higher taxonomic level, the phytoplankton community remained largely unaltered and was dominated by diatoms [21]. Under nutrient-replete as well as nutrient-limiting conditions, elevated pCO_2 resulted in an increased abundance of picoeukaryotes [21]. Specific changes within phytoplankton groups will be discussed elsewhere in this PLOS collection (see S1 Table in [21]). With regard to the dominating role of diatoms in our experiment, several studies found this group to enhance their C_i fixation rates in response to elevated pCO_2, which was often attributed to the down-regulation in the CCM activities under these conditions [e.g. 38-40]. Such enhanced OA-driven efficiencies in C_i fixation may, at least partially, have contributed to the higher phytoplankton biomass during the second bloom in our experiment.

Our results indicate an OA-dependent increase in primary production during certain times of the spring-to-summer phytoplankton succession, particularly under NO_3^- limitation (phase III) being accompanied by a significant increase in picoeukaryotes during this period [21]. With respect to higher trophic levels, OA showed differential growth effects on several predominant mesozooplankton species, though as a whole, the community remained rather unaltered under OA (Algueró-Muñiz et al. *in prep.*). OA led, however, to an increase in the survival rate of

herring larvae (being planted in the mesocosms on t63), which could be linked to higher prey abundances (Sswat et al. *in prep.*). Hence, the observed changes in primary production under OA have a high potential to restructure phytoplankton communities in the future coastal North Sea with likely consequences for higher trophic levels.

Acknowledgements

We thank the Sven Lovén Centre for Marine Sciences, Kristineberg, for their hospitality and help during the field work. We thank Amy Forsberg-Grivogiannis for her great help during the field work. We also gratefully acknowledge the captain and crew of RV ALKOR for their work transporting, deploying and recovering the mesocosms during cruises AL406 and AL420. This project was funded by the German Federal Ministry of Science and Education (BMBF) in the framework of the BIOACID II project (grant no. FKZ 03F0655A). SW, TE and DBvdW received support from the EU FP7 research infrastructure initiative 'Association of European Marine Biological Laboratories' (ASSEMBLE, grant no. 227799), and SW from the Royal Swedish Academy of Sciences.

References

1. **Wolf-Gladrow** DA, Riebesell U, Burkhardt S, Bijma J. Direct effects of CO_2 concentration on growth and isotopic composition of marine plankton. Tellus B. 1999; 51: 461–476.

2. **Caldeira** K, Wickett ME. Anthropogenic carbon and ocean pH. Nature. 2003; 425: 365.

3. **Stocker** TF, Qin D, Plattner G-K, Tignor M, Allen SK, Boschung J, et al. (eds.). 2013. In: climate change 2013: the physical science basis. Contribution of working group I to the fifth assessment report of the intergovernmental panel on climate change. Cambridge University Press, USA.

4. **Roy** T, Bopp L, Gehlen M, Schneider B, Cadule P, Frölicher TL, et al. Regional impacts of climate change and atmospheric CO_2 on future ocean carbon uptake: A multimodel linear feedback analysis. J. Clim. 2011; 24: 2300–2318.

5. **Sabine** CL, Feely RA, Gruber N, Key RM, Lee K, Bullister JL, et al. The oceanic sink for anthropogenic CO_2. Science. 2004; 305: 367–371.

6. **Raven** JA. Inorganic carbon acquisition by marine autotrophs. Adv. Bot. Res. 1997; 27: 85–209.

7. **Badger** MR, Andrews TJ, Whitney SM, Ludwig M, Yellowlees DC, Leggat W, Price GD. The diversity and coevolution of Rubisco, plastids, pyrenoids, and chloroplast-based CO_2-concentrating mechanisms in algae. Can. J. Bot. 1998; 76: 1052–1071.

8. **Young** JN, Heureux AMC, Sharwood RE, Rickaby REM, Morel FMM, Whitney SM. Large variation in the Rubisco kinetics of diatoms reveals diversity among their carbon-concentrating mechanisms. J. Exp. Bot. 2016; doi: 10.1093/jxb/erw163.

9. **Raven** JA. Physiology of inorganic C acquisition and implications for resource use efficiency by marine phytoplankton: relation to increased CO_2 and temperature. Plant Cell Environ. 1991; 14: 779–794.

10. **Giordano** M, Beardall J, Raven JA. CO_2 concentrating mechanisms in algae: mechanisms, environmental modulation, and evolution. Annu. Rev. Plant. Biol. 2005; 56: 99–131.

11. **Rost** B, Zondervan I, Wolf-Gladrow D. Sensitivity of phytoplankton to future changes in ocean carbonate chemistry: current knowledge, contradictions and research directions. Mar. Ecol. Prog. Ser. 2008; 373: 227–237.

12. **Reinfelder** JR. Carbon concentrating mechanisms in eukaryotic marine phytoplankton. Annu. Rev. Mar. Sci. 2011; 3: 291–315.

13. **Raven** JA, Beardall J, Giordano M. Energy costs of carbon dioxide concentrating mechanisms in aquatic organisms. Photosynth Res. 2014; 121(2-3):111–24.

14. **Burkhardt** S, Zondervan I, Riebesell U. Effect of CO_2 concentration on C:N:P ratio in marine phytoplankton: a species comparison. Limnol. Oceanogr. 1999; 44: 683–690.

15. **Kranz** SA, Sültemeyer D, Richter K-U, Rost B. Carbon acquisition by *Trichodesmium*: the effect of pCO_2 and diurnal changes. Limnol. Oceanogr. 2009; 54: 548–559.

16. **Eberlein** T, Van de Waal DB, Brandenburg KM, John U, Voss M, Achterberg EP, Rost B. Interactive effects of ocean acidification and nitrogen limitation on two bloom-forming dinoflagellate species. Mar. Ecol. Prog. Ser. 2016; 543: 127–140.

17. **Hutchins** DA, Fu F-X, ZhangY, Warner ME, Feng Y, Portune K, et al. CO_2 control of *Trichodesmium* N_2 fixation, photosynthesis, growth rates, and elemental ratios: Implications for past, present, and future ocean biogeochemistry. Limnol. Oceanogr. 2007; 52(4): 1293–1304.

18. **Brading** P, Warner ME, Smith DJ, Suggett DJ. Contrasting modes of inorganic carbon acquisition amongst *Symbiodinium* (Dinophyceae) phylotypes. New Phytol. 2013; 200: 432−442.

19. **Schaum** E, Rost B, Millar AJ, Collins S. Variation in plastic responses of a globally distributed picoplankton species to ocean acidification. Nat. Clim. Change. 2013; 3: 298–302.

20. **Riebesell** U, Tortell PD. Effects of ocean acidification on pelagic organisms and ecosystems. In: Gattuse, J.P., Hansson, L. (Eds.), Ocean Acidification. Oxford University Press, Oxford, UK, 2011; 99–121.

21. **Bach** LT, Taucher J, Boxhammer T, Ludwig A, The Kristineberg KOSMOS Consortium, Achterberg EP, et al. Influence of Ocean Acidification on a Natural Winter-to-Summer Plankton Succession: First Insights from a Long-Term Mesocosm Study Draw Attention to Periods of Low Nutrient Concentrations. PLoS ONE. 2016; 11(8). e0159068.

22. **Tiselius** P, Kuylenstierna M. Growth and decline of a diatom spring bloom: phytoplankton species composition, formation of marine snow and the role of heterotrophic dinoflagellates. J. Plankton. Res. 1996; 18: 133–155.

23. **Waite** AM, Lindahl O. Bloom and decline of the toxic flagellate *Chattonella marina* in a Swedish fjord. Mar. Ecol. Prog. Ser. 2006; 326: 77–83.

24. **Steemann Nielsen** E. The use of radioactive carbon (^{14}C) for measuring primary production in the sea. J. Cons. Perm. Int. Explor. Mer. 1952; 18: 117–140.

25. **Riebesell** U, Czerny J, Bröckel KV, Boxhammer T, Büdenbender J, Deckelnick M et al. Technical Note: A mobile sea-going mesocosm system–new opportunities for ocean change research. Biogeosciences. 2013; 10(3): 1835–1847.

26. **Boxhammer** T, Bach LT, Czerny J, Riebesell U. Technical note: Sampling and processing of mesocosm sediment trap material for quantitative biogeochemical analysis. Biogeosciences. 2016; 13: 2849–2858.

27. **Bender** M, Grande K, Johnson K, Marra J, Williams PJ LeB, Sieburth J et al. A comparison of four methods for determining planktonic community production. Limnol. Oceanogr. 1987; 32(5): 1085–1098.

28. **Lindahl** O. Long-term studies of primary production in the Gullmar fjord, Sweden. *In*: Skjoldal, H. R., C. Hopkins, K. E. Erikstad, H. P Leinaas [eds.] Ecology of fjords and coastal waters. Elsevier Science Publishers, New York. 1995; 105–112.

29. **Lindahl** O, Belgrano A, Davidsson L, Hernroth B. Primary production, climatic oscillations, and physico-chemical processes: the Gullmar Fjord time-series data set (1985–1996). ICES J. Mar. Sci. 1998; 55 (4): 723–729.

30. **Egge** JK, Thingstad TF, Larsen A, Engel A, Wohlers J, Bellerby RGJ, Riebesell U. Primary production during nutrient-induced blooms at elevated CO_2 concentrations. Biogeosciences. 2009; 6: 877–885.

31. **Paul** AJ, Bach LT, Schulz KG, Boxhammer T, Czerny J, Achterberg EP, et al. Effect of elevated CO_2 on organic matter pools and fluxes in a summer Baltic Sea plankton community. Biogeosciences. 2015; 12: 6181–6203.

32. **Sala** MM, Aparicio FL, Balagué V, Boras JA, Borrull E, Cardelús C. Contrasting effects of ocean acidification on the microbial food web under different trophic conditions. Ices. J. Mar. Sci. 2015; doi:10.1093/icesjms/fsv130.

33. **Hopkinson** BM, Xu Y, Shi D, McGinn PJ, Morel FMM. The effect of CO_2 on the photosynthetic physiology of phytoplankton in the Gulf of Alaska. Limnol. Oceanogr. 2010; 55(5): 2011–2024.

34. **Elser** JJ, Bracken MES, Cleland EE, Gruner DS, Harpole WS, Hillebrand H, Ngai JT, Seabloom EW, Shurin JB, Smith JE. Global analysis of nitrogen and phosphorus limitation of primary producers in freshwater, marine and terrestrial ecosystems. Ecol. Lett. 2007; 10: 1135−1142.

35. **Moore** CM, Mills MM, Arrigo KR, Berman-Frank I, Bopp L, Boyd PW, et al. Processes and patterns of oceanic nutrient limitation. Nat. Geosci. 2013; 6: 701−710.

36. **Riebesell** U, Schulz KG, Bellerby RGJ, Botros M, Fritsche P, Meyerhofer M, Neill C, Nondal G, Oschlies A, Wohlers J, Zollner E. Enhanced biological carbon consumption in a high CO_2 ocean. Nature. 2007; 450: 545–548.

37. **Engel** A, Borchard C, Piontek J, Schulz KG, Riebesell U, Bellerby R. CO_2 increases ^{14}C primary production in an Arctic plankton community. Biogeosciences. 2013; 10: 1291–1308.

38. **Trimborn** S, Lundholm N, Thoms S, Richter K-U, Krock B, Hansen PJ, Rost B. Inorganic carbon acquisition in potentially toxic and non-toxic diatoms: the effect of pH-induced changes in seawater carbonate chemistry. Physiol. Plant. 2008; 133: 92–105.

39. **Wu**, Y, K. Gao, Riebesell U. CO_2-induced seawater acidification affects physiological performance of the marine diatom *Phaeodactylum tricornutum*. Biogeosciences. 2010; 7: 2915–2923.

40. **Hoppe** CJM, Holtz L-M, Trimborn S, Rost B. Ocean Acidification decreases the light use efficiency in an Antarctic diatom under dynamic but not constant light, New Phytol. 2015; 207: 159–171.

Supplement data

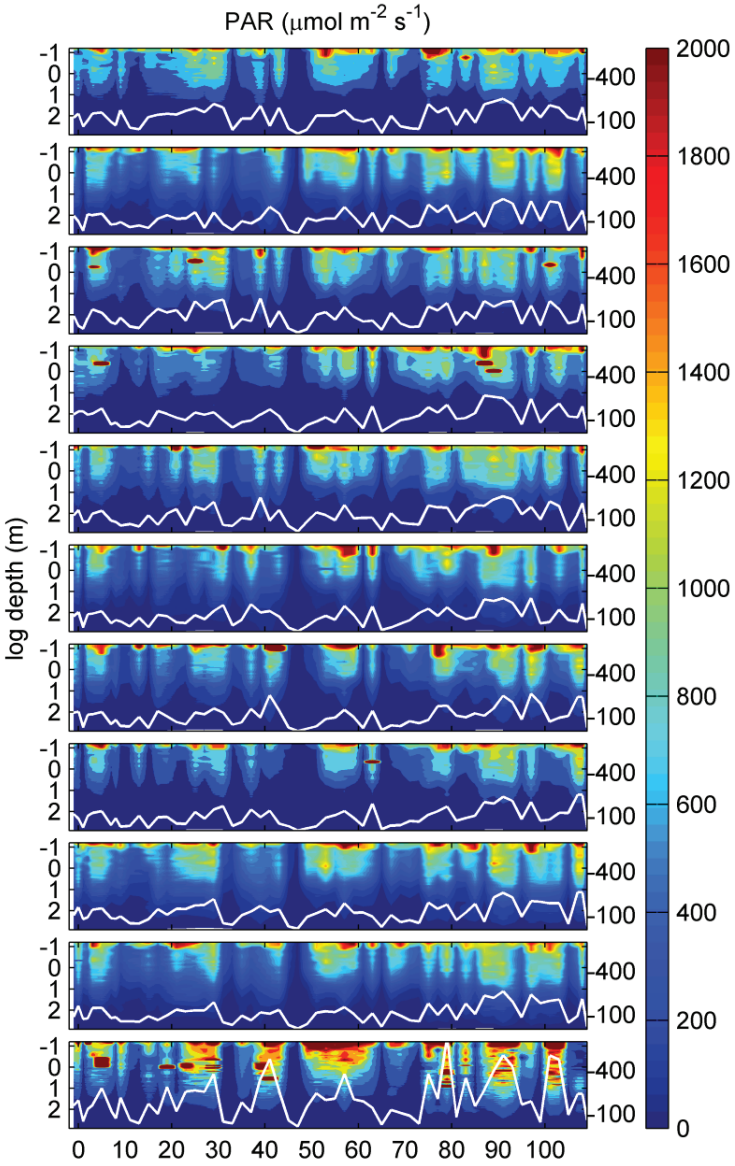

S1 Fig. PAR (µmol m^{-2} s^{-1}) inside the mesocosms during the time of the experiment.

S1 Table. Photoacclimation raw data obtain with the photosynthesis-irradiance response curves.

Time (days)	Mesocosm	CO2 treatment (Low/High)	Parameters PP(T)	Chl a	P(max)	I(k)	alpha
			(µmol C L-1 d-1)	(µg Chl a L-1)	(µg C (µg Chl a)-1 h-1)	(µmol potons m-2 s-1)	
1	M1	L	1.88	38.52	2.61	101	0.027
5	M1	L	1.75	29.37	3.06	73	0.043
9	M1	L	1.96	29.89	2.83	92	0.031
13	M1	L	1.69	23.68	3.60	99	0.036
17	M1	L	1.48	16.66	3.27	110	0.030
21	M1	L	2.63	17.72	3.85	82	0.047
25	M1	L	6.08	21.70	4.31	278	0.059
29	M1	L	9.48	14.45	4.77	69	0.071
33	M1	L	15.94	30.39	2.48	100	0.025
37	M1	L	7.70	27.50	6.06	82	0.078
41	M1	L	8.91	57.64	2.75	116	0.024
45	M1	L	5.10	21.94	3.24	168	0.019
49	M1	L	5.65	17.52	1.18	114	0.010
53	M1	L	9.01	23.47	4.73	49	0.096
57	M1	L	9.69	25.58	3.75	67	0.056
61	M1	L	6.77	22.06	0.76	43	0.018
65	M1	L	5.77	19.29	5.38	84	0.064
69	M1	L	3.13	13.68	3.21	85	0.038
73	M1	L	1.05	7.29	1.53	65	0.025
77	M1	L	3.68	28.53	2.20	130	0.017
81	M1	L	2.40	14.71	3.39	308	0.011
85	M1	L	2.16	29.77	2.53	122	0.021
89	M1	L	1.10	12.48	7.56	215	0.036
93	M1	L	0.29	4.15	6.51	113	0.061
97	M1	L	1.29	17.50	5.73	208	0.028
101	M1	L	0.83	9.32	2.42	94	0.026
105	M1	L	0.78	8.27	2.93	76	0.038
109	M1	L	1.05	15.82	4.94	231	0.022
1	M2	H	1.34	28.77	2.59	80	0.034
5	M2	H	1.97	35.95	3.84	108	0.036
9	M2	H	2.16	28.85	2.07	113	0.018
13	M2	H	1.60	20.16	2.95	80	0.037
17	M2	H	1.53	17.75	3.32	101	0.033
21	M2	H	2.15	15.10	3.79	96	0.040
25	M2	H	4.60	19.13	4.44	62	0.046
29	M2	H	6.88	13.44	5.09	100	0.051

33	M2	H	5.04	18.21	1.81	91	0.020
37	M2	H	3.40	16.24	5.81	184	0.034
41	M2	H	3.08	22.54	3.11	92	0.035
45	M2	H	2.73	13.09	5.39	227	0.025
49	M2	H	8.65	28.58	3.33	219	0.015
53	M2	H	4.90	15.54	3.54	38	0.100
57	M2	H	6.15	26.37	2.90	69	0.042
61	M2	H	7.60	49.53	0.98	33	0.030
65	M2	H	4.71	27.30	5.18	30	0.024
69	M2	H	2.54	13.32	2.65	143	0.019
73	M2	H	1.75	14.16	1.75	92	0.020
77	M2	H	0.90	9.96	1.21	213	0.006
81	M2	H	0.39	3.85	2.93	186	0.016
85	M2	H	1.28	19.82	6.12	400	0.015
89	M2	H	1.13	15.86	3.07	75	0.041
93	M2	H	0.52	6.82	3.42	115	0.031
97	M2	H	0.57	9.74	2.71	120	0.024
101	M2	H	0.63	13.40	2.59	323	0.008
105	M2	H	0.85	6.59	3.21	116	0.028
109	M2	H	1.65	21.11	3.50	98	0.036
1	M3	L	0.85	18.20	3.37	143	0.024
5	M3	L	1.29	21.28	2.71	83	0.033
9	M3	L	1.25	17.11	2.83	196	0.014
13	M3	L	1.26	15.22	2.49	80	0.032
17	M3	L	1.83	23.80	4.12	139	0.030
21	M3	L	2.04	15.29	3.33	139	0.024
25	M3	L	2.81	11.57	3.99	104	0.034
29	M3	L	4.68	10.87	4.64	106	0.044
33	M3	L	4.92	19.39	1.78	181	0.010
37	M3	L	3.29	12.00	1.752	108	0.016
41	M3	L	5.25	24.00	1.72	35	0.050
45	M3	L	6.98	21.50	2.44	164	0.016
49	M3	L	2.45	8.11	0.67	35	0.019
53	M3	L	4.93	20.31	3.31	113	0.029
57	M3	L	3.91	18.78	3.56	68	0.055
61	M3	L	2.78	20.75	1.53	35	0.043
65	M3	L	1.24	16.91	3.76	55	0.076
69	M3	L	1.06	12.63	1.47	80	0.020
73	M3	L	0.69	8.90	0.84	52	0.019
77	M3	L	0.85	13.45	1.69	96	0.019
81	M3	L	0.72	7.49	1.54	81	0.020
85	M3	L	1.35	30.32	2.53	79	0.034
89	M3	L	1.02	19.16	4.36	208	0.021

93	M3	L	0.73	10.67	1.75	88	0.021
97	M3	L	1.01	11.81	2.89	101	0.031
101	M3	L	0.41	8.23	1.93	71	0.027
105	M3	L	1.91	23.32	4.49	106	0.044
109	M3	L	0.48	6.94	2.35	62	0.040
1	M4	H	1.42	29.65	3.30	107	0.033
5	M4	H	2.04	35.96	4.05	106	0.039
9	M4	H	2.30	25.30	2.09	117	0.018
13	M4	H	2.22	26.28	3.21	95	0.035
17	M4	H	1.48	16.33	4.17	90	0.048
21	M4	H	2.46	19.01	3.39	89	0.039
25	M4	H	4.22	18.80	3.95	79	0.046
29	M4	H	8.39	13.50	4.52	89	0.052
33	M4	H	22.40	31.82	3.15	142	0.022
37	M4	H	9.70	23.26	8.12	213	0.038
41	M4	H	16.59	68.85	4.17	110	0.040
45	M4	H	5.25	21.16	4.93	244	0.020
49	M4	H	8.10	20.09	1.84	48	0.039
53	M4	H	14.08	27.71	3.85	77	0.050
57	M4	H	9.96	24.24	7.05	200	0.035
61	M4	H	13.59	40.83	2.04	61	0.033
65	M4	H	4.10	17.43	2.37	53	0.045
69	M4	H	3.80	22.25	4.80	96	0.051
73	M4	H	1.71	12.67	2.71	190	0.014
77	M4	H	1.94	17.82	2.51	133	0.019
81	M4	H	2.05	16.92	2.50	157	0.016
85	M4	H	0.88	13.94	3.39	129	0.028
89	M4	H	1.52	17.97	4.73	278	0.017
93	M4	H	1.23	37.18	5.452	210	0.061
97	M4	H	0.43	10.71	6.17	417	0.015
101	M4	H	1.02	11.87	2.93	204	0.014
105	M4	H	0.99	10.02	3.44	70	0.052
109	M4	H	0.65	17.66	3.27	97	0.034
1	M5	L	1.44	34.84	3.03	123	0.026
5	M5	L	2.15	36.21	3.39	97	0.036
9	M5	L	1.93	27.38	2.36	101	0.024
13	M5	L	2.02	27.53	2.82	115	0.025
17	M5	L	0.85	10.92	2.71	123	0.022
21	M5	L	1.77	14.99	4.05	182	0.045
25	M5	L	2.65	14.08	3.67	95	0.043
29	M5	L	3.27	8.57	3.30	84	0.041
33	M5	L	13.20	26.52	2.58	90	0.030
37	M5	L	4.05	17.90	6.05	459	0.013

41	M5	L	2.02	18.10	2.59	153	0.019
45	M5	L	2.50	15.39	2.49	219	0.011
49	M5	L	3.43	16.52	0.69	58	0.012
53	M5	L	5.80	25.83	3.27	71	0.050
57	M5	L	9.95	33.33	2.66	67	0.041
61	M5	L	3.42	17.00	1.01	61	0.017
65	M5	L	4.49	28.96	2.25	141	0.016
69	M5	L	1.85	19.14	1.99	92	0.023
73	M5	L	0.65	6.85	1.40	94	0.015
77	M5	L	0.53	11.37	1.02	121	0.010
81	M5	L	0.86	11.87	1.59	129	0.012
85	M5	L	0.75	15.38	2.19	63	0.035
89	M5	L	1.08	18.52	2.55	137	0.020
93	M5	L	0.81	19.55	1.91	131	0.015
97	M5	L	0.19	3.48	1.26	125	0.011
101	M5	L	1.30	27.48	3.32	103	0.032
105	M5	L	2.11	17.21	5.54	119	0.047
109	M5	L	1.34	10.48	1.80	95	0.019
1	M6	H	1.46	28.91	3.10	143	0.022
5	M6	H	2.58	40.73	3.37	63	0.054
9	M6	H	2.27	28.72	3.13	120	0.026
13	M6	H	2.22	26.81	2.83	80	0.036
17	M6	H	1.43	15.67	3.41	106	0.033
21	M6	H	3.07	22.85	2.92	86	0.034
25	M6	H	2.92	13.60	4.83	70	0.048
29	M6	H	6.45	12.47	6.73	111	0.062
33	M6	H	15.47	27.60	2.83	152	0.019
37	M6	H	7.62	23.34	5.84	127	0.047
41	M6	H	5.11	38.90	5.65	162	0.036
45	M6	H	5.48	22.66	3.19	87	0.038
49	M6	H	8.60	22.98	3.62	63	0.061
53	M6	H	12.51	30.30	3.69	93	0.039
57	M6	H	10.87	31.08	3.11	71	0.044
61	M6	H	6.64	24.09	2.24	70	0.034
65	M6	H	6.21	24.01	2.32	76	0.031
69	M6	H	2.83	13.87	2.29	76	0.030
73	M6	H	1.84	10.57	2.40	88	0.029
77	M6	H	1.97	18.79	2.79	159	0.018
81	M6	H	1.93	17.99	2.91	182	0.016
85	M6	H	0.98	15.29	1.73	82	0.021
89	M6	H	1.40	17.69	2.54	109	0.025
93	M6	H	0.80	16.14	3.02	121	0.026
97	M6	H	0.47	10.00	3.35	149	0.023

101	M6	H	0.64	8.98	3.54	85	0.045
105	M6	H	1.98	20.97	5.78	102	0.058
109	M6	H	0.54	18.87	2.87	81	0.035
1	M7	H	0.95	21.04	2.63	56	0.047
5	M7	H	2.12	32.12	3.11	65	0.048
9	M7	H	1.96	27.33	2.53	72	0.036
13	M7	H	1.81	26.92	3.20	70	0.045
17	M7	H	2.13	23.77	3.69	120	0.031
21	M7	H	1.34	10.04	3.21	111	0.029
25	M7	H	4.70	19.06	5.17	60	0.052
29	M7	H	7.77	11.80	7.13	97	0.075
33	M7	H	18.89	31.20	2.67	107	0.025
37	M7	H	8.37	22.25	4.36	70	0.062
41	M7	H	5.17	25.91	4.74	112	0.043
45	M7	H	5.07	27.28	4.90	244	0.020
49	M7	H	4.10	11.19	3.35	64	0.055
53	M7	H	17.43	37.07	5.61	74	0.077
57	M7	H	9.84	21.73	4.10	97	0.042
61	M7	H	13.83	44.45	3.21	79	0.041
65	M7	H	4.98	18.73	2.83	87	0.033
69	M7	H	3.69	19.26	2.19	53	0.042
73	M7	H	3.36	20.73	2.15	59	0.037
77	M7	H	1.70	17.49	2.31	160	0.015
81	M7	H	2.41	14.05	2.88	213	0.014
85	M7	H	1.07	10.07	0.77	37	0.021
89	M7	H	3.74	27.43	3.49	116	0.030
93	M7	H	1.98	16.67	3.32	137	0.025
97	M7	H	1.44	18.36	2.76	99	0.032
101	M7	H	0.44	7.57	2.19	61	0.038
105	M7	H	0.86	7.98	4.45	105	0.044
109	M7	H	1.63	17.08	2.58	85	0.030
1	M8	H	0.08	1.14	2.13	88	0.024
5	M8	H	1.96	32.28	3.26	59	0.055
9	M8	H	2.01	30.22	3.25	104	0.031
13	M8	H	1.57	23.20	2.98	101	0.030
17	M8	H	2.03	23.05	3.32	100	0.033
21	M8	H	1.66	13.01	2.58	92	0.028
25	M8	H	2.98	14.95	3.85	127	0.028
29	M8	H	3.30	7.31	5.13	179	0.029
33	M8	H	18.73	27.99	2.56	85	0.031
37	M8	H	5.65	18.63	6.64	204	0.033
41	M8	H	5.68	37.06	2.97	120	0.026
45	M8	H	3.66	17.82	2.86	62	0.049

49	M8	H	7.59	16.80	2.91	118	0.025
53	M8	H	7.65	15.44	2.24	11	0.034
57	M8	H	3.59	7.63	2.56	64	0.040
61	M8	H	9.15	33.62	2.35	38	0.065
65	M8	H	4.08	22.68	3.94	116	0.035
69	M8	H	3.17	20.60	2.54	135	0.019
73	M8	H	0.92	6.71	2.26	89	0.026
77	M8	H	1.22	11.72	2.51	70	0.040
81	M8	H	2.40	14.66	2.61	146	0.018
85	M8	H	1.01	9.16	2.97	210	0.014
89	M8	H	2.37	39.41	1.43	87	0.017
93	M8	H	0.94	15.75	3.59	122	0.030
97	M8	H	0.98	14.82	3.16	91	0.038
101	M8	H	0.95	14.82	3.25	86	0.041
105	M8	H	0.85	7.32	4.37	95	0.048
109	M8	H	1.60	16.81	2.92	116	0.026
1	M9	L	1.16	27.59	3.08	93	0.033
5	M9	L	1.82	34.03	3.62	89	0.042
9	M9	L	1.93	27.48	2.76	95	0.030
13	M9	L	1.80	23.38	3.22	104	0.032
17	M9	L	1.88	20.43	3.89	80	0.049
21	M9	L	1.34	9.09	2.49	87	0.029
25	M9	L	5.34	19.26	4.42	69	0.053
29	M9	L	7.88	11.58	6.34	83	0.077
33	M9	L	6.16	17.16	1.38	62	0.023
37	M9	L	1.45	9.50	7.88	323	0.024
41	M9	L	6.32	75.60	3.96	158	0.026
45	M9	L	5.14	29.26	3.88	124	0.034
49	M9	L	3.16	10.28	3.79	170	0.023
53	M9	L	3.89	12.73	2.11	61	0.036
57	M9	L	12.80	52.70	1.95	80	0.025
61	M9	L	7.24	35.15	2.04	35	0.058
65	M9	L	5.90	29.43	4.46	89	0.050
69	M9	L	4.55	23.50	1.71	60	0.029
73	M9	L	1.58	10.58	2.95	161	0.018
77	M9	L	1.41	12.92	1.95	89	0.023
81	M9	L	1.36	12.05	1.77	101	0.018
85	M9	L	0.65	9.22	3.18	157	0.020
89	M9	L	0.67	10.03	6.71	114	0.061
93	M9	L	0.83	11.38	4.08	201	0.021
97	M9	L	1.27	21.71	3.51	157	0.024
101	M9	L	0.50	14.61	2.94	112	0.027
105	M9	L	0.35	12.27	4.65	128	0.036

109	M9	L	0.48	19.75	2.92	116	0.026
1	M10	L	1.28	31.76	2.73	74	0.037
5	M10	L	2.26	38.77	3.69	78	0.047
9	M10	L	1.65	22.97	2.30	90	0.026
13	M10	L	1.68	26.07	2.75	86	0.032
17	M10	L	1.61	22.11	3.45	67	0.055
21	M10	L	2.72	17.12	3.87	135	0.029
25	M10	L	7.05	23.22	6.05	72	0.053
29	M10	L	10.79	13.54	8.24	106	0.077
33	M10	L	21.83	35.67	2.82	132	0.021
37	M10	L	10.47	22.34	4.87	125	0.039
41	M10	L	7.65	35.63	3.35	102	0.035
45	M10	L	5.70	24.14	2.94	90	0.034
49	M10	L	7.15	22.82	7.11	313	0.023
53	M10	L	6.41	19.75	4.08	98	0.042
57	M10	L	5.10	11.82	5.33	98	0.056
61	M10	L	10.85	32.17	3.27	54	0.063
65	M10	L	7.90	26.03	2.74	50	0.056
69	M10	L	2.97	13.58	1.77	46	0.041
73	M10	L	2.62	16.49	3.67	127	0.030
77	M10	L	2.77	27.08	4.29	208	0.022
81	M10	L	1.79	11.99	1.78	79	0.023
85	M10	L	2.49	22.39	4.79	270	0.018
89	M10	L	2.83	26.35	4.58	117	0.042
93	M10	L	0.65	7.77	2.69	108	0.027
97	M10	L	1.79	13.50	4.14	145	0.031
101	M10	L	0.52	6.35	2.09	97	0.023
105	M10	L	0.62	14.61	2.85	102	0.028
109	M10	L	0.66	20.41	1.68	191	0.009

3. Synthesis

Consequences of OA are considered to be among the major environmental challenges mankind has to face within the next centuries (Herr et al. 2014). Although underlying chemical processes are well understood and changes in seawater chemistry (based on various CO_2 emission scenarios) can be estimated for our near future, anticipated consequences of these changes for the marine biota are less clear (Turley and Gattuso 2012). While the knowledge on some groups is more advanced, others groups, like the dinoflagellates, are less well understood. To shed more light on this, I studied the effects of OA on the eco-physiology of dinoflagellates under N-replete (Publication I) and N-limited conditions (Publication II) as well as OA effects on primary production in a coastal North Sea phytoplankton community (Publication III). Here, I highlight the main findings of these studies and furthermore point out overarching concepts that arise from these experimental results.

3.1 Main findings of this thesis

With a type II RubisCO, dinoflagellates possess a carboxylating enzyme with the lowest CO_2 affinities among all eukaryotic phytoplankton (Morse et al. 1995; Badger et al. 1998). Our studies on *S. trochoidea* and *A. fundyense* show, however, that within this group of dinoflagellates, effective CCMs are able to compensate for these kinetic shortcomings (*Publication I*). Our measured $K_{1/2}$ values for C fixation fall in the same order of magnitude as those employed in diatoms, with the difference that diatoms are equipped with a highly-affine type I RubisCO (Young et al. 2006). The consequently higher energetic costs for dinoflagellates in running their CCMs may partly explain why they generally exhibit lower growth rates and higher respiration rates (*Publication I*). To some extent, this could also

explain why diatoms often lead the succession of phytoplankton and prevail against dinoflagellates under nutrient-rich and well-mixed surface water. Under oligotrophic and more stratified conditions, which occur after the spring blooms, dinoflagellates often dominate (Margalef 1978). This observation can be attributed to the heterotrophic behavior of many dinoflagellates allowing them to use organic compounds as an additional nutrient source for growth (Tiselius and Kuylenstierna 1996; Waite and Lindahl 2006). Such traits may have greatly contributed to their overall success, i.e. occupying an ecological niche in which they do not have to compete with fast growing (and often energetically very efficient) phytoplankton species.

We furthermore found a trade-off between maximum rates and affinities of C fixation in both *S. trochoidea* and *A. fundyense* (Fig. 7A; *Publication I*). This trade-off even subsisted when maximum rates and affinities of carbon fixation changed under different CO_2 environments. This relationship of having either high maximum rates or high affinities in C acquisition may represent fundamental constrains in enzyme kinetics, i.e. operating fast comes at the expense of lower substrate affinities and *vice versa*.

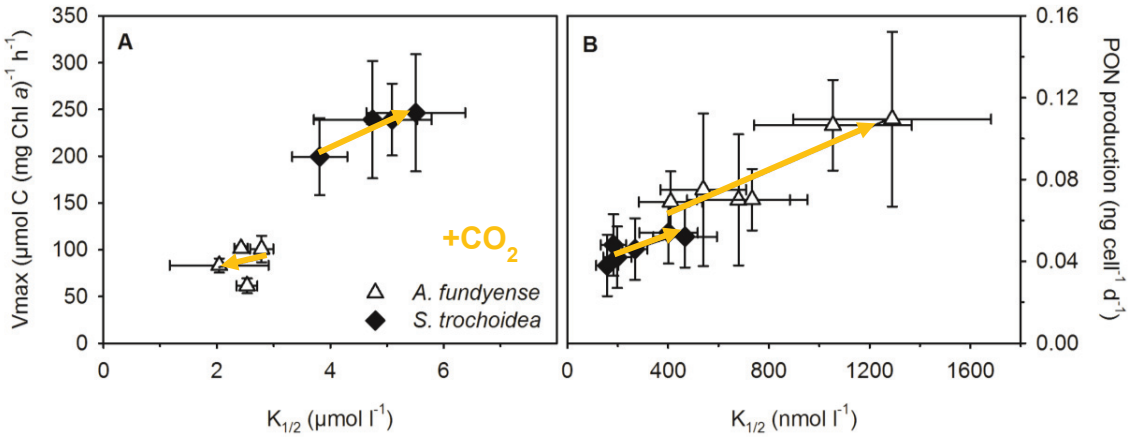

Fig. 7: V_{max} versus $K_{1/2}$ of photosynthetic C fixation (A) and PON production rates versus half-saturation concentrations ($K_{1/2}$; residual DIN concentration) of growth (B) over a range of pCO_2 of *Scrippsiella trochoidea* and *Alexandrium fundyense*, respectively. The orange arrows indicate the increase in CO_2 concentrations in the incubations. Figs. from *publication I* and *II*.

Based on the limited number of studies, however, the observed correlation shows large variation among the different phytoplankton groups and even appear to be absent in diatoms (Young et al. 2016). Further investigations on the complex catalytic mechanisms and potential relationships therein are needed, particularly if we want to understand how other phytoplankton groups, featuring different types of RubisCO and CCMs, may respond to OA.

Publication II also shows a trade-off that changed with pCO_2, but this time dealing with N acquisition under N-limiting conditions. More specifically, while PON production rates were increased, affinities to take up DIN were lowered towards elevated pCO_2 (Fig. 7B). This shift could imply a reduction in stress imposed by N limitation. Such changes in N assimilation most likely derive from the reallocation of energy from a CO_2-driven down-regulation of a CCM. Acquiring C_i under OA may become less cost-intensive and the 'surplus' of energy can be directed into N assimilation. Interestingly, the expected benefit from elevated pCO_2 on growth and elemental composition (as well as toxin production in *A. fundyense*) was relatively small under nutrient-replete conditions. This may possibly be a result of saturated CO_2 fixation already at low CO_2 concentrations (*Publication I*). Nevertheless, due to the high energy expenditure of cells in C and N assimilation and the close linking between the C and N pathways (Flynn 1991), saving energy in C_i acquisition may allow for a fast redirection of energy resources into N acquisition.

As illustrated in Fig. 8, during N assimilation, glutamine (Gln) reacts with 2-oxoglutarate (2-OG) to form two molecules of glutamate (Glu), which resembles the primary product of N assimilation. 2-OG derives from the tricarboxylic acid cycle (TCA), which itself is replenished by the primary product of C assimilation, 3-Phosphoglyceric acid (PGA). Based on the assumption that the CCM is down-regulated under elevated pCO_2, the link between both C and N pathways (Fig. 8; orange arrows) may simplify the shunting of energy between

the two pathways. In case more 2-OG is produced under elevated pCO_2, it may allow a faster incorporation of N and provide to some extent an explanation of the results from *publication II*. The question remains which of the observed changes in C_i acquisition (*publication I*) may provide an energy source for N assimilation under elevated pCO_2. One way to approach this question could be to perform C_i flux measurements with cultures acclimated to N-limiting conditions and elevated pCO_2 and to compare these results with our findings under N-replete conditions (*publication I*). To perform adequate C_i flux measurements would, however, require much more biomass (i.e. a set-up with larger culture flasks) than our continuous culture system provides under N-limited conditions. So more of the continuous culture systems would have to be deployed simultaneously, since a simple increase in population densities becomes more difficult to control under steady-state conditions and could quickly differ from representative concentrations for natural assemblages of these species.

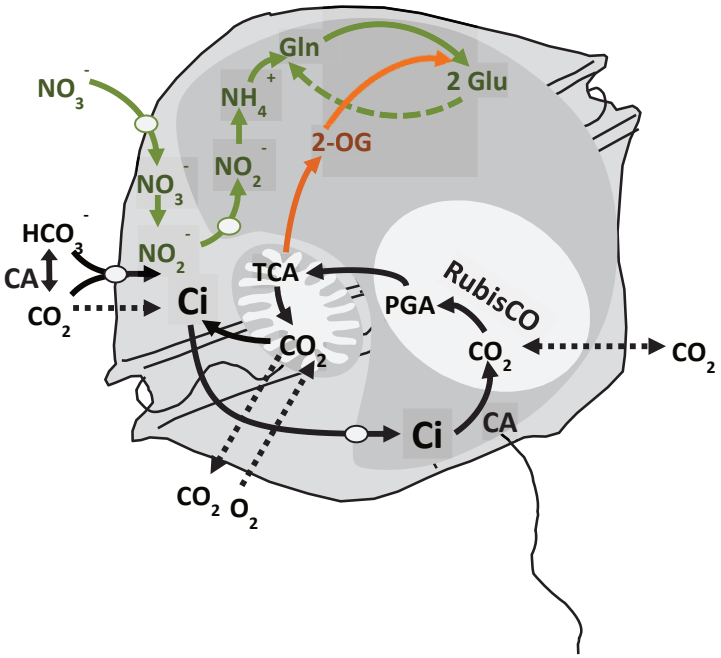

Fig. 8: Schematic overview of C_i assimilation (black color) and N assimilation (green color) in dinoflagellates. The link between the C and N pathways is indicated in orange color. Modified after Van de Waal et al. (2013).

Another possibility of how elevated pCO_2 may lead to a reduction in energy requirements for N assimilation is through the increase in the CO_2/O_2 ratio of the environment. The competitive inhibition of RubisCO by O_2 may consequently have been lowered. A reduction in photorespiration decreases the production as well as the risk to loose NH_3 from the amino acid pool as well as the cost for re-fixation. These effects could also have contributed to the increased PON production in both dinoflagellates under elevated pCO_2.

In a natural community, the mode of nutrient acquisition largely determines the competitive ability of species. According to resource competition theory, trade-offs in nutrient uptake, such as were presented in *publication I* and *II*, play an important role in niche development and facilitate co-existence of species (Tilman 1976; Tilman et al 1980). Depending on the direction of shifts in such trade-offs, species may gain a competitive advantage or disadvantage over other species. In the oceans, there are regions where *S. trochoidea* and *A. fundyense* co-exist (Fistarol et al. 2004; McCollin et al. 2011). Based on the N uptake kinetics and the respective changes under elevated pCO_2, the relative dominance may shift in low nutrient oceanic waters. *S. trochoidea* could prevail in numbers where it co-occurs with *A. fundyense*, showing higher DIN affinities (i.e. a lower $K_{1/2}$) over the whole range of the applied pCO_2 (Fig. 7). Furthermore, *S. trochoidea* can sustain a higher maximum growth rate under nutrient-replete conditions, and higher cell abundances at a higher dilution rate under nutrient-limiting conditions in continuous culture experiments, which may allow it to outgrow *A. fundyense*. Nonetheless, other traits can have a severe effect on the outcome of such experiments as well. For instance, the production of allelopathic compounds of *A. fundyense* can trigger encystment of *S. trochoidea* (Fistarol et al. 2004). In our continuous culture systems with a fixed dilution rate, this would automatically lead to a loss of *S. trochoidea* and allow *A. fundyense* to prevail.

With respect to the natural environment, predicting the competitive ability and subsequent dominance of species in future ocean waters is difficult, firstly, because the ocean is much more complex than our applied indoor experiments and secondly, due to the various species-specific traits which can be found among dinoflagellates and the lack of knowledge on the impact of global change on such. Regarding toxin production (PSP toxins), which is one these traits, N limitation had an expected negative effect in *A. fundyense.* Measured quotas were about four times lower compared to N-replete conditions (Van de Waal et al. 2014), this negative effect was reduced when *A. fundyense* was exposed to elevated pCO_2 (*publication II*). Contributions of the toxin analogues STX and GTX1+4 to total toxin content of *A. fundyense* under N-limited conditions and increasing pCO_2 showed opposite trends than those observed und N-replete conditions (Van de Waal et al. 2014). To my knowledge, there has so far no mechanism been described that could explain such changes in sulfonated PSP toxin synthesis. In view of the increasing number of reports on HAB events, there is a great need to understand the impacts of global change on PSP toxin synthesis (Fu et al. 2012), particularly as OA may not only alleviate the negative effects of N limitation on dinoflagellate species in general, but furthermore facilitate the synthesis of N-rich compounds such PSP toxins (*publication II*).

Besides toxin production, mixotrophy may play an important role in the competition for resources as well, particularly when available inorganic resources are reduced to very low concentrations. For instance, in a summer bloom in Masan Bay, Korea, mixotrophy determined the succession among dinoflagellate species, and while *P. minimum* and *P. triestinum* fed on *Amphidinium carterae*, the species *C. polykrikoides* and *P. micans* fed on *H. akashiwo* (Jeong et al. 2005). *A. fundyense* and *S. trochoidea* have as well been reported to feed on various phytoplankton species by engulfing their prey, including *Amphidinium*

carterae, *Prorocentrum minimum* (Jeong et al. 2005). The effect of OA on nutrient assimilation and feeding behavior among dinoflagellates has to my knowledge not been investigated. Yet, under nutrient-limiting conditions, mixotrophy may be the driving force in the succession of dominant species. Future experiments could approach this question by performing multi species experiments with the co-existing *A. fundyense* and *S. trochoidea* and build on the knowledge one has on these two species as described in this thesis.

So far, most of our knowledge is based on short-term single species experiments, which tested individual environmental drivers over a relatively short time scales (Riebesell and Tortell 2011). To forecast implications for ecosystems from such experiments is limited, because multiple changes could hamper the prediction based on these kind of "bottle experiments". Although large-scale experiments on plankton communities are difficult to interpret and require large teams, they still allow multiple environmental drivers to interact (Kroeker et al. 2010; Riebesell and Gattuso 2015). Hence, having started with such single species and single environmental driver experiments and the approach towards a process-based understanding (p*ublication I and II*), I then participated in a mesocosm experiment in Sweden to investigate the potential effects of OA on entire phytoplankton communities. This KOSMOS 2013 mesocosm experiment was designed to capture potential effects of OA on a coastal, winter to summer plankton succession. The long-term experiment furthermore provided an opportunity to investigate the effects of OA on mixotrophic dinoflagellates, which were often shown to bloom in these waters towards the end of the phytoplankton succession under low nutrient conditions, imposing a strong grazing pressure, e.g. controlling the growth of diatoms (Tiselius and Kuylenstierna 1996). The experiment followed a plankton succession for 109 days during which time two phytoplankton blooms were observed. While nutrients were reduced to very low concentrations and terminated the first

bloom, a second bloom appeared under NO_3^--limited conditions (Fig. 8). During both bloom events, total primary production seemed to be higher under OA, but this applied only to a marginally significant increase during the peak of the second phytoplankton bloom (t53-t61; Fig. 8; *publication III*). An enhanced effect of elevated pCO_2 on phytoplankton productivity under nutrient limitation has been described earlier (Egge et al. 2009; Paul et al. 2015; Sala et al. 2015) and indicate the need of multiple stressor experiments to unravel the impact of OA on natural phytoplankton assemblages (*publication II*).

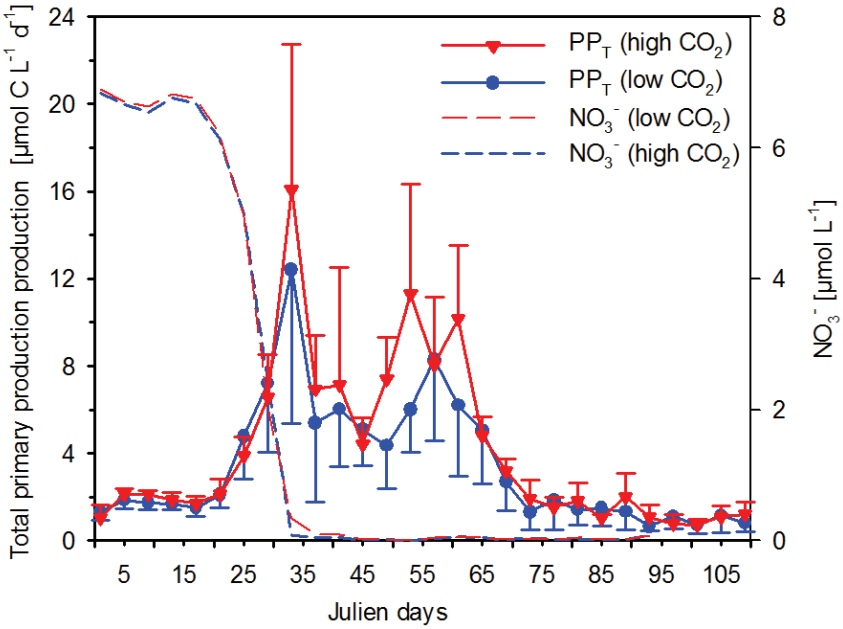

Fig. 9: Total primary production (PP_T; from ^{14}C based 24 h incubations) and NO_3^- concentrations in the mesocosms. Triangles (red; high CO_2) and circles (blue; low CO_2) represent the mean PP_T and ± SD of five biological replicates. Dashed lines show NO_3^- measurements from every other day (nutrient data from *E. Achterberg*).

Both blooms in the mesocosms as well as in the fjord where most of the time dominated by diatoms (Bach et al. 2016). Dinoflagellates were observed in the Gullmar Fjord during the experimental period as well. Life cycles of dinoflagellates often include the formation of cysts, which may follow sexual reproduction or allow them to resist unfavorable

environmental conditions such as low light and temperatures (Head 1996). To account for dinoflagellates emerging from cysts later in the season and other species coming up during the phytoplankton succession in the fjord, a so-called "seeding" took place every fourth day, during which 22 L of seawater, which was collected with a submersible pump down to a depth of about 19 meter in the fjord, were transferred to each mesocosm (Bach et al. 2016). Compared to a total mesocosm water volume of about 50 m^3, the seeded volumes (about 0.3 %) were presumably too small to sufficiently introduce dinoflagellates into the mesocosms. Thus, a dinoflagellate bloom did not occur in the mesocosms, which would otherwise have allowed us to test some of our ideas emerging from *publication II*.

Regarding the performed photosynthesis versus irradiance (P/I) curves during the Gullmar Fjord experiment, no apparent effect of OA on photoacclimation parameters of the phytoplankton community was detected (*publication III*). This could be of advantage for future field work, indicating that the use of pre-defined light levels during ^{14}C incubations for 24 h may, if at all, have only a minor effect on the outcome and analysis of the results. We therefore suggest that 24 h incubations with fixed light levels such as we performed in *publication III* may be adequate to determine potential effects of OA on primary production.

3.2 Conclusion

The use of single species and single environmental drivers in laboratory experiments gives us specific insight into eco-physiological changes, e.g. towards OA. Such process-based understanding, even if obtained for many different key species, will not allow us to forecast phytoplankton prevalence in a future ocean, recalling that the world is not as simple as a bottle. A multitude of species (and genotypes) in a natural environment respond to a

multitude of alterations at the same time and it remains unclear how additional environmental drivers may influence the effects caused by OA. Therefore, to be more precise in anticipating responses of phytoplankton to global change, it is unavoidable to account for potential interactions among physical, chemical and biological drivers as well. After all, aspects such as competition, grazing, and invasion also affect the success of a species in the oceans. Experiments on natural phytoplankton communities, which consider several of these aspects, are rare and still in need of improvement (e.g. regarding invasion: see our unsuccessful attempt to introduce dinoflagellates to the mesocosms). Interpretation of the results is challenging, as these large-scale experiments often miss an understanding of underlying processes. So each approach is (so far) not expedient on its own and future attempts should try to put the knowledge gained from these different approaches together into one big picture. One way to assess the impacts of OA on HABs or marine phytoplankton communities in general is to synthesize information from short and long-term studies, single and multiple species experiments as well as laboratory and field studies with respect to multiple environmental drivers in order to ‘tighten the noose’ around our target (Fig. 9).

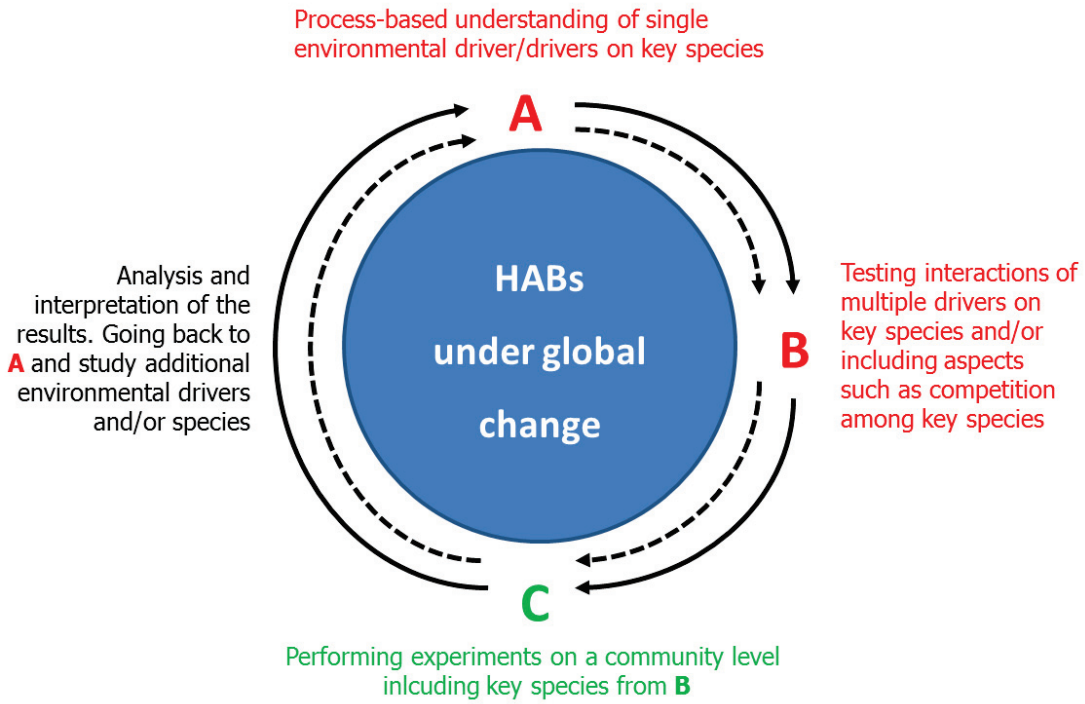

Fig. 10: Schematic overview of how to approach the impacts of global change on HABs. Red color indicates the attempts to gain a process-based understanding (normally laboratory-based bottle experiments), green color indicates large-scale outdoor experiments.

This brings us back to the central question of the thesis: "Will there be *good tidings for red tides*?" My findings support the line of reasoning that dinoflagellates are among those taxa that also have the capability to adjust their CCM under OA. Although *A. fundyense* and *S. trochoidea* did not invest their potential energy savings from a down regulated CCM into growth, they can presumably redirect it into other processes when facing unfavorably nutrient conditions. This may be of advantage since OA will most likely be accompanied by nutrient limitation in the surface oceans through an increased thermal stratification. Under N limitation, species invested in 'biomass quality' (i.e. lower cell abundances with a PON content similar to N-replete conditions) rather than 'biomass quantity' (i.e. higher cell abundances with a reduced PON content), which might be of an advantage for PSP toxin producing *A. fundyense*. Under grazing pressure, PSP toxins may provide a defensive role

and reduce its mortality rate compared to non-toxic species (Wohlrab et al. 2010). Yet, at the same time, affinities for DIN uptake was lowered, decreasing the competitive ability for N assimilation of both tested dinoflagellates. Thus, when competing with other species, which show an unaltered or even increased affinity for N, the *tidings may be not so good*.

In the end, our knowledge is still too limited to make robust forecasts on HABs in a future ocean. Based on their large variety of physiological traits and their possibility to adapt to future ocean conditions being investigated in this thesis, I am positive that dinoflagellates will persist or even gain an advantage under global change. The more we learn about this group, the more we will be astonished about the unexpected features.

4. References

Anderson, D. M., J. M. Burkholder, W. P. Cochlan, P. M. Glibert, C. J. Gobler, C. A. Heil, R. M. Kudela, M. L. Parsons, J. E. J. Rensel, D. W. Townsend, V. L. Trainer, and G. A. Vargo. 2008. Harmful algal blooms and eutrophication: Examining linkages from selected coastal regions of the United States. Harmful Algae 8: 39–53.

Anderson, D. M., A. D. Cembella, and G. M. Hallegraeff. 2012*a*. Progress in understanding Harmful algal blooms: Paradigm shifts and new technologies for research, monitoring, and management. Annu. Rev. Marine Sci. 4:143-176.

Anderson, D. M., T. J. Alpermann, A. D. Cembella, Y. Collos, E. Masseret, M. Montresor. 2012*b*. The globally distributed genus *Alexandrium*: multifaceted roles in marine ecosystems and impacts on human health. Harmful Algae 14: 10–35.

Badger, M. R., T. J. Andrews, S. M. Whitney, M. Ludwig, D. C. Yellowlees, W. Leggat, and G. D. Price. 1998. The diversity and coevolution of Rubisco, plastids, pyrenoids, and chloroplast-based CO_2-concentrating mechanisms in algae. Can. J. Bot. 76: 1052–1071.

Bach, L.T., J. Taucher, T. Boxhammer, A. Ludwig, The Kristineberg KOSMOS Consortium, E.P. Achterberg, et. al. Influence of Ocean Acidification on a Natural Winter-to-Summer Plankton Succession: First Insights from a Long-Term Mesocosm Study Draw Attention to Periods of Low Nutrient Concentrations. PLoS ONE. 2016; 11(8). e0159068.

Beardall, J., and M. Giordano. 2002. Ecological implications of microalgal and cyanobacterial CO_2 concentrating mechanisms, and their regulation. Funct. Plant. Biol. 29: 335–347.

Beardall, J. and J. A. Raven. 2004. The potential effects of global climate change on microalgal photosynthesis, growth and ecology. Phycologia 43(1): 26-40.

Behrenfeld, M. J., R. T. O'Malley, D. A. Siegel, C. R. McClain, J. L. Sarmiento, G. C. Feldman, A. J. Milligan, P. G. Falkowski, R. M. Letelier, and E. S. Boss. 2006. Climate-driven trends in contemporary ocean productivity. Nature 444: 752-755.

Beman, J. M., C.-E. Chow, A. L. King, Y. Feng, J. A. Fuhrman, A. Andersson, N. R. Bates, B. N. Popp, and D. A. Hutchins. 20011. Global declines in oceanic nitrification rates as a consequence of ocean acidification. PNAS 108(1): 208-213.

Berner, R. A. 1997. The rise of plants and their effect on weathering and atmospheric CO_2. Science. 276(5312): 544-546.

Boyer, G. L., J. J. Sullivan, , R. J. Anderson, P. J. Harrison, and F. J. R. Taylor. 1987. Effects of nutrient limitation on toxin production and composition in the marine dinoflagellate *Protogonyaulax tamarensis*. Mar. Biol. 96: 123–128.

Burkholder, J. M. 1998. Implications of harmful microalgae and heterotrophic dinoflagellates in management of sustainable marine fisheries. Ecol. Appl. 8: 37–S62.

Caldeira, K., and M. E. Wickett. 2003. Anthropogenic carbon and ocean pH. Nature 425(6956): 365–365.

Capone, D. G., J. P. Zehr, H. W. Paerl, B. Bergman, and E. J. Carpenter. 1997. *Trichodesmium*, a globally significant marine cyanobacterium. Science. 276: 1221-1229.

Cembella, A. D. 1998. Ecophysiology and metabolism of paralytic shellfish toxins in marine microalgae, p. 281–403 *In*: D. M. Anderson, A. D. Cembella, and G. M. Hallegraeff [eds.], Physiological ecology of harmful algal blooms. Springer-Verlag.

Colman, B., I. E. Huertas, S. Bhatti, and J. S. Dason. 2002. The diversity of inorganic carbon acquisition mechanisms in eukaryotic microalgae. Funct. Plant. Biol. 29: 261–270.

Dason, J. S., I. E. Huertas, and B. Colman. 2004. Source of inorganic carbon for photosynthesis in two marine dinoflagellates. J. Phycol. 40: 229–434.

De La Rocha, C. L., and U. Passow. 2007. Factors influencing the sinking of POC and the efficiency of the biological carbon pump. Deep-Sea Res II 54: 639–658.

Dickson, A. G. 1981. An exact definition of total alkalinity and a procedure for the estimation of alkalinity and total inorganic carbon from titration data. Deep Sea Research Part A. 28(6): 609–623.

Doney, S. C., V. J. Fabry, R. A. Feely, and J. A. Kleypas. 2009. Ocean acidification: The other CO_2 problem. Annu. Rev. Mar. Sci. 1:169–92.

Dugdale R. C., and J. J. Goering. 1967. Uptake of new and regenerated forms of nitrogen in primary productivity. Limnol. Oceanogr. 12(2): 196-206.

Egge, J. K., T. F. Thingstad, A. Larsen, A. Engel, J. Wohlers, R. G. J. Bellerby, and U. Riebesell. 2009. Primary production during nutrient-induced blooms at elevated CO_2 concentrations. Biogeosciences 6: 877-885.

Elser, J. J., M. E. S. Bracken, E. E. Cleland, D. S. Gruner, W. S. Harpole, H. Hillebrand, J. T. Ngai, E. W. Seabloom, J. B. Shurin, and J. E. Smith. 2007. Global analysis of nitrogen and phosphorus limitation of primary producers in freshwater, marine and terrestrial ecosystems. Ecol. Lett. 10: 1135–1142.

Eppley, R. W. and B. J. Peterson. 1979. Particulate organic matter flux and planktonic new production in the deep ocean. Nature 282: 677-680.

Falkowski, P. G. and J. A. Raven. 1997. Aquatic photosynthesis. Blackwell Scientific Publishers, Oxford. 375 pp.

Falkowski, P. G., R. T. Barber, and Victor Smetacek. 1998. Biogeochemical controls and feedbacks on ocean primary production. Science 281: 200-206.

Falkowski, P. G., R. J. Scholes, E. Boyle, J. Canadell, D. Canfield, J. Elser, N. Gruber, K. Hibbard, P. Högberg, S. Linder, F. T. Mackenzie, B. Moore III, T. Pedersen, Y. Rosenthal, S. Seitzinger, V. Smetacek, and W. Steffen. 2000. The global carbon cycle: A test of our knowledge of earth as a system. Science 290(5490): 291-296.

Fistarol, G. O., C. Legrand, K. Rengefors, and E. Graneli. 2004. Temporary cyst formation in phytoplankton: a response to allelopathic competitors? Environ. Microbiol. 6(8): 791-798.

Flynn K. J. 1991. Algal carbon-nitrogen metabolism: a biochemical basis for modelling the interactions between nitrate and ammonium uptake. J. Plankton. Res. 13(2): 373-387.

Fu, F.-X., A. O. Tatters, and D. A. Hutchins. 2012. Global change and the future of harmful algal blooms in the ocean. Mar. Ecol. Prog. Ser. 470: 207–233.

Giordano, M., J. Beardall, and J. A. Raven. 2005. CO_2 concentrating mechanisms in algae: mechanisms, environmental modulation, and evolution. Annu. Rev. Plant. Biol. 56: 99–131.

Glibert, P. M., E. Mayorga, and S. Seitzinger. 2008. *Prorocentrum minimum* tracks anthropogenic nitrogen and phosphorus inputs on a global basis: application of spatially explicit nutrient export models. Harmful Algae 8: 33–38

Granéli, E. and J. T. Turner. 2006. Ecology of Harmful Algae. Springer-Verlag, Berlin, Germany

Hansen, J., M. Sato, R. Ruedy, K. Lo, D. W. Lea, and M. Medina-Elizade. 2006. Global temperature change. PNAS 103 (39): 14288-14293.

Hansen, P. J., N. Lundholm, B. Rost. 2007. Growth limitation in marine red-tide dinoflagellates: effects of pH versus inorganic carbon availability. Mar. Ecol. Prog. Ser. 334: 63–71

Head, M. J. 1996. Modern dinoflagellate cysts and their biological affinities. In Jansonius, J. & McGregor, D.C. [eds.], Palynology: principles and applications. American Association of Stratigraphic Palynologists Foundation 3: 1197-1248.

Henderson, C. 2006. Ocean acidification: the other CO_2 problem. New Scientist.

Herr, D., K. Isensee, E. Harrould-Kolieb, and C. Turley. 2014. Ocean Acidification: International Policy and Governance Options. Gland, Switzerland: IUCN.

Hutchins, D. A., M. R. Mulholland, and F. Fu. 2009. Nutrient cycles and marine microbes in a CO_2-enriched ocean. Oceanography 22(4): 128-145.

IPCC 1999. Climate Change 1992: The supplementary report to the IPCC scientific assessment. J. Leggett, W.J. Pepper, R.J. Swart, J. Edmonds, L.G. Meira Filho, I. Mintzer, M.X. Wang, and J. Watson. 1992. Emissions Scenarios for the IPCC: an Update. Cambridge University Press, UK, pp. 68-95.

IPCC. 2013. Climate change 2013: The physical science basis. Contribution of working group I to the fifth assessment report of the intergovernmental panel on climate change. Stocker, T. F., D. Qin, G.-K. Plattner, M. Tignor, S. K. Allen, J. Boschung, A. Nauels, Y. Xia, V. Bex, and P. M. Midgley [eds.]. Cambridge University Press.

Jeong, H. J., Y. D. Yoo, J. Y. Park, J. Y. Song, S. T. Kim, S. H. Lee, K. Y. Kim, and W. H. Yih. 2005. Feeding by phototrophic red-tide dinoflagellates: five species newly revealed and six species previously known to be mixotrophic. Aquat Microb Ecol 40: 133–150.

John, U., R. Wayne Litaker, M. Montresor, S. Murray, M. L. Brosnahan, and D. M. Anderson. 2014. Formal revision of the *Alexandrium tamarense* species complex (Dinophyceae) Taxonomy: The introduction of five species with emphasis on molecular-based (rDNA) classification. Protist 65(6): 779–804.

Karl, T.R. and K. E. Trenberth. 2003. Modern Global Climate Change. Science 302: 1719-1723.

Katz, M. E., Z. V. Finkel, D. Grzebyk, A. H. Knoll, and Paul G. Falkowski. 2004. Evolutionary trajectories and biogeochemical impacts of marine eukaryotic phytoplankton. Annu. Rev. Ecol. Evol. Syst. 35: 523–556.

Klausmeier, C.A., E. Litchman, T. Daufresne, and S. A. Levin. 2004. Optimal nitrogen-to-phosphorus stoichiometry of phytoplankton. Nature 429: 171–174.

Kremp, A., A. Godhe, J. Egardt, S. Dupont, S. Suikkanen, S. Casabianca, and A. Penna. 2012. Intraspecific variability in the response of bloom-forming marine microalgae to changed climate conditions. Ecol. Evol. 2: 1195–1207.

Kroeker, K. J., R. L. Kordas, R. N. Crim, and G. G. Singh. 2010. Meta-analysis reveals negative yet variable effects of ocean acidification on marine organisms. Ecol. Lett. 13: 1419–1434.

Leggat, W., M. R. Badger, and D. Yellowlees. 1999. Evidence for an inorganic carbon-concentrating mechanism in the symbiotic dinoflagellate *Symbiodinium sp*. Plant Phys. 121: 1247–1255.

Le Quéré, C., O. Aumont, P. Monfray, and J. Orr. 2003. Propagation of climatic events on ocean stratification, marine biology, and CO_2: Case studies over the 1979–1999 period. J. Geophys. Res. 108: C12, 3375.

Levitus, S., J. I. Antonov, T. P. Boyer, O. K. Baranova, H. E. Garcia, R. A. Locarnini, A. V. Mishonov, J. R. Reagan, D. Seidov, E. S. Yarosh, and M. M. Zweng. 2012. World ocean heat content and thermosteric sea level change (0–2000 m), 1955–2010. Geophys. Res. Lett. 39: L10603.

Lüthi, D., M. Le Floch, B. Bereiter, T. Blunier, J.-M. Barnola, U. Siegenthaler, D. Raynaud, J. Jouzel, H. Fischer, K. Kawamura, and T. F. Stocker. 2008. High-resolution carbon dioxide concentration record 650,000–800,000 years before present. Nature 453: 379-382.

McCollin, T., D. Lichtman, E. Bresnan, and B. Berx. 2011. A study of phytoplankton communities along a hydrographic transect on the north east coast of Scotland. Marine Scotland Science Report 04/11, Marine Scotland, Aberdeen.

MacIntyre, J. G., J. J. Cullen, and A. D. Cembella. 1997. Vertical migration, nutrition and toxicity in the dinoflagellate *Alexandrium tamarense*. Mar Ecol Prog Ser 148: 201–216.

Mahaffey, C., A. F. Michaels, and D. G. Capone. 2005. The conundrum of marine N_2 fixation. Am. J. Sci. 305: 546-595.

Margalef, R. 1978. Life-forms of phytoplankton as survival alternatives in an unstable environment. Oceanologica Acta 1(4): 493-509.

Masseret, E., D. Grzebyk, S. Nagai, B. Genovesi, B. Lasserre, M. Laabir, Y. Collos, A. Vaquer, and P. Berrebi. 2009. Unexpected genetic diversity among and within populations of the toxic dinoflagellate *Alexandrium catenella* as revealed by nuclear microsatellite markers. Appl. Environ. Microbiol. 75(7): 2037-2045.

Moore, C. M., M. M. Mills, K. R. Arrigo, I. Berman-Frank, L. Bopp, P. W. Boyd, E. D. Galbraith, R. J. Geider, C. Guieu, S. L. Jaccard, T. D. Jickells, J. La Roche, T. M. Lenton, N. M. Mahowald, E. Marañón, I. Marinov, J. K. Moore, T. Nakatsuka, A. Oschlies, M. A. Saito, T. F. Thingstad, A. Tsuda, and O. Ulloa. 2013. Processes and patterns of oceanic nutrient limitation. Nat. Geosci. 6: 701–710.

Morse, D., P. Salois, P. Markovic, and J. W. Hastings. 1995. A nuclear-encoded form II RuBisCO in dinoflagellates. Science 268: 1622–1624.

NASA. 1994. Composition, chemistry, and climate of the atmosphere. Hanwant B. Singh [ed.] p 19-49.

Paul, A. J., L. T. Bach, K.-G. Schulz, T. Boxhammer, J. Czerny, E. P. Achterberg, D. Hellemann, Y. Trense, M. Nausch, M. Sswat, and U. Riebesell. 2015. Effect of elevated CO_2 on organic matter pools and fluxes in a summer Baltic Sea plankton community. Biogeosciences 12: 6181–6203.

Petit, J. R., J. Jouzel, D. Raynaud, N. I. Barkov, J.-M. Barnola, I. Basile, M. Bender, J. Chappellaz, M. Davisk, G. Delaygue, M. Delmotte, V. M. Kotlyakov, M. Legrand, V. Y. Lipenkov, C. Lorius, L. Pepin, C. Ritz, E. Saltzmank, and M. Stievenard. 1999. Climate and atmospheric history of the past 420,000 years from the Vostok ice core, Antarctica. Nature 399(6735): 429–436.

Polovina, J. J., E. A. Howell, and M. Abecassis. 2008. Ocean's least productive waters are expanding. Geophys. Res. Lett. 35: L03618, doi:10.1029/2007GL031745.

Ratti S., and M. Giordano. 2007. CO_2-concentrating mechanisms of the potentially toxic dinoflagellate *Protoceratium reticulatum* (Dinophyceae, Gonyaulacales). J. Phycol. 43: 693–701.

Raven, J.A., J. Beardall, and M. Giordano. 2014. Energy costs of carbon dioxide concentrating mechanisms in aquatic organisms. Photosynth. Res. 121: 111. doi:10.1007/s11120-013-9962-7

Redfield, A. C. "The biological control of chemical factors in the environment." American Scientist 46(3): 205–221.

Redfield, A. C., B. H. Ketchum, and F. A. Richards. 1963. The influence of organisms on the composition of sea-water. In M. N. Hill [ed.], Comparative and descriptive oceanography. The sea: ideas and observations on progress in the study of the seas.

Riebesell, U., and P. D. Tortell. 2011. Effects of ocean acidification on pelagic organisms and ecosystems. In: Gattuso, J. P. and L. Hansson (Eds.), Ocean Acidification. Oxford University Press, Oxford, UK, pp. 99–121.

Riebesell, U., and J.-P. Gattuso. 2015. Lessons learned from ocean acidification research. Nature 5: 12-14.

Rost, B., K.-U. Richter, U. Riebesell, and P. J. Hansen. 2006. Inorganic carbon acquisition in red tide dinoflagellates. Plant Cell Environ. 29: 810–822.

Rost, B., I. Zondervan, and D. A. Wolf-Gladrow. 2008. Sensitivity of phytoplankton to future changes in ocean carbonate chemistry: current knowledge, contradictions and research directions. Mar Ecol Prog Ser. 373: 227–237.

Sabine, C. L., and R. A. Feely. 2007. The oceanic sink for carbon dioxide. In D. S. Reay, N. Hewitt, J. Grace, and K. Smith [eds.], Greenhouse Gas Sinks. CABI Publishing.

Sala, M. M., F. L. Aparicio, V. Balagué, J. A. Boras, E. Borrull, C. Cardelús, L. Cros, A. Gomes, A. López-Sanz, A. Malits, R. A. Martínez, M. Mestre, J. Movilla, H. Sarmento, E. Vázquez-Domínguez, D. Vaqué, J. Pinhassi, A. Calbet, E. Calvo, J. M. Gasol, C. Pelejero, and C. Marrasé. 2015. Contrasting effects of ocean acidification on the microbial food web under different trophic conditions. Ices J. Mar. Sci. fsv130.

Sarmiento, J. L., R. Murnane, and C. Le Quéré. 1995. Air-sea CO_2 transfer and the carbon budget of the North Atlantic. Phil. Trans. R. Soc. Lond. B. 348: 211-219.

Sarmiento, J. L., R. Slater, R. Barber, L. Bopp, S. C. Doney, A. C. Hirst, J. Kleypas, R. Matear, U. Mikolajewicz, P. Monfray, V. Soldatov, S. A. Spall, and R. Stouffer. 2004. Response of ocean ecosystems to climate warming. Global. Biochem. Cy. 18: GB3003.

Schlitzer, R. 2000. Applying the adjoint method for biogeochemical modeling: Export of particulate organic matter in the World Ocean, inverse methods in biogeochemical cycles. Geophys. Monogr. Ser. 114: 107-124.

Smetacek, V. 1999. Diatoms and the Ocean Carbon Cycle. Protist 150: 25-32.

Tilman, D. 1976. Ecological competition between algae: Experimental confirmation of resource-based competition theory. Science 192 (4238): 463-465.

Tilman, D., S. S. Kilham, and P. Kilham. 1980. Phytoplankton Community Ecology: The Role of Limiting Nutrients. Annu. Rev. Ecol. Evol. Syst. 13: 349-372.

Tiselius, P., and M. Kuylenstierna. 1996. Growth and decline of a diatom spring bloom: phytoplankton species compesition, formation of a marine snow and the role of heterotrophic dinoflagellates. J Plankton Res. 18(2): 133-155.

Turley, C. and J.-P. Gattuso. 2012. Future biological and ecosystem impacts of ocean acidification and their socioeconomic-policy implications. Curr. Opin. Environ. Sustainability. 4: 278–286.

Van de Waal, D. B., U. Tillmann, M. Zhu, B. P. Koch, B. Rost, U. John. 2013. Nutrient pulse induces dynamic changes in cellular C:N:P, amino acids, and paralytic shellfish poisoning toxins in *Alexandrium tamarense.* Mar. Ecol. Prog. Ser. 493: 57–69.

Van de Waal, D. B., T. Eberlein, U. John, S. Wohlrab, and B. Rost. 2014. Impact of elevated pCO_2 on paralytic shellfish poisoning toxin content and composition in *Alexandrium tamarense*. Toxicon 78: 58–67.

Volk, T. and M. I. Hoffert. 1985. Ocean carbon pumps: Analysis of relative strengths and efficiencies in ocean-driven atmospheric CO_2 changes. In E.T. Sundquist and W.S. Broecker [eds.], The carbon cycle and atmospheric CO: natural variations Archean to present. American Geophysical Union, Washington, D. C.

Voss, M., H. W. Bange, J. W. Dippner, J. J. Middelburg, J. P. Montoya, and B. Ward. 2013. The marine nitrogen cycle: recent discoveries, uncertainties and the potential relevance of climate change. Phil. Trans. R. Soc. B 368: 20130121.

Waite, A. M., and O. Lindahl. 2006. Bloom and decline of the toxic flagellate *Chattonella marina* in a Swedish fjord. Mar. Ecol. Prog. Ser. 326: 77-83.

Walther, G.-R., E. Post, P. Convey, A. Menzel, C. Parmesank, T. J. C. Beebee, J.-M. Fromentin, O. Hoegh-Guldberg, and F. Bairlein. 2002. Ecological responses to recent climate change. Nature 416: 389-395.

Wells, M. L., V. L. Trainer, T. J. Smayda, B. S. O. Karlson, C. G. Trick, R. M. Kudela, A. Ishikawa, S. Bernard, A. Wulff, D. M. Anderson, and W. P. Cochlan. 2015. Harmful algal blooms and climate change: Learning from the past and present to forecast the future. Harmful Algae 49: 68–93.

Wiese, M., P. M. D'Agostino, T. K. Mihali, M. C. Moffitt, and B. A. Neilan. 2010. Neurotoxic alkaloids: Saxitoxin and its analogs. Mar. Drugs 8: 2185–2211.

Wohlrab, S., M. H. Iversen, and U. John. 2010. A Molecular and Co-Evolutionary Context for Grazer Induced Toxin Production in Alexandrium tamarense. PLoS ONE 5(11): e15039.

Wolf-Gladrow, D. A., R. E. Zeebe, C. Klaas, A. Körtzinger, and A. G. Dickson. 2007. Total alkalinity: The explicit conservative expression and its application to biogeochemical processes. Mar. Chem. 106: 287–300.

Young, N. J., A. M. C. Heureux, R. E. Sharwood, R. E. M. Rickaby, F. M.M. Morel, and S. M. Whitney. 2016. Large variation in the Rubisco kinetics of diatoms reveals diversity among their carbon-concentrating mechanisms. J. Exp. Bot.: 67 (11): 3445-3456.

Zeebe, R.E. and D. A. Wolf-Gladrow. 2001. CO_2 in seawater: equilibrium, kinetics, isotopes, Elsevier Science.

5. Appendix

5.1 **Publication:** Shake it easy: a gently mixed continuous culture system for dinoflagellates.

Journal of
Plankton Research
plankt.oxfordjournals.org

J. Plankton Res. (2014) 36(3): 889–894. First published online January 23, 2014 doi:10.1093/plankt/fbt138

SHORT COMMUNICATION

Shake it easy: a gently mixed continuous culture system for dinoflagellates

DEDMER B. VAN DE WAAL[1,2]*, TIM EBERLEIN[2], YVETTE BUBLITZ[2], UWE JOHN[3] AND BJÖRN ROST[2]

[1]DEPARTMENT OF AQUATIC ECOLOGY, NETHERLANDS INSTITUTE OF ECOLOGY (NIOO-KNAW), POST OFFICE BOX 50, 6700 AB WAGENINGEN, THE NETHERLANDS, [2]MARINE BIOGEOSCIENCES, ALFRED-WEGENER-INSTITUT HELMHOLTZ-ZENTRUM FÜR POLAR- UND MEERESFORSCHUNG, AM HANDELSHAFEN 12, 27570 BREMERHAVEN, GERMANY AND [3]ECOLOGICAL CHEMISTRY, ALFRED-WEGENER-INSTITUT HELMHOLTZ-ZENTRUM FÜR POLAR- UND MEERESFORSCHUNG, AM HANDELSHAFEN 12, 27570 BREMERHAVEN, GERMANY

*CORRESPONDING AUTHOR: d.vandewaal@nioo.knaw.nl

Received June 3, 2013; accepted December 28, 2013

Corresponding editor: John Dolan

An important requirement for continuous cultures is a homogeneous distribution of resources and microorganisms, often achieved by rigorous mixing. Many dinoflagellate species are known to be vulnerable to turbulence. Here, we present a newly developed continuous culture system based on gentle mixing in which the two dinoflagellate species *Scrippsiella trochoidea* and *Alexandrium tamarense*, with different turbulence sensitivities, grew well under steady state conditions. We also show that the continuous culture system can be applied at low nutrient conditions and low population densities.

KEYWORDS: continuous culture; nutrient limitation; chemostat; *Scrippsiella*; *Alexandrium*

Continuous cultures allow for a wide range of environmental factors to be tested under well-defined growth conditions, and have therefore contributed greatly to our understanding of microbial physiology and ecology (Monod, 1950; Novick and Szilard, 1950; Fredrickson, 1977; Huisman *et al.*, 2002; Bull, 2010). In conventional batch cultures, population growth will deplete one or more resources. Consequently, growth rates and resource concentrations can substantially change during the course of an experiment. In a continuous culture system, the population growth rate is controlled by the dilution rate (D). With a fixed dilution rate and a sufficiently low initial population density, resource conditions may support transient growth rates greater than the dilution

available online at www.plankt.oxfordjournals.org

JOURNAL OF PLANKTON RESEARCH | VOLUME 36 | NUMBER 3 | PAGES 889–894 | 2014

rate ($\mu > D$). As a consequence, population densities will increase until a resource becomes growth limiting, causing the net population growth rate to decrease until it equals dilution rate, and a so-called steady state is reached ($\mu = D$). Once in steady state, growth rate, resource conditions and population densities remain constant. Thus, net population growth is fixed by the dilution rate, which in turn controls the extent to which resources become limiting.

The application of continuous cultures has a long history (Monod, 1950; Novick and Szilard, 1950), and has been applied for a variety of organisms including bacteria, fungi, as well as phytoplankton (Bull, 2010). Continuous cultures have been used to study the impact of growth and resource limitation on phytoplankton physiology, for instance on their biochemical composition (Droop, 1974; Goldman *et al.*, 1979). Continuous cultures have also been applied to study ecological processes such as competition for various resources (Tilman, 1982; Passarge *et al.*, 2006; Van de Waal *et al.*, 2011), evolutionary processes like mutation and selection (Novick and Szilard, 1950; Rosenzweig *et al.*, 1994), and natural community dynamics (Harrison and Davis, 1979; Sommer, 1985; Hutchins *et al.*, 2003).

An important requirement of continuous cultures is a homogeneous distribution of resources and cells, needed for a representative dilution of the system. This is typically achieved by rigorous mixing via aeration and/or stirring. Clearly, this mixing should not negatively affect the species of interest. Here, we describe a continuous culture system based on gentle mixing, and test its applicability for two dinoflagellate species, *Alexandrium tamarense* and *Scrippsiella trochoidea*. Many dinoflagellate species are known to be vulnerable to turbulence, and often show decreased or even arrested growth rates (Berdalet *et al.*, 2007). Both species tested here have been shown to differ in their sensitivity to turbulence, with *A. tamarense* being insensitive to moderately sensitive (White, 1976; Sullivan and Swift, 2003) and *S. trochoidea* being highly sensitive (Berdalet and Estrada, 1993), especially to high shaking levels.

We grew *S. trochoidea* GeoB267 (culture collection of the University of Bremen) and *A. tamarense* Alex5 (Tillmann *et al.*, 2009) at 15°C in 0.2 μm filtered North Sea water (salinity 34) containing 18 μM NO_3^-, 0.8 μM NH_4^+ and 0.3 μM PO_4^{3-}. The seawater was enriched with vitamins, trace metals and 36 μM PO_4^{3-} according to the recipe of f/2 medium (Guillard and Ryther, 1962), with additional 10 nM H_2SeO_3 and 6.3 nM $NiCl_2$ according to the recipe of K medium (Keller *et al.*, 1987). In the first series of experiments, cultures were grown under high nutrient conditions, by adding 100 μM NO_3^- to the medium, which yielded an initial concentration of 118 μM NO_3^-. A second series of experiments was conducted under low nutrient conditions. In that case, the medium did not contain additional NO_3^-, which allowed us to test whether the continuous cultures are also applicable at low population densities. Culture medium was pre-aerated with moistened air containing 380 μatm CO_2 (Fig. 1). Cultures were grown in custom-made glass tubes (diameter 95 mm; length 370 mm) closed by Duran GLS80 caps at both ends, yielding a working volume of 2100 ± 50 mL. The glass tubes were placed on a three-dimensional orbital shaker (TL10; Edmund Bühler GmbH, Hechingen, Germany), set at an angle of 9° with a shaking speed of 16 rpm, to allow homogenous mixing (i.e. rocking) by moving a 55 mm diameter polyoximethylene ball and a 50–100 mL headspace back and forth (Fig. 1). Light was provided from above by day light tubes (18W/965 Biolux; OSRAM GmbH, München, Germany) at a light:dark cycle of 16:8 h and average

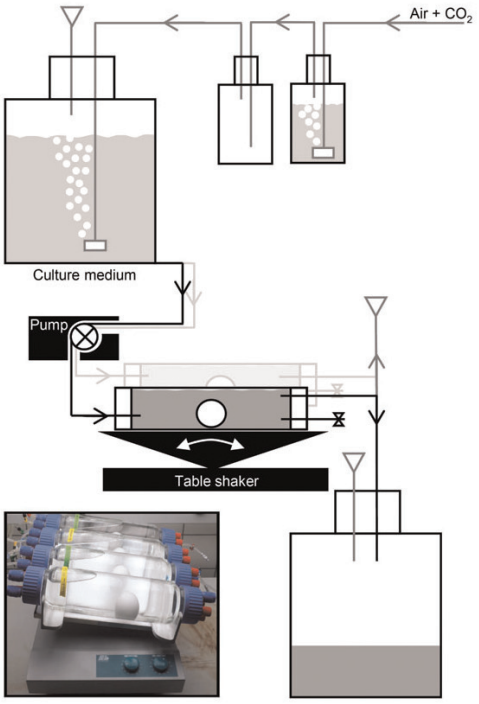

Fig. 1. Schematic overview of the continuous culture system. Culture medium is pre-aerated with humidified air containing 380 μatm CO_2. The culture medium is pumped at a fixed rate (i.e. dilution rate) into the culture vessel. Mixing in the culture vessels is achieved by gentle rocking, where ball and headspace move in opposite direction, covering the entire length of the vessel. The culture medium containing cell material runs out of the culture vessel by overpressure, and is transported to a waste container. The air outlet allows for stabilization of overpressure.

incident irradiance of 200 ± 25 μmol photons m^{-2} s^{-1}. Medium was continuously supplied using a peristaltic pump with a dilution rate $D = 0.14$ day^{-1} for the high nutrient incubation with *S. trochoidea*, and $D = 0.11$ day^{-1} for high nutrient incubation with *A. tamarense*. To further lower population densities in the low nutrient incubations, dilution rates were increased to $D = 0.2$ day^{-1}. Prior to the experiments, cells were acclimated to the respective culture medium and experimental conditions for at least seven generations.

Samples for population density, pH and dissolved inorganic nitrogen (DIN) were taken every second or third day, except for the *A. tamarense* high nutrient incubations for which no DIN samples were taken. Population densities were assessed as cell number and biovolume by means of automated cell counts, applying triplicate counts of 2×1 mL culture suspension with a Multisizer III Coulter Counter (Beckman-Coulter, Fullerton, CA, USA). Automatic cell counts were regularly confirmed by microscopic cell counts with an inverted light microscope (Axiovert 40C), using a settling chamber containing 0.2–10 mL culture suspension fixed with Lugol's solution (2% final concentration). Because cell volume changed during the transient phase, average growth rate was based on biovolume according to: $\mu = D + (\ln(N_2) - \ln(N_1))/(t_2 - t_1)$, where N_1 and N_2 represent the average total biovolumes at times t_1 and t_2, respectively (Bull, 2010). The calculated growth rate was corrected for the dilution rate by adding D. pH was measured with a pH electrode (Schott Instruments, Mainz, Germany), applying a two-point calibration on the NBS scale prior to each measurement. For DIN analyses (i.e. NO_3^-, NO_2^- and NH_4^+), 15 mL of culture suspension was filtered over a 0.45 μm membrane filter and duplicates were measured colorimetrically using an Evolution III continuous flow analyzer (Alliance Instruments, Salzburg, Austria) according to Grasshoff *et al.* (Grasshoff *et al.*, 1999).

Both dinoflagellate species grew well in the continuous culture system and showed a gradual increase in population density reaching steady state after 21–29 days at the high nutrient incubations (Fig. 2A and B), and after 14–17 days at the low nutrient incubations (Fig. 3A

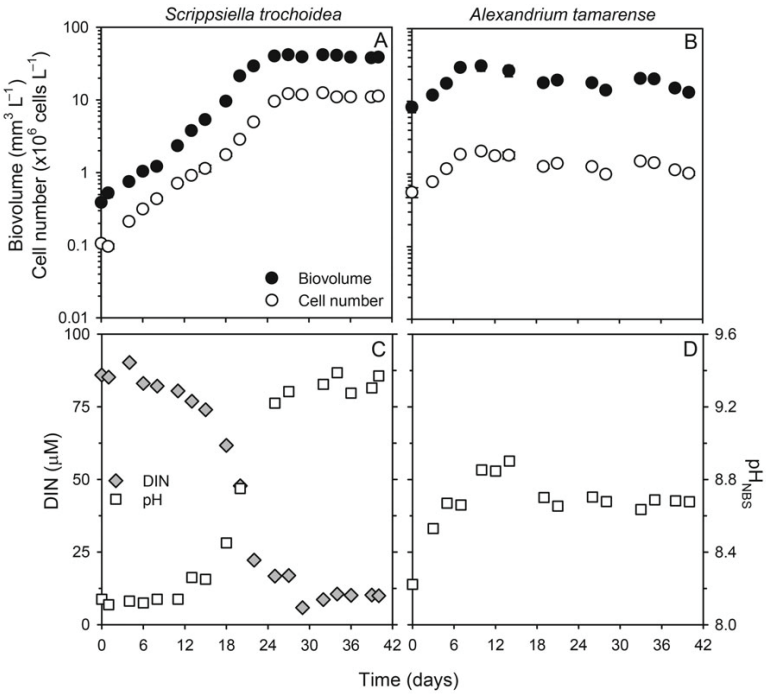

Fig. 2. Dynamic changes in population densities, given in cell number and biovolume, and pH in the high nutrient incubations of (**A** and **B**) *S. trochoidea*, and (**C** and **D**) of *A. tamarense*. For *S. trochoidea*, dissolved inorganic nitrogen (DIN) is also shown (C). Values for population densities indicate mean ± SD ($n = 3$).

JOURNAL OF PLANKTON RESEARCH | VOLUME 36 | NUMBER 3 | PAGES 889–894 | 2014

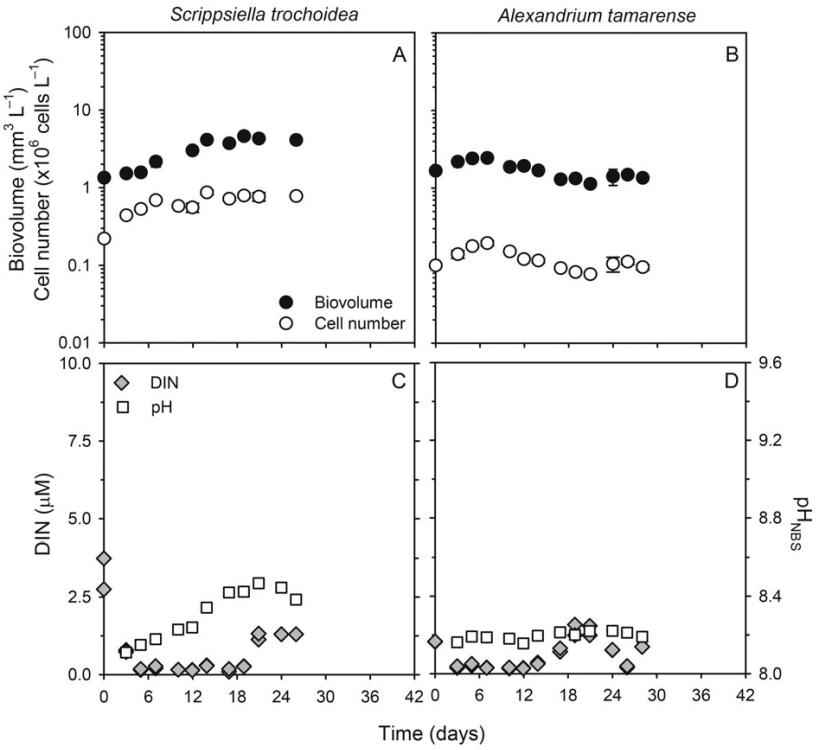

Fig. 3. Dynamic changes in population densities, given in cell number and biovolume, and dissolved inorganic nitrogen (DIN), and pH in the low nutrient incubations (**A** and **B**) of *S. trochoidea*, and (**C** and **D**) of *A. tamarense*. Values for population densities indicate mean ± SD ($n = 3$).

and B). The average growth rates achieved during the transient phase at the high nutrient incubations were 0.46 (0.31–0.64) day^{-1} for *S. trochoidea* and 0.33 (0.30–0.36) day^{-1} for *A. tamarense*, which were somewhat lower in the low nutrient incubations with 0.30 (0.22–0.36) day^{-1} for *S. trochoidea* and 0.27 (0.25–0.29) day^{-1} for *A. tamarense*. Relatively stable cell numbers were reached at steady state, with $11.5 \pm 0.2 \times 10^6$ cells L^{-1} and $1.3 \pm 0.1 \times 10^6$ cells L^{-1} in the high nutrient incubations, and $0.76 \pm 0.03 \times 10^6$ cells L^{-1} and $0.10 \pm 0.02 \times 10^6$ cells L^{-1} in the low nutrient incubations, for *S. trochoidea* and *A. tamarense*, respectively (Figs 2A and B, 3A and B). The associated biovolumes at steady state were 40.1 ± 1.5 mm^3 L^{-1} and 17.2 ± 2.9 mm^3 L^{-1} in the high nutrient incubations and 4.2 ± 0.3 mm^3 L^{-1} and 1.3 ± 0.1 mm^3 L^{-1} in the low nutrient incubations, for *S. trochoidea* and *A. tamarense*, respectively. In both *A. tamarense* incubations, we observed a slight decrease in population density prior to reaching steady state. This is presumably the result of initial cell growth towards higher population densities than can be sustained under the given experimental conditions. Consequently, cell growth and population densities decrease to a level where growth equals D, and steady state is reached.

Regular microscopic inspection throughout the experiment revealed no visual changes in cell morphology or motility of the dinoflagellate species tested, suggesting that there were no direct negative effects of the applied mixing. Furthermore, test batch experiments with the highly sensitive *S. trochoidea* under the same experimental conditions without shaking, with shaking but without the ball, or with shaking and with the ball, showed comparable growth rates as observed in our high nutrient incubation, yielding average growth rates of 0.51 (0.31–0.61) day^{-1}, 0.48 (0.25–0.65) day^{-1} and 0.46 (0.33–0.63) day^{-1}, respectively. Thus, growth of *S. trochoidea* does not seem to be affected by the induced mixing, which presumably also applies to *A. tamarense*. The growth rates attained during the transient phase of the high nutrient incubations are also consistent with values reported earlier in batch experiments with the same *A. tamarense*

strain, and another strain of *S. trochoidea* (Tillmann and Hansen, 2009). This further confirms that growth of both species remained unaffected by the mixing conditions applied. The lower growth rates during the transient phase in the low nutrient incubations are presumably caused by the low initial DIN concentrations, which limited growth even at the start of the experiment. It remains to be tested whether other dinoflagellates will also be unaffected by the mixing technique used. However, many dinoflagellates show a comparable or lower sensitivity towards turbulence as does *S. trochoidea* (Berdalet *et al.*, 2007, and references therein). It is thus likely that our continuous culture system will be applicable to many more dinoflagellate species.

The increase in biomass was associated with a decrease in DIN and an increase in pH (Figs 2C and D, 3C and D). In the high nutrient incubation with *S. trochoidea*, DIN decreased from about 86 μM measured at the start of the experiments to 10.2 ± 3.6 μM at steady state. At the same time, pH increased from about 8.1 to 9.33 ± 0.05 (Fig. 2C). In the high nutrient incubation with *A. tamarense*, pH increased from about 8.2 at the start to 8.68 ± 0.02 at steady state (Fig. 2D). In the low nutrient incubations, changes in pH were substantially smaller, increasing from about 8.1 at the start of the experiment to 8.43 ± 0.04 at steady state for *S. trochoidea*, while remaining stable around 8.20 ± 0.02 for *A. tamarense* (Fig. 3C and D). Also in terms of DIN, changes were much lower in the low nutrient incubation compared with the high nutrient incubation. More specifically, in the *S. trochoidea* culture, DIN decreased from about 3.3 μM measured at the start down to 0.73 ± 0.63 μM at steady state (Fig. 3C). In the low nutrient incubations with *A. tamarense*, DIN was about 1.0 μM at the start, decreased upon cell growth, but increased afterwards reaching 1.08 ± 0.37 μM at steady state (Fig. 3D). The increase in DIN at the end of the low nutrient incubations may be associated with a small decrease in population densities (observed for *A. tamarense*), or by bacterial mineralization of organic nitrogen, which may occur in non-axenic cultures. Under such low nutrient concentrations, fluctuations caused by minor shifts in nutrient uptake by the dinoflagellate species tested, or by bacterial mineralization of organic nitrogen, are relatively strong. Future experiments should proceed for a longer period in order to better assess the residual nutrient concentrations at steady state.

In the high nutrient incubations, increasing population densities not only caused a strong decrease in DIN (only available for *S. trochoidea*, Fig. 2C), but also a substantial increase in pH (Fig. 2C and D). Although initial NO_3 concentrations were lowered compared with full f/2 medium (118 μM compared with 883 μM), the concentrations were sufficiently high to support substantial biomass build-up. The high population densities also caused a pH drift towards values potentially affecting dinoflagellate growth, as has been demonstrated for the tested strain of *A. tamarense*, and for another strain of *S. trochoidea* (Tillmann and Hansen, 2009). Consequently, growth at steady state is presumable also controlled by the shift in carbonate chemistry. With the low nutrient incubations, we show that a lowering of the initial NO_3 concentration can prevent such a strong drift in carbonate chemistry and ensures that cultures become limited by DIN only, maintaining low and relatively stable population densities (Fig. 3).

Our findings presented here demonstrate that both *S. trochoidea* and *A. tamarense* are able to grow well towards stable population densities at steady state in the continuous culture system based on gentle mixing. Population densities and accompanied changes in carbonate chemistry can be modulated by changing the supply of nutrients, as well as by adjusting other chemical parameters such as pH or the CO_2 concentration used for aeration of the medium, which may prove valuable in testing the consequences of ocean acidification. We believe this gently mixed continuous culture system to be very suitable for eco-physiological studies with dinoflagellates and possibly other turbulence sensitive phytoplankton species as well.

ACKNOWLEDGEMENTS

The authors thank Janna Hölscher for assistance with the sample analyses, Karen Brandenburg for her help with the test batch experiments and Klaus-Uwe Richter for the fruitful discussions during the development of the new continuous culture system. We also thank three anonymous reviewers for their constructive comments.

FUNDING

This work was supported by BIOACID, financed by the German Ministry of Education and Research, and by the European Community's Seventh Framework Programme (FP7/2007–2013)/ERC grant agreement no. 205150 and contributes to EPOCA under the grant agreement no. 211384. D.B.v.d.W., B.R. and U.J. thank BIOACID, financed by the German Ministry of Education and Research.

REFERENCES

Berdalet, E. and Estrada, M. (1993) Effects of turbulence on several phytoplankton species. In Smayda, T. J. and Shimizu, Y. (eds), *Toxic*

JOURNAL OF PLANKTON RESEARCH | VOLUME 36 | NUMBER 3 | PAGES 889–894 | 2014

Phytoplankton Blooms in the Sea: Proceedings of the Fifth International Conference on Toxic Marine Phytoplankton. Elsevier, New York, USA.

Berdalet, E., Peters, F., Koumandou, V. L. *et al.* (2007) Species-specific physiological response of dinoflagellates to quantified small-scale turbulence. *J. Phycol.*, **43**, 965–977.

Bull, A. T. (2010) The renaissance of continuous culture in the post-genomics age. *J. Ind. Microbiol. Biotechnol.*, **37**, 993–1021.

Droop, M. R. (1974) The nutrient status of algal cells in continuous culture. *J. Mar. Biol. Assoc. U.K.*, **54**, 825–855.

Fredrickson, A. G. (1977) Behavior of mixed cultures of microorganisms. *Annu. Rev. Microbiol.*, **31**, 63–87.

Goldman, J. C., McCarthy, J. J. and Peavey, D. G. (1979) Growth-rate influence on the chemical composition of phytoplankton in oceanic waters. *Nature*, **279**, 210–215.

Grasshoff, K., Kremling, K. and Ehrhardt, M. (1999) *Methods of Seawater Analysis*. Wiley-VCH, Weinheim, Germany.

Harrison, P. J. and Davis, C. O. (1979) The use of outdoor phytoplankton continuous cultures to analyse factors influencing species selection. *J. Exp. Mar. Biol. Ecol.*, **41**, 9–23.

Guillard, R. R. and Ryther, J. H. (1962) Studies of marine planktonic diatoms: I. *Cyclotella nana* Hustedt, and *Detonula confervacea* (Cleve). *Gran. Can. J. Microbiol./Rev. Can. Microbiol.*, **8**, 229–239.

Huisman, J., Matthijs, H. C. P., Visser, P. M. *et al.* (2002) Principles of the light-limited chemostat: theory and ecological applications. *Antonie Van Leeuwenhoek*, **81**, 117–133.

Hutchins, D. A., Pustizzi, F., Hare, C. E. *et al.* (2003) A shipboard natural community continuous culture system for ecologically relevant low-level nutrient enrichment experiments. *Limnol. Oceanogr. Methods*, **1**, 82–91.

Keller, M. D., Selvin, R. C., Claus, W. *et al.* (1987) Media for the culture of oceanic ultraphytoplankton. *J. Phycol.*, **23**, 633–638.

Monod, J. (1950) La technique de culture continue, theorie et applications. *Annales d'Institute Pasteur*, **79**, 390–410.

Novick, A. and Szilard, L. (1950) Experiments with the chemostat on spontaneous mutations of bacteria. *PNAS*, **36**, 708–719.

Passarge, J., Hol, S., Escher, M. *et al.* (2006) Competition for nutrients and light: stable coexistence, alternative stable states, or competitive exclusion? *Ecol. Monogr.*, **76**, 57–72.

Rosenzweig, R. F., Sharp, R. R., Treves, D. S. *et al.* (1994) Microbial evolution in a simple unstructured environment: genetic differentiation in *Escherichia coli*. *Genetics*, **137**, 903–917.

Sommer, U. (1985) Comparison between steady-state and non-steady state competition: experiments with natural phytoplankton. *Limnol. Oceanogr.*, **30**, 335–346.

Sullivan, J. M. and Swift, E. (2003) Effects of small-scale turbulence on net growth rate and size of ten species of marine dinoflagellates. *J. Phycol.*, **39**, 83–94.

Tillmann, U., Alpermann, T. L., da Purificacao, R. C. *et al.* (2009) Intra-population clonal variability in allelochemical potency of the toxigenic dinoflagellate *Alexandrium tamarense*. *Harmful Algae*, **8**, 759–769.

Tillmann, U. and Hansen, P. J. (2009) Allelopathic effects of *Alexandrium tamarense* on other algae: evidence from mixed growth experiments. *Aquat. Microb. Ecol.*, **57**, 101–112.

Tilman, G. D. (1982) *Resource Competition and Community Structure*. Princeton University Press, Princeton, NJ, USA.

Van de Waal, D. B., Verspagen, J. M. H., Finke, J. F. *et al.* (2011) Reversal in competitive dominance of a toxic versus non-toxic cyanobacterium in response to rising CO_2. *ISME J.*, **5**, 1438–1450.

White, A. W. (1976) Growth inhibition caused by turbulence in the toxic marine dinoflagellate *Gonyaulax excavata*. *J. Fish. Res. Board Can.*, **33**, 2598–2602.

5.2 Publication: Impact of elevated pCO_2 on paralytic shellfish poisoning toxin content and composition in *Alexandrium tamarense*.

Toxicon 78 (2014) 58–67

Contents lists available at ScienceDirect

Toxicon

journal homepage: www.elsevier.com/locate/toxicon

Impact of elevated pCO_2 on paralytic shellfish poisoning toxin content and composition in *Alexandrium tamarense*

Dedmer B. Van de Waal [a,b,*], Tim Eberlein [b], Uwe John [c], Sylke Wohlrab [c], Björn Rost [b]

[a] Department of Aquatic Ecology, Netherlands Institute of Ecology (NIOO-KNAW), Post Office Box 50, 6700 AB Wageningen, The Netherlands
[b] Marine Biogeosciences, Alfred Wegener Institute for Polar and Marine Research, Am Handelshafen 12, 27570 Bremerhaven, Germany
[c] Ecological Chemistry, Alfred Wegener Institute for Polar and Marine Research, Am Handelshafen 12, 27570 Bremerhaven, Germany

ARTICLE INFO

Article history:
Received 16 May 2013
Received in revised form 15 November 2013
Accepted 20 November 2013
Available online 1 December 2013

Keywords:
Ocean acidification
Dinoflagellates
Harmful Algal Blooms
Saxitoxin
Gene regulation
Sulfur metabolism

ABSTRACT

Ocean acidification is considered a major threat to marine ecosystems and may particularly affect primary producers. Here we investigated the impact of elevated pCO_2 on paralytic shellfish poisoning toxin (PST) content and composition in two strains of *Alexandrium tamarense*, Alex5 and Alex2. Experiments were carried out as dilute batch to keep carbonate chemistry unaltered over time. We observed only minor changes with respect to growth and elemental composition in response to elevated pCO_2. For both strains, the cellular PST content, and in particular the associated cellular toxicity, was lower in the high CO_2 treatments. In addition, Alex5 showed a shift in its PST composition from a non-sulfated analogue towards less toxic sulfated analogues with increasing pCO_2. Transcriptomic analyses suggest that the ability of *A. tamarense* to maintain cellular homeostasis is predominantly regulated on the post-translational level rather than on the transcriptomic level. Furthermore, genes associated to secondary metabolite and amino acid metabolism in Alex5 were down-regulated in the high CO_2 treatment, which may explain the lower PST content. Elevated pCO_2 also induced up-regulation of a putative sulfotransferase *sxtN* homologue and a substantial down-regulation of several sulfatases. Such changes in sulfur metabolism may explain the shift in PST composition towards more sulfated analogues. All in all, our results indicate that elevated pCO_2 will have minor consequences for growth and elemental composition, but may potentially reduce the cellular toxicity of *A. tamarense*.

1. Introduction

Since the industrial revolution, atmospheric CO_2 levels are rising at an unprecedented rate (Solomon et al., 2007). This increase in atmospheric pCO_2 affects the carbonate chemistry of ocean waters, which shifts towards higher concentrations of CO_2 and bicarbonate (HCO_3^-), lower concentrations of carbonate (CO_3^{2-}), and a reduction in pH, i.e. ocean acidification (Caldeira and Wickett, 2003; Wolf-Gladrow et al., 1999). Such changes in ocean carbonate chemistry will have implications for phytoplankton that convert inorganic carbon into organic biomass. For instance, increasing concentrations of CO_2 and HCO_3^- were shown to promote phytoplankton growth and photosynthesis (Hein and SandJensen, 1997; Tortell et al., 2008), whereas decreasing pH and concentrations of CO_3^{2-} were hold responsible for the adverse effects observed in calcification (Beaufort et al., 2011; Riebesell et al., 2000).

* Corresponding author. Department of Aquatic Ecology, Netherlands Institute of Ecology (NIOO-KNAW), Post Office Box 50, 6700 AB Wageningen, Netherlands. Tel.: +31 317 473 553.
E-mail addresses: d.vandewaal@nioo.knaw.nl (D.B. Van de Waal), tim.eberlein@awi.de (T. Eberlein), uwe.john@awi.de (U. John), sylke.wohlrab@awi.de (S. Wohlrab), bjoern.rost@awi.de (B. Rost).

0041-0101/$ – see front matter © 2013 Elsevier Ltd. All rights reserved.
http://dx.doi.org/10.1016/j.toxicon.2013.11.011

Our current knowledge about the sensitivity of phytoplankton towards ocean acidification is almost entirely based on the work with diatoms, coccolithophores, and cyanobacteria (see Riebesell and Tortell, 2011). Relatively little is yet known about the responses of autotrophic dinoflagellates (Brading et al., 2011; Burkhardt et al., 1999; Van de Waal et al., 2013a), in particular of toxin producing species (Fu et al., 2010; Hallegraeff, 2010; Kremp et al., 2012). This is surprising because, among all eukaryotic phytoplankton species, dinoflagellates feature the primary carboxylating enzyme ribulose1,5-bisphosphate carboxylase/oxygenase (RubisCO) with lowest affinities for its substrate CO_2 (Badger et al., 1998). Thus, the predicted increase of CO_2 concentrations in the future ocean may particularly favour this group.

Some toxic dinoflagellate species can proliferate under favourable environmental conditions, thereby producing Harmful Algal Blooms (HABs) that may cause mass mortalities of fish, illness and death of marine mammals, seabirds, and humans (Anderson et al., 2012b; Granéli and Turner, 2006). Of all the dinoflagellate HAB species, the genus *Alexandrium* is among the most prominent with respect to the diversity and distribution of its globally widespread blooms (Anderson et al., 2012a). Moreover, *Alexandrium* blooms are often responsible for the outbreak of paralytic shellfish poisoning (PSP), which is caused by the neurotoxin saxitoxin (STX) and its analogues, from which neosaxitoxin (NEO), gonyautoxins (GTX1, 2, 3 and 4), C1 and C2 are often most abundant. Although non-sulfated STX and NEO are highly toxic (LD_{50} i.p. mice ~8 μg kg^{-1}), the addition of one sulfate group in GTXs reduces this toxicity by ~40%, and subsequent incorporation of a sulfonyl group in C1 + C2 reduces its toxicity by up to 99% (Wiese et al., 2010). Thus, the cellular toxicity of these PST producing HAB species is not only determined by their PST content, but also by the relative composition of the different PST analogues.

Toxin production by HAB species is strongly affected by changes in resource availabilities, such as light and nutrients (Cembella, 1998; Granéli and Flynn, 2006; Neilan et al., 2013; Sivonen and Jones, 1999; Van de Waal et al., 2013b). Current changes in ocean carbonate chemistry may have consequences as well. For instance, elevated pCO_2 was found to cause an increase or a decrease in the production of domoic acid by the diatom *Pseudo-nitzschia multiseries* (Sun et al., 2011; Trimborn et al., 2008). Elevated pCO_2 was also shown to affect the composition of karlotoxins in the dinoflagellates *Karlodinium veneficum*, which shifted towards a more toxic analogue (Fu et al., 2010). Furthermore, PST content and composition differentially changed in various *Alexandrium ostenfeldii* strains (Kremp et al., 2012). The observed responses in these studies have been attributed to CO_2-induced changes in growth and energy allocation, even though the mechanisms underlying the production and composition of these toxins remain unclear.

Here we investigated the impact of elevated pCO_2 on PST content and composition in two strains of *Alexandrium tamarense* (Alex5 and Alex2), which were isolated from the same population at the Scottish east coast of the North Sea (Alpermann et al., 2009; Tillmann et al., 2009). Both *A. tamarense* strains differ in their growth rate, PST content as well as in their PST composition, comprising distinct contributions of STX, NEO, C1 + C2, GTX and decarbamoylated dcSTX (Tillmann et al., 2009). Earlier experiments with these strains illustrated that their PST production as well as the regulation of their genome can be affected by abiotic and biotic factors such as nutrient availability and grazing (Van de Waal et al., 2013b; Wohlrab et al., 2010). Little is yet known about the regulation of genes involved in PST synthesis by dinoflagellates (Hackett et al., 2013), and no study thus far investigated the impact of elevated pCO_2 on toxin production and gene regulation in *A. tamarense*.

2. Materials and methods

2.1. Culture conditions

Cultures of *Alexandrium tamarense* Alex5 and Alex2 (Alpermann et al., 2009; Tillmann et al., 2009) were grown as dilute batch in 2.4 L air-tight borosilicate bottles. Filtered natural seawater (0.2 μm pore size; Satorius, Goettingen, Germany) was enriched with metals and vitamins according to the recipe of f/2-medium (Guillard and Ryther, 1962), except for $FeCl_3$ (1.9 μmol L^{-1}), H_2SeO_3 (10 nmol L^{-1}), and $NiCl_2$ (6.3 nmol L^{-1}). The added concentrations of NO_3 and PO_4^{3-} were 100 μmol L^{-1} and 6.25 μmol L^{-1}, respectively. Cultures were grown at a light:dark cycle of 16:8 h and an incident light intensity of 250 ± 25 μmol photons m^{-2} s^{-1} provided by daylight lamps (Lumilux HO 54W/965, Osram, München, Germany). Bottles were kept at 15 °C and placed on a roller table to avoid sedimentation. Prior to inoculation, the culture medium was equilibrated with air containing a pCO_2 of 180 μatm (~Last Glacial Maximum), 380 μatm (~present-day), 800 μatm (~2100 scenario), and 1200 μatm (>2100 scenario). Each treatment was performed in triplicate.

2.2. Carbonate chemistry

Carbonate chemistry was assessed by total alkalinity (TA), dissolved inorganic carbon (DIC), and pH_{NBS}. For TA analyses, 25 mL of culture suspension was filtered over glass-fibre filters (GF/F, ~0.6 μm pore size; Whatman, Maidstone, UK) and stored in gas-tight borosilicate bottles at 3 °C. Duplicate samples were analysed by means of potentiometric titrations using an automated TitroLine burette system (SI Analytics, Mainz, Germany). For DIC analyses, 4 mL culture suspension was filtered over cellulose-acetate filters (0.2 μm pore size; Thermo Fisher Scientific Inc. Waltham, USA), and stored headspace free in gas-tight borosilicate bottles at 3 °C. Duplicate samples for DIC were analysed colorimetrically with a QuAAtro autoanalyser (Seal Analytical, Mequon, USA). pH was measured immediately after sampling with a pH electrode (Schott Instruments, Mainz, Germany), applying a two-point calibration on the NBS scale prior to each measurement. Calculations of the carbonate system were based on TA and pH and performed with the program CO2sys (Pierrot et al., 2006). An average phosphate concentration of 6.4 μmol L^{-1} was assumed, the dissociation constant of carbonic acid was based on Mehrbach et al. (1973), refit by Dickson and Millero (1987), and the dissociation constant of sulfuric acid was taken from Dickson (1990).

2.3. Population densities and growth rate

In order to ensure dilute batch conditions, cell densities were kept below <400 cells mL $^{-1}$. Prior to the experiments, cells were acclimated to the respective CO_2 concentrations for at least 7 cell divisions. During the experiments, cell growth was followed for 8 days, a period comprising at least 4 cell divisions. Cell densities were determined daily or every other day by means of single or duplicate cell counts with an inverted light microscope (Axiovert 40C, Zeiss, Germany), using 1–18 mL culture suspension fixed with Lugol's solution (2% final concentration). Triplicate cell counts were performed on the last day of each experiment, i.e. on day 8. Growth rates were estimated from each biological replicate by means of an exponential function fitted through all cell counts over time, according to $N_t = N_0 \exp^{\mu t}$, where N_t refers to the population density at time t, N_0 to the population density at the start of the experiment, and μ to the growth rate (Figs. A.1 and A.2).

2.4. Organic carbon and nitrogen

For organic carbon and nitrogen analyses, 250–500 mL cell suspension was filtered over precombusted GF/F filters (12 h, 500 °C) and stored at −25 °C in precombusted Petri dishes. Prior to measurements, 200 μL of 0.2 N HCl (analytical grade) was added to the filters to remove all inorganic carbon, and filters were dried overnight. Filters were analysed on carbon and nitrogen content in duplicate on an Automated Nitrogen Carbon Analyser mass spectrometer (ANCA-SL 20-20, SerCon Ltd., Crewe, UK). Carbon production rates were estimated by multiplication of the organic carbon content with μ.

2.5. PST analogues

Different analogues of PSTs were analysed and included the non-sulfated STX, NEO and dcSTX, the mono-sulfated GTX1 + 4 and GTX2 + 3, and the di-sulfated C1 + C2. The cellular toxicity was estimated based on the cellular PST content and the relative toxicity of each PST analogue (Wiese et al., 2010). For analyses of the different PST analogues, 200–500 mL of culture suspension was filtered over polycarbonate filters (0.8 μm pore size; Whatman) and stored in Eppendorf tubes at −25 °C. Prior to analyses, cells were re-suspended in 1.2 mL 0.03 mol L $^{-1}$ acetic acid and lysed for 1 min with a Sonifier 250 ultrasonic probe (Branson Ultrasonics, Danbury, CT, USA). Subsequently, samples were transferred into new 1.5 mL reaction vials and centrifuged for 15 min at 10,000 g at 4 °C. The supernatant was transferred into an LC vial and analysed by liquid chromatography via fluorescence detection (LC-FD) with post-column derivatization (Krock et al., 2007).

2.6. RNA extraction

For RNA extraction, 500 mL of culture suspension was concentrated to 50 mL with a 10 μm mesh sized sieve, and subsequently centrifuged at 15 °C for 15 min at 4000 g. Cell pellets were immediately mixed with 1 mL 60 °C TriReagent (Sigma–Aldrich, Steinheim, Germany), frozen with liquid nitrogen and stored at −80 °C. Subsequently, cell suspensions were transferred to a 2 mL cryovial containing acid washed glass beads. Cells were lysed using a BIO101 FastPrep instrument (Thermo Savant, Illkirch, France) at maximum speed (6.5 m s $^{-1}$) for 2 × 30 s, with an additional incubation of 5 min at 60 °C in between. For RNA isolation, 200 μL chloroform was added to each vial, vortexed for 20 s and incubated for 10 min at room temperature. The samples were subsequently centrifuged for 15 min at 4 °C with 12,000 g. The upper aqueous phase was transferred to a new vial and 2 μL 5 M linear acrylamide, 10% volume fraction of 3 μmol L $^{-1}$ sodium acetate, and an equal volume of 100% isopropanol were added. Mixtures were vortexed and subsequently incubated overnight at −20 °C in order to precipitate the RNA. The RNA pellet was collected by 20 min centrifugation at 4 °C and 12,000 g. The pellet was washed twice, first with 70% ethanol and afterwards with 96% ethanol, air-dried and dissolved with 100 μL RNase free water (Qiagen, Hilden, Germany). The RNA sample was further cleaned with the RNeasy Kit (Qiagen) according to manufacturer's protocol for RNA clean-up including on-column DNA digestion. RNA quality check was performed using a NanoDrop ND-100 spectrometer (PeqLab, Erlangen, Germany) for purity, and the RNA Nano Chip Assay with a 2100 Bioanalyzer (Agilent Technologies, Böblingen, Germany) was performed in order to examine the integrity of the extracted RNA. Only high quality RNAs ($OD_{260}/OD_{280} > 1.8$ and $OD_{260}/OD_{230} > 1.8$) as well as RNA with intact ribosomal peaks (obtained from the Bioanalyzer readings) were used for microarrays.

2.7. Microarray hybridizations

For microarray hybridizations, RNA Spike-In Mix (Agilent, p/n 5188-5279) was added to the RNA samples prior to the labelling substances as an internal standard for hybridization performance (Agilent RNA Spike-In Kit protocol). 200 ng total RNA from samples was reversely transcribed, and the resulting cDNA was linear amplified into labelled cRNA (two-colour Low Input Quick Amp Labeling kit, p/n 5190-2306). Incorporation of labelled cytidine 5′-triphosphate (Perkin Elmer, Waltham, USA) into the cRNA from the 180, 380 and 800 μatm CO_2 treatments (Cy-3) as well as for the pooled reference cRNA (380 μatm CO_2, Cy-5) was verified photometrically using the NanoDrop ND1000 (PeqLab). Labelling efficiencies were calculated as pmol dye (ng cRNA) $^{-1}$. Microarray hybridizations of the 180, 380 and 800 μatm CO_2 treatments were carried out in biological triplicates against the reference pool using SureHyb hybridization chambers (Agilent, p/n G2534A). 300 ng of each Cy-3 and Cy-5 labelled cRNA was hybridized to 8 × 60 K custom-built microarrays (Agilent). Probe design was done using Agilent's eArray online platform. Following the Two-Color Microarray-based Gene Expression Analysis protocol (Agilent, p/n 5188-5242), hybridization was performed in a hybridization oven at 65 °C for 17 h at an agitation of 6 rpm. After hybridization, microarrays were disassembled in Wash Buffer 1 (Agilent, p/n 5188-5325), washed with Wash Buffer 1, Wash Buffer 2 (Agilent, p/n 5188-5326), acetonitrile (VWR, Darmstadt, Germany) and 'Stabilization and Drying Solution' (Agilent,

p/n 5185-5979) according to manufacturer's instructions. Stabilization and Drying Solution, an ozone scavenger, protects the Cy-dye signal from degradation. Arrays were immediately scanned with a G2505C microarray scanner (Agilent) using standard photomultiplier tube (PMT) settings and 3 μm scan resolution.

2.8. Data analysis

Normality and equality of variances of growth, elemental composition, and PST data were confirmed using the Shapiro-Wilk and Levene's test, respectively. Variables were log-transformed if this improved normality and the homogeneity of variances. Significant differences between strains and treatments were tested using a mixed effect two-way ANOVA, with CO_2 treatment as fixed factor and strain as random factor, and followed by post hoc comparison of the means using Tukey's HSD test ($\alpha = 0.05$; Quinn and Keough, 2002). For PST composition, significant differences between treatments were tested using a one-way ANOVA followed by post hoc comparison of the means using Tukey's HSD test.

Microarray raw data of Alex5 was extracted with Feature Extraction Software version 9.0 (Agilent), incorporating the GE2_105_Dec08 protocol. Array quality was monitored using the QC Tool v1.0 (Agilent) with the metric set GE2_QCMT_Feb07. Analysis was performed using GeneSpring 12 (Agilent). Raw data including LOWESS-normalized data were submitted to the MIAMExpress database hosted by the European Bioinformatics Institute (accession code E-MEXP-3946). Differential gene expression was evaluated using the GeneSpring GX software platform version 12 (Agilent). After combining biological replicates, the 180 and 800 μatm CO_2 treatments were tested against the 380 μatm CO_2 treatment using a one-way ANOVA. Genes were considered to be differential expressed when $P < 0.05$ and fold changes > 1.5. Obtained differential expressed genes were categorized according to KOG with the batch web CD-search tool (Marchler-Bauer et al., 2011) and an *e*-value cut-off of e^{-7}.

3. Results

3.1. Carbonate chemistry

The drift in carbonate chemistry as result of biomass built-up remained below 4% with respect to alkalinity and DIC in all incubations (Table B.1). The applied CO_2 treatments clearly differed from each other with respect to pCO_2 and pH throughout the experiment. In the incubations with Alex5, pCO_2 values ranged from 162 ± 24 μatm to 995 ± 248 μatm, accompanied by a pH of 8.50 ± 0.06 and 7.83 ± 0.12, respectively. For Alex2, pCO_2 values ranged from 151 ± 9 μatm to 1167 ± 112 μatm, which was accompanied by a pH of 8.51 ± 0.02 to 7.75 ± 0.04, respectively (Table B.1).

3.2. Growth and elemental composition

Alex2 clearly exhibited a lower growth rate (two-way ANOVA, $F_{1,16} = 287.0$, $P < 0.001$) and organic carbon production rate (two-way ANOVA, $F_{1,16} = 102.5$, $P = 0.002$) as compared to Alex5 (Table 1). Growth rates of Alex2 decreased by up to 25% (two-way ANOVA, $F_{3,16} = 7.2$, $P = 0.003$) and carbon production rates by up to 35% (two-way ANOVA, $F_{3,16} = 13.7$, $P < 0.001$) from the lowest to the higher pCO_2 treatments. Growth and carbon production rates of Alex5 remained largely unaffected in response to elevated pCO_2. The carbon content in both strains was comparable at the lowest CO_2 treatment and increased with elevated pCO_2 in Alex5. As a consequence, Alex5 contained more carbon in all but the lowest CO_2 treatment (two-way ANOVA, $F_{3,16} = 5.0$, $P = 0.012$). In both strains, the nitrogen content remained unaltered by the applied changes in pCO_2. The cellular nitrogen content of Alex5 was up to 79% higher as compared to Alex2 (two-way ANOVA, $F_{1,16} = 100.9$, $P = 0.002$), resulting in up to 33% lower C:N ratios (two-way ANOVA, $F_{1,16} = 51.9$, $P = 0.006$).

3.3. PST content and composition

Alex5 showed a substantially higher cellular PST content (two-way ANOVA, $F_{1,16} = 1041$, $P < 0.001$) and toxicity (two-way ANOVA, $F_{1,16} = 1035$, $P < 0.001$) as compared to Alex2 (Fig. 1). In both strains, cellular PST content and toxicity were significantly affected by elevated pCO_2 (Fig. 1), decreasing by up to 21% in Alex5 (two-way ANOVA, $F_{3,16} = 7.0$, $P = 0.004$) and 26% in Alex2 (two-way ANOVA, $F_{3,16} = 5.0$, $P = 0.009$). The most abundant PST analogues produced by both strains were C1 + C2, STX and NEO, contributing up to 74% and 98% of the total PSTs in Alex5 and Alex2, respectively (Fig. 2). Cellular contents of GTXs were lower, particularly in Alex2, and trace amounts of dcSTX (<0.3%) were found in Alex5 (data not shown). In

Table 1
Growth and elemental composition in the different CO_2 treatments. Values indicate mean (±S.D., $n = 3$). For each strain, significant differences between treatments are indicated by a different superscript letter (two-way ANOVA, $P < 0.05$).

	pCO_2 treatment	Growth (d^{-1})	C production (pg cell $^{-1}$ d^{-1})	C content (pg $cell^{-1}$)	N content (pg $cell^{-1}$)	C:N ratio (molar)
Alex5	180	0.41 (0.03)	1466 (76)^{a}	3169 (254)	642 (65)	5.8 (0.1)
	380	0.42 (0.03)	1676 (117)^{b}	3620 (308)	731 (25)	5.8 (0.3)
	800	0.43 (0.01)	1669 (55)^{b}	3455 (153)	703 (42)	5.7 (0.1)
	1200	0.44 (0.02)	1545 (61)^{ab}	3461 (165)	721 (40)	5.6 (0.1)
Alex2	180	0.24 (0.01)^{a}	702 (83)^{a}	2964 (283)	439 (14)	7.9 (0.8)^{a}
	380	0.20 (0.01)^{ab}	498 (25)^{b}	2455 (191)	401 (33)	7.1 (0.1)^{ab}
	800	0.18 (0.02)^{b}	434 (55)^{b}	2364 (37)	399 (5)	6.9 (0.2)^{b}
	1200	0.20 (0.03)^{b}	455 (47)^{b}	2342 (425)	409 (66)	6.7 (0.2)^{b}

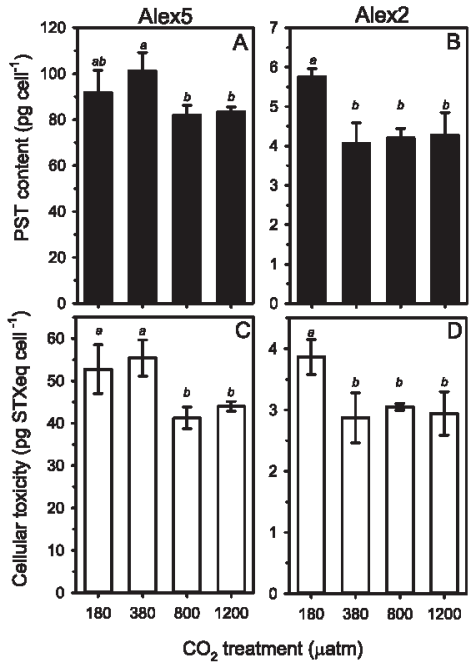

Fig. 1. PST content and cellular toxicity of Alex5 (A,C) and Alex2 (B,D) at the different CO_2 treatments. Error bars denote standard deviation ($n = 3$). Letters above bars indicate significant differences between treatments (two-way ANOVA, $P < 0.05$).

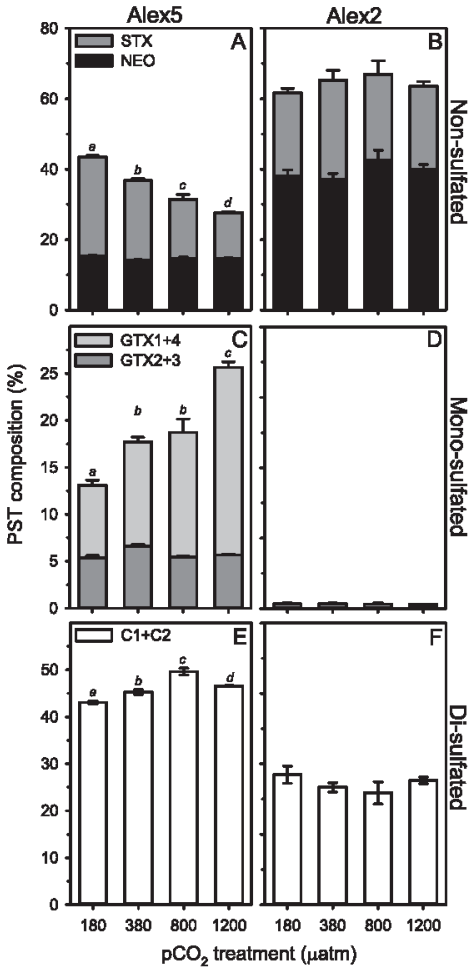

Fig. 2. Relative composition of PST analogues grouped as non-sulfated (A,B), mono-sulfated (C,D) and di-sulfated (E,F), in Alex5 (A,C,E) and Alex2 (B,D,F) at the different CO_2 treatments. Error bars denote standard deviation ($n = 3$). Letters above bars indicate significant differences between treatments of grouped toxins, as well as STX (A) and GTX1 + 4 (C) (one-way ANOVA, $P < 0.05$).

Alex2, the change in toxicity is caused by a reduction in toxin content, while its PST composition did not change (Fig. 2B,D,F). In Alex5, the PST composition was strongly affected by elevated pCO_2 (Fig. 2A,C,E). Specifically, the cellular contribution of non-sulfated STX decreased by 54% (one-way ANOVA, $F_{3,8} = 225.6$, $P < 0.001$), the mono-sulfated GTX1 + 4 increased by 159% (one-way ANOVA, $F_{3,8} = 109.4$, $P < 0.001$), and di-sulfated analogues C1 + C2 increased by 8% from the lowest to the highest CO_2 treatment (one-way ANOVA, $F_{3,8} = 98.4$, $P < 0.001$). This shift in PST composition towards less toxic analogues explains about half of the overall reduction in cellular toxicity of Alex5.

3.4. Gene expression profiles

A substantial number of genes in Alex5 were differentially expressed as compared to the control treatment (i.e. 380 µatm), with a total of 894 genes in the 180 µatm CO_2 and 1238 genes in the 800 µatm CO_2 treatment (Fig. 3A). Part of the regulated genes could be annotated and were grouped according to KOG categories representing various cellular functions (Figs. 3B and A.3; Appendix C). In both treatments, the highest number of regulated genes was related to the KOG categories 'Signal transduction mechanisms [T]' and 'Post-translational modification, protein turnover, chaperones [O]', together representing about 35% of the total number of annotated genes. Another 31% of the total number of annotated genes was associated to transport and metabolism of inorganic ions, carbohydrates, lipids, secondary metabolites and amino acids (Fig. 3B). Generally, the number of genes being differentially expressed was higher in the 800 µatm CO_2 as compared to the 180 µatm CO_2 treatment, particularly those genes related to post-translational modification and the transport and metabolism of carbohydrates (Fig. 3B). In only a few KOG categories, the number of regulated genes clearly differed between the high and low CO_2 treatment. Specifically, the number of down-regulated genes associated to the categories 'Secondary metabolites biosynthesis, transport and catabolism [Q]' and 'Amino acid transport and

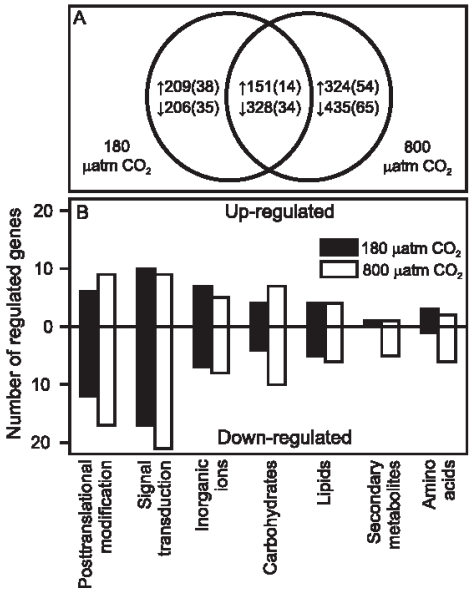

Fig. 3. Venn diagram showing the total and annotated number (between brackets) of differentially expressed genes in Alex 5 (A), and the regulation of annotated genes grouped by most represented KOG categories (B). Values indicate the actual number of genes being up-regulated (↑) and down-regulated (↓) in the 180 µatm CO_2 (A, left circle; B, black bar) and 800 µatm CO_2 (A, right circle; B, white bar) treatments in comparison to the control treatment of 380 µatm CO_2. Short KOG category names refer to 'Post-translational modification, protein turnover and chaperones [O]', 'Signal transduction mechanisms [T]', 'Inorganic ion transport and metabolism [P]', 'Carbohydrate transport and metabolism [G]', 'Lipid transport and metabolism [I]', 'Secondary metabolite biosynthesis, transport and catabolism [Q]' and 'Amino acid transport and metabolism [E]'.

metabolism [E]' was higher in the 800 µatm CO_2 as compared to the 180 µatm CO_2 treatment (Figs. 3 and A.3).

In view of the pronounced changes in toxin composition of Alex5 from non-sulfated to sulfated PST analogues, we analysed the genes involved in sulfur metabolism more closely. A total of 17 genes within the sulfur metabolism were found to be regulated in the 180 and 800 µatm CO_2 treatment compared to the 380 µatm CO_2 treatment (Table 2). In response to elevated pCO_2, we also observed a significant up-regulation of a gene with strong resemblance to a sulfotransferase in the cyanobacterium *Cylindrospermopsis*, which may thus be a putative *sxtN* homologue involved in the synthesis of sulfated PST analogues (Hackett et al., 2013; Moustafa et al., 2009; Soto-Liebe et al., 2010; Stucken et al., 2010). However, the relative change was small (i.e. 1.3 fold; Tables 2 and B.2) and we did not observe differential expression of other putative homologues of STX genes.

4. Discussion

While growth and carbon production remained largely unaffected with elevated pCO_2 (Table 1), the cellular PST content and associated toxicity were clearly reduced under high pCO_2 in both strains (Fig. 1). Furthermore, PST composition in Alex5 shifted towards more sulfated analogues with increasing pCO_2, whereas PST composition in Alex2 remained unaltered (Fig. 2). The observed decrease in PST content of Alex5 may be explained by a decrease in the relative expression of genes involved in amino acid metabolism (Fig. 3), presumably including arginine which is an important precursor in PST biosynthesis. The shift in PST composition towards more sulfated analogues is in line with CO_2-dependent changes in the expression of genes involved in sulfur metabolism, notably a putative sulfotransferase *sxtN* homologue associated to PST synthesis (Table 2; Hackett et al., 2013; Moustafa et al., 2009; Soto-Liebe et al., 2010). The largest number of genes being differentially expressed compared to the control was related to signal transduction and post-translational modification. This suggests that the ability of Alex5 to maintain cellular homeostasis with respect to growth and elemental composition is predominantly achieved by post-translational modification of general physiological processes rather than a specific transcriptomic regulation.

4.1. CO_2 effects on growth and PST contents

The minor changes of growth and carbon production rates in response to elevated pCO_2 are somewhat surprising, as dinoflagellates were expected to be sensitive to changes in CO_2 due to their low affine RubisCO. This suggests that both *A. tamarense* strains do not rely on diffusive CO_2 supply alone and instead operate a carbon concentrating mechanism (CCM), as has been shown for several red-tide dinoflagellate species (Rost et al., 2006). Such a CCM may be regulated as a function of CO_2 supply, enabling the cell to keep its growth relatively unaffected over the tested CO_2 range. Regarding the gene expression in Alex5, we observed a significant down-regulation of a gene homologous to carbonic anhydrase (CA) with elevated pCO_2 (Appendix C). As CA accelerates the interconversion between HCO_3 and CO_2, it often plays an important role in the functioning of CCMs (Giordano et al., 2005a; Reinfelder, 2011). The lowered expression of CA homologues under elevated pCO_2 is in line with the often observed down-regulation of CA activities (Sültemeyer et al., 1989 Trimborn et al., 2013), and may therefore be taken as an indication for a down-regulation of the CCM. In Alex5, we further observed a larger number of genes associated to carbohydrate transport and metabolism being regulated in the high CO_2 treatment (Fig. 3B), which points towards re-constellation of internal carbon fluxes helping to maintain homeostasis in terms of growth and elemental composition.

In Alex2, highest growth rate as well as PST content was observed in the lowest CO_2 treatment, whereas in all other treatments the growth rate and toxin content were consistently lower. Furthermore, PST contents in the faster growing Alex5 were much higher than in slower growing Alex2, hinting towards a general relationship between growth and toxin content. When nutrients are in ample supply, cellular PST content has indeed been dependent on the growth cycle and tend to increase with growth rate (Cembella, 1998; Taroncher-Oldenburg et al., 1997). The

Table 2
Regulated genes coding for proteins involved in sulfur metabolism.

pCO_2	Regulation	Probe identifier	Pfam domain	Putative gene function [product]	Fold change
180	Down	42752174	2Fe–2S iron–sulfur cluster binding domain	Citric acid cycle & electron transport chain [succinate dehydrogenase]	1.5
		Atam22716	Radical SAM superfamily	Sulfur insertion	1.7
		Tc_01299	Rieske [2Fe–2S] domain	Oxidation-reduction processes	1.9
	Up	Atam05776	Nitrite/Sulfite reductase ferredoxin-like half domain	Sulfite reduction [sulfite reductase]	1.6
		Atam07846	Taurine catabolism dioxygenaseTauD, TfdA family	Release of sulfite from taurine	3.2
		Contig03677	Thiamine pyrophosphate enzyme	Thiamine consuming reactions, sulfur containing co-factor	1.7
		Contig51258	Sulfatase	Hydrolysis of sulfate esters	1.6
		Contig52974	Sulfate transporter family	Sulfate transporter	3.5
800	Down	42752174	2Fe-2S iron-sulfur cluster binding domain	Citric acid cycle & electron transport chain [succinde dehydrogenase]	2.2
		Atam05776	Nitrite/Sulfite reductase ferredoxin-like half domain	Sulfite reduction [sulfite reductase]	1.9
		Atam22716	Radical SAM superfamily	Sulfur insertion	3.2
		Contig03677	Thiamine pyrophosphate enzyme	Thiamine consuming reactions, sulfur containing co-factor	2.7
		Contig52312	Sulfatase	Hydrolysis of sulfate esters	2.6
		Tc_01299	Rieske [2Fe–2S] domain	Oxidation-reduction processes	2.2
	Up	Atam07846	Taurine catabolism dioxygenaseTauD, TfdA family	Release of sulfite from taurine	2.8
		Contig52974	Sulfate transporter family	Sulfate transporter	3.0
		Contig05268	Pyridine nucleotide-disulphide oxidoreductase	Oxidoreductase activity	2.8
		Atam20042	Sulfotransfer_3	*SxtN* gene candidate *A. tamarense*	1.3

growth rates of Alex5 were in line with earlier reported values in conventional batch cultures, while growth rates of Alex2 were lower (Zhu and Tillmann, 2012). This may be the result of differences in experimental conditions, suggesting that Alex2 may not have been growing optimally under the imposed conditions. Our findings seem to confirm that growth rate plays an important role in determining the PST content in *A. tamarense*.

Cells of Alex5 have lower C:N ratios than Alex2 and hence contain relatively more nitrogen. This nitrogen can be allocated to nitrogen containing metabolites, such as amino acids and PSTs, which would be in line with the observed differences in PST content between both strains of *A. tamarense*. Transcriptomic analyses in Alex5 furthermore reveal a down-regulation of amino acid transport and metabolism with elevated pCO_2 (Fig. 3). This down-regulation may also affect the availability of arginine, an important precursor of PSTs (Shimizu, 1996), and thus may explain the decreased PST content with elevated pCO_2. Additional studies including both amino acid composition and transcriptome analyses should further elucidate the role of amino acid metabolism in the synthesis of PSTs.

4.2. CO_2 effects on PST composition

PST composition in Alex5 shifted from a non-sulfated towards sulfated PST analogues with increasing pCO_2 (Fig. 2A,C,E), which implies that sulfation of PSTs is enhanced under these conditions. Sulfotransferases play a key role in sulfation of PST analogues and their activity is therefore important in determining the PST composition (Moustafa et al., 2009; Sako et al., 2001; Soto-Liebe et al., 2010). We observed a small, yet significant up-regulation in the expression of a putative sulfotransferase *sxtN* homologue in our high CO_2 treatment. Furthermore, we found substantial regulation in the expression of genes coding for sulfatases, which catalyse the hydrolysis of sulfate esters, and thereby possibly affect the PST composition (Fig. 4; Taroncher-Oldenburg et al., 1997). In the high CO_2 treatment, expression of sulfatase significantly decreased, whereas it increased in the low CO_2 treatment (Table 2). In other words, the transformation of di-sulfated and mono-sulfated PST analogues to mono-sulfated and non-sulfated PST analogues, respectively, is less likely to occur at elevated pCO_2, whereas these reactions are potentially more frequent at low pCO_2 (Fig. 4). We also observed a significant decrease in the expression of genes involved in sulfite reduction in the high CO_2 treatment, whereas it increased in the low CO_2 treatment. Sulfite reductase plays a role in the assimilation of sulfur into amino acids, starting with the production of cysteine (Fig. 4; Giordano et al., 2005b; Shibagaki and Grossman, 2008). Our data thus suggests that with elevated pCO_2, more sulfur is allocated in sulfated PST analogues, while less is assimilated to cysteine (Fig. 4). Although the exact processes remain to be elucidated, our results clearly demonstrate that elevated pCO_2 can affect sulfur metabolism in *A. tamarense* and thereby causes a shift in PST composition towards more sulfated analogues.

PST composition in Alex2 was not affected by changes in pCO_2. Given that the same treatments have been applied to both strains, the observed differences in CO_2-sensitivity are presumably strain-specific (Alpermann et al., 2010; Tillmann et al., 2009). There have been earlier attempts to assess strain-specific differences in the response of PST composition towards elevated pCO_2 in *Alexandrium ostenfeldii* (Kremp et al., 2012). The observed trends in the latter study remain inconclusive, however, due to the large shifts in carbonate chemistry that occurred during the experiments. Hence, further experiments are needed to test

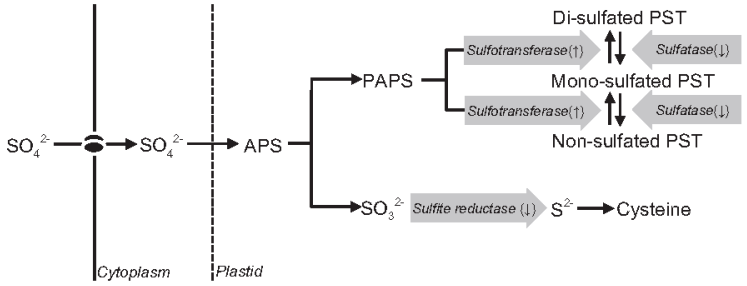

Fig. 4. Schematic diagram of observed CO_2 effects on sulfate (SO_4^{2-}) assimilation in Alex5. Vertical arrows next to enzymes indicate up-regulation (↑) or down-regulation (↓) in relevant genes under elevated CO_2. After taken up by the cell, SO_4^{2-} is transported to the plastid and activated to 5′-adenylsulfate (APS). This APS can be reduced to sulfite (SO_3^{2-}) and subsequently to sulfide (S^{2-}). The latter reaction is catalysed by SO_3^{2-} reductase. The resulting free S^{2-} is immediately incorporated into cysteine, the first stable sulfur containing organic biochemical. APS can also undergo a second phosphorylation, yielding 3′-phosphoadenosine 5′-phosphosulfate (PAPS), which can be used by sulfotransferases to catalyse sulfation of various metabolites, including PSTs. Transformation of di-sulfated and mono-sulfated PST analogues to mono-sulfated and non-sulfated PST analogues is catalysed by sulfatases.

whether elevated pCO_2 indeed alters sulfur metabolism and subsequently the production of sulfated PST analogues in *Alexandrium* as well as other PST producers.

4.3. Ecological implications

What will be the impact of elevated pCO_2 on PST production in natural occurring blooms of *A. tamarense*? Obviously, the natural system is far more complex than our dilute batch experiments, and blooms of *A. tamarense* comprise many more genotypes with different growth rates and PST characteristics than can be tested in laboratory studies (Alpermann et al., 2009; Alpermann et al., 2010; Tillmann et al., 2009; Yoshida et al., 2001). Being aware of this, we chose the two strains with different properties, for instance in terms of growth rate, elemental composition, PST characteristics, and most notably their allelopathic properties (Tillmann et al., 2009). We also worked with low cell densities in our experiments (i.e. <400 cells mL^{-1}) in order to be comparable with population densities of *Alexandrium* that may be reached during blooms (Wyatt and Jenkinson, 1997). Hence, natural blooms will likely be exposed to similar CO_2 levels as tested here, which may lead to the conclusion that with a decrease in the cellular toxicity of *A. tamarense*, future blooms may become less toxic.

A. tamarense blooms with population densities exceeding those reached in our experiments can shift seawater carbonate chemistry towards lower CO_2 concentrations and a higher pH. Ultimately, this may cause phytoplankton to become limited by CO_2, or to become negatively affected by the high pH (Hansen, 2002; Hansen et al., 2007; Tillmann and Hansen, 2009). Such a change in carbonate chemistry may have contrasting consequences for the toxicity of *A. tamarense* as compared to elevated pCO_2, i.e. the cellular toxicity could increase (Fig. 1). On top of that, elevated pCO_2 may promote higher population densities as cells can presumably sustain growth for a longer period before becoming CO_2 limited, or before reaching their pH limit. Hence, even if their cellular toxicity is not affected, higher population densities will increase the toxicity of an *A. tamarense* bloom. Experiments with natural occurring blooms of *A. tamarense* are required in order to understand the complex interactions that exist between carbonate chemistry, phytoplankton growth, and the toxicity of HABs.

Ecological consequences of changes in PST contents and composition will depend on the role of these compounds. It has been suggested that PSTs play a role in grazer defense (Selander et al., 2012, 2006; Wohlrab et al., 2010), act as pheromones (Wyatt and Jenkinson, 1997), and may have physiological functions as well (Cembella, 2003). Recent findings have further suggested that PST may play a role in the maintenance of cellular ion homeostasis (Pomati et al., 2004; Soto-Liebe et al., 2012), and this putative function seems to become more pronounced under elevated pH (Pomati et al., 2004). In our study, the highest PST content was indeed associated to the treatments with highest pH, i.e. the treatment with the lowest pCO_2 (Table B.1). It remains to be determined, however, whether the observed changes in PST content are primarily due to shifts in pH or by changes in CO_2 availability.

4.4. Conclusions

Here we show that growth and elemental composition in *A. tamarense* remain largely unaltered in response to elevated pCO_2. This ability to maintain cellular homeostasis under substantial changes in carbonate chemistry appears to be achieved primarily by post-translational regulation. In both *A. tamarense* strains, cellular PST content and particularly the associated toxicity were lower in the highest CO_2 treatments. In Alex5, PST composition further shifted towards more sulfated analogues under these conditions. These CO_2-dependent changes in PST content and composition are accompanied by substantial regulation of multiple genes, including those associated to secondary metabolite and amino acid metabolism. Notably, we found that elevated pCO_2 caused an opposing regulation of sulfotransferase and sulfatase, leading to an enhanced production of less toxic sulfated PST analogues. All in all, our findings suggest that elevated pCO_2 may have minor

consequences for growth and elemental composition of *A. tamarense*, yet may potentially cause a decrease in its cellular toxicity.

Acknowledgements

The authors like to thank Hannah Thörner for assistance with the experiments, Annegret Müller for helping with the PST analyses and Nancy Kühne for support with the molecular analyses. D.B.v.d.W., U.J., S.W., and B.R. thank BIOACID, financed by the German Ministry of Education and Research. Furthermore, this work was supported by the European Community's Seventh Framework Programme (FP7/2007-2013)/ERC grant agreement No. 205150, and contributes to project EPOCA under the grant agreement No. 211384. The funders had no role in study design, data collection and analysis, decision to publish, or preparation of the manuscript.

Appendices A, B, and C. Supplementary material

Supplementary material related to this article can be found at http://dx.doi.org/10.1016/j.toxicon.2013.11.011.

Conflict of interest statement

The authors declare that there are no conflicts of interest.

References

Alpermann, T.J., Beszteri, B., John, U., Tillmann, U., Cembella, A.D., 2009. Implications of life-history transitions on the population genetic structure of the toxigenic marine dinoflagellate *Alexandrium tamarense*. Mol. Ecol. 18, 2122–2133.

Alpermann, T.J., Tillmann, U., Beszteri, B., Cembella, A.D., John, U., 2010. Phenotypic variation and genotypic diversity in a planktonic population of the toxigenic marine dinoflagellate *Alexandrium tamarense* (Dinophyceae). J. Phycol. 46, 18–32.

Anderson, D.M., Alpermann, T.J., Cembella, A.D., Collos, Y., Masseret, E., Montresor, M., 2012a. The globally distributed genus *Alexandrium*: multifaceted roles in marine ecosystems and impacts on human health. Harmful Algae 14, 10–35.

Anderson, D.M., Cembella, A.D., Hallegraeff, G.M., 2012b. Progress in understanding harmful algal blooms: paradigm shifts and new technologies for research, monitoring, and management. Annu. Rev. Mar. Sci. 4, 143–176.

Badger, M.R., Andrews, T.J., Whitney, S.M., Ludwig, M., Yellowlees, D.C., Leggat, W., Price, G.D., 1998. The diversity and coevolution of Rubisco, plastids, pyrenoids, and chloroplast-based CO_2-concentrating mechanisms in algae. Can. J. Bot./Rev. Can. Bot. 76, 1052–1071.

Beaufort, L., Probert, I., de Garidel-Thoron, T., Bendif, E.M., Ruiz-Pino, D., Metzl, N., Goyet, C., Buchet, N., Coupel, P., Grelaud, M., Rost, B., Rickaby, R.E.M., de Vargas, C., 2011. Sensitivity of coccolithophores to carbonate chemistry and ocean acidification. Nature 476, 80–83.

Brading, P., Warner, M.E., Davey, P., Smith, D.J., Achterberg, E.P., Suggett, D.J., 2011. Differential effects of ocean acidification on growth and photosynthesis among phylotypes of *Symbiodinium* (Dinophyceae). Limnol. Oceanogr. 56, 927–938.

Burkhardt, S., Zondervan, I., Riebesell, U., 1999. Effect of CO_2 concentration on C:N: P ratio in marine phytoplankton: a species comparison. Limnol. Oceanogr. 44, 683–690.

Caldeira, K., Wickett, M.E., 2003. Anthropogenic carbon and ocean pH. Nature 425, 365–366.

Cembella, A.D., 1998. Ecophysiology and metabolism of paralytic Shellfixh toxins in marine microalgae. In: Anderson, D.M., Cembella, A.D., Hallegraeff, G.M. (Eds.), Physiological Ecology of Harmful Algal Blooms. Springer-Verlag, Berlin Heidelberg, Germany, pp. 281–403.

Cembella, A.D., 2003. Chemical ecology of eukaryotic microalgae in marine ecosystems. Phycologia 42, 420–447.

Dickson, A.G., 1990. Standard potential of the reaction: AgCl(s) + 1/2 H_2(g) = Ag(s) + HCl(aq), and the standard acidity constant of the ion HSO_4^- in synthetic seawater from 273.15 to 318.15 K. J. Chem. Thermodyn. 22, 113–127.

Dickson, A.G., Millero, F.J., 1987. A comparison of the equilibrium constants for the dissociation of carbonic acid in seawater media. Deep Sea Res. (I Oceanogr. Res. Pap.) 34, 1733–1743.

Fu, F.X., Place, A.R., Garcia, N.S., Hutchins, D.A., 2010. CO_2 and phosphate availability control the toxicity of the harmful bloom dinoflagellate *Karlodinium veneficum*. Aquat. Microb. Ecol. 59, 55–65.

Giordano, M., Beardall, J., Raven, J.A., 2005a. CO_2 concentrating mechanisms in algae: mechanisms, environmental modulation, and evolution. Annu. Rev. Plant Biol. 56, 99–131.

Giordano, M., Norici, A., Hell, R., 2005b. Sulfur and phytoplankton: acquisition, metabolism and impact on the environment. New Phytol. 166, 371–382.

Granéli, E., Flynn, K., 2006. Chemical and physical factors influencing toxin content. In: Granéli, E., Turner, J.T. (Eds.), Ecology of Harmful Algae. Springer-Verlag, Berlin Heidelberg, pp. 229–241.

Granéli, E., Turner, J.T., 2006. Ecology of Harmful Algae. Springer-Verlag, Berlin, Heidelberg, Germany.

Guillard, R.R.L., Ryther, J.H., 1962. Studies of marine planktonic diatoms: I. *Cyclotella nana* Hustedt, and *Detonula confervacea* (Cleve) Gran. Can. J. Microbiol./Rev. Can. Microbiol. 8, 229–239.

Hackett, J.D., Wisecaver, J.H., Brosnahan, M.L., Kulis, D.M., Anderson, D.M., Bhattacharya, D., Plumley, F.G., Erdner, D.L., 2013. Evolution of Saxitoxin synthesis in cyanobacteria and dinoflagellates. Mol. Biol. Evol. 30, 70–78.

Hallegraeff, G.M., 2010. Ocean climate change, phytoplankton community responses, and harmful algal blooms: a formidable predictive challenge. J. Phycol. 46, 220–235.

Hansen, P.J., 2002. Effect of high pH on the growth and survival of marine phytoplankton: implications for species succession. Aquat. Microb. Ecol. 28, 279–288.

Hansen, P.J., Lundholm, N., Rost, B., 2007. Growth limitation in marine red-tide dinoflagellates: effects of pH versus inorganic carbon availability. Mar. Ecol. Prog. Ser. 334, 63–71.

Hein, M., SandJensen, K., 1997. CO_2 increases oceanic primary production. Nature 388, 526–527.

Kremp, A., Godhe, A., Egardt, J., Dupont, S., Suikkanen, S., Casabianca, S., Penna, A., 2012. Intraspecific variability in the response of bloom-forming marine microalgae to changed climate conditions. Ecol. Evol. 2, 1195–1207.

Krock, B., Seguel, C.G., Cembella, A.D., 2007. Toxin profile of *Alexandrium catenella* from the Chilean coast as determined by liquid chromatography with fluorescence detection and liquid chromatography coupled with tandem mass spectrometry. Harmful Algae 6, 734–744.

Marchler-Bauer, A., Lu, S.N., Anderson, J.B., Chitsaz, F., Derbyshire, M.K., DeWeese-Scott, C., Fong, J.H., Geer, L.Y., Geer, R.C., Gonzales, N.R., Gwadz, M., Hurwitz, D.I., Jackson, J.D., Ke, Z.X., Lanczycki, C.J., Lu, F., Marchler, G.H., Mullokandov, M., Omelchenko, M.V., Robertson, C.L., Song, J.S., Thanki, N., Yamashita, R.A., Zhang, D.C., Zhang, N.G., Zheng, C.J., Bryant, S.H., 2011. CDD: a conserved domain database for the functional annotation of proteins. Nucleic Acids Res. 39, D225–D229.

Mehrbach, C., Culberson, C.H., Hawley, J.E., Pytkowicz, R.M., 1973. Measurement of the apparent dissociation constants of carbonic acid in seawater at atmospheric pressure. Limnol. Oceanogr. 18, 897–907.

Moustafa, A., Loram, J.E., Hackett, J.D., Anderson, D.M., Plumley, F.G., Bhattacharya, D., 2009. Origin of saxitoxin biosynthetic genes in cyanobacteria. PLoS ONE 4.

Neilan, B.A., Pearson, L.A., Muenchhoff, J., Moffitt, M.C., Dittmann, E., 2013. Environmental conditions that influence toxin biosynthesis in cyanobacteria. Environ. Microbiol. 15, 1239–1253.

Pierrot, D.E., Lewis, E., Wallace, D.W.R., 2006. MS Exel Program Developed for CO2 System Calculations. ORNL/CDIAC-105a. Carbon Dioxide Information Analysis Centre, Oak Ridge National Laboratory, US Department of Energy, Oak Ridge, Tennessee, USA.

Pomati, F., Rossetti, C., Manarolla, G., Burns, B.P., Neilan, B.A., 2004. Interactions between intracellular Na^+ levels and saxitoxin production in *Cylindrospermopsis raciborskii* T3. Microbiology 150, 455–461.

Quinn, G.P., Keough, M.J., 2002. Experimental Design and Data Analysis for Biologists. Cambridge University Press, Cambridge, UK.

Reinfelder, J.R., 2011. Carbon concentrating mechanisms in eukaryotic marine phytoplankton. Annu. Rev. Mar. Sci. 3, 291–315.

Riebesell, U., Tortell, P.D., 2011. Effects of ocean acidification on pelagic organisms and ecosystems. In: Gattuse, J.P., Hansson, L. (Eds.), Ocean Acidification. Oxford University Press, Oxford, UK, pp. 99–121.

Riebesell, U., Zondervan, I., Rost, B., Tortell, P.D., Zeebe, R.E., Morel, F.M.M., 2000. Reduced calcification of marine plankton in response to increased atmospheric CO_2. Nature 407, 364–367.
Rost, B., Richter, K.U., Riebesell, U., Hansen, P.J., 2006. Inorganic carbon acquisition in red tide dinoflagellates. Plant Cell Environ. 29, 810–822.
Sako, Y., Yoshida, T., Uchida, A., Arakawa, O., Noguchi, T., Ishida, Y., 2001. Purification and characterization of a sulfotransferase specific to N-21 of saxitoxin and gonyautoxin 2 + 3 from the toxic dinoflagellate *Gymnodinium catenatum* (Dinophyceae). J. Phycol. 37, 1044–1051.
Selander, E., Fagerberg, T., Wohlrab, S., Pavia, H., 2012. Fight and flight in dinoflagellates? Kinetics of simultaneous grazer-induced responses in *Alexandrium tamarense*. Limnol. Oceanogr. 57, 58–64.
Selander, E., Thor, P., Toth, G., Pavia, H., 2006. Copepods induce paralytic shellfish toxin production in marine dinoflagellates. Proc. R. Soc. Lond., Ser. B: Biol. Sci. 273, 1673–1680.
Shibagaki, N., Grossman, A., 2008. The state of sulfur metabolism in algae: from ecology to genomics. In: Hell, R., Dahl, C., Knaff, D.B., Leustek, T. (Eds.), Advances in Photosynthesis and Respiration: Sulfur Metabolism in Phototrophic Organisms. Springer, Dordrecht, The Netherlands, pp. 231–267.
Shimizu, Y., 1996. Microalgal metabolites: a new perspective. Annu. Rev. Microbiol. 50, 431–465.
Sivonen, K., Jones, G., 1999. Cyanobacterial toxins. In: Chorus, I., Bartram, J. (Eds.), Toxic Cyanobacteria in Water: A Guide to their Public Health Consequences, Monitoring and Management. E & FN Spon, WHO, London, pp. 41–112.
Solomon, S., Qin, D., Manning, M., Marquis, M., Averyt, K., Tignor, M.M.B., Miller Jr., H.L., Zhenlin, C., 2007. Climate Change 2007: The Physical Science Basis. Contribution of Working Group I to the Fourth Assessment Report of the Intergovernmental Panel on Climate Change. Cambridge University Press, Cambridge, UK.
Soto-Liebe, K., Mendez, M.A., Fuenzalida, L., Krock, B., Cembella, A., Vásquez, M., 2012. PSP toxin release from the cyanobacterium *Raphidiopsis brookii* D9 (Nostocales) can be induced by sodium and potassium ions. Toxicon 60, 1324–1334.
Soto-Liebe, K., Murillo, A.A., Krock, B., Stucken, K., Fuentes-Valdés, J.J., Trefault, N., Cembella, A., Vásquez, M., 2010. Reassessment of the toxin profile of *Cylindrospermopsis raciborskii* T3 and function of putative sulfotransferases in synthesis of sulfated and sulfonated PSP toxins. Toxicon 56, 1350–1361.
Stucken, K., John, U., Cembella, A., Murillo, A.A., Soto-Liebe, K., Fuentes-Valdés, J.J., Friedel, M., Plominsky, A.M., Vásquez, M., Glöckner, G., 2010. The smallest known genomes of multicellular and toxic cyanobacteria: comparison, minimal gene sets for linked traits and the evolutionary implications. PLoS ONE 5.
Sültemeyer, D.F., Miller, A.G., Espie, G.S., Fock, H.P., Canvin, D.T., 1989. Active CO_2 transport by the green-alga *Chlamydomonas reinhardtii*. Plant Physiol. 89, 1213–1219.
Sun, J., Hutchins, D.A., Feng, Y.Y., Seubert, E.L., Caron, D.A., Fu, F.X., 2011. Effects of changing pCO_2 and phosphate availability on domoic acid production and physiology of the marine harmful bloom diatom *Pseudo-nitzschia multiseries*. Limnol. Oceanogr. 56, 829–840.
Taroncher-Oldenburg, G., Kulis, D.M., Anderson, D.M., 1997. Toxin variability during the cell cycle of the dinoflagellate *Alexandrium fundyense*. Limnol. Oceanogr. 42, 1178–1188.
Tillmann, U., Alpermann, T.L., da Purificacao, R.C., Krock, B., Cembella, A., 2009. Intra-population clonal variability in allelochemical potency of the toxigenic dinoflagellate *Alexandrium tamarense*. Harmful Algae 8, 759–769.
Tillmann, U., Hansen, P.J., 2009. Allelopathic effects of *Alexandrium tamarense* on other algae: evidence from mixed growth experiments. Aquat. Microb. Ecol. 57, 101–112.
Tortell, P.D., Payne, C.D., Li, Y.Y., Trimborn, S., Rost, B., Smith, W.O., Riesselman, C., Dunbar, R.B., Sedwick, P., DiTullio, G.R., 2008. CO_2 sensitivity of Southern Ocean phytoplankton. Geophys. Res. Lett. 35.
Trimborn, S., Brenneis, T., Sweet, E., Rost, B., 2013. Sensitivity of Antarctic phytoplankton species to ocean acidification: growth, carbon acquisition, and species interaction. Limnol. Oceanogr. 58, 997–1007.
Trimborn, S., Lundholm, N., Thoms, S., Richter, K.U., Krock, B., Hansen, P.J., Rost, B., 2008. Inorganic carbon acquisition in potentially toxic and non-toxic diatoms: the effect of pH-induced changes in seawater carbonate chemistry. Physiol. Plant 133, 92–105.
Van de Waal, D.B., John, U., Ziveri, P., Reichart, G.J., Hoins, M., Sluijs, A., Rost, B., 2013a. Ocean acidification reduces growth and calcification in a marine dinoflagellate. PLoS ONE 8, e65987.
Van de Waal, D.B., Tillmann, U., Zhu, M.M., Koch, B.P., Rost, B., John, U., 2013b. Nutrient pulse induces dynamic changes in cellular C: N:P, amino acids, and paralytic shellfish poisoning toxins in *Alexandrium tamarense*. Mar. Ecol. Prog. Ser. in press.
Wiese, M., D'Agostino, P.M., Mihali, T.K., Moffitt, M.C., Neilan, B.A., 2010. Neurotoxic alkaloids: Saxitoxin and its analogs. Mar. Drugs 8, 2185–2211.
Wohlrab, S., Iversen, M.H., John, U., 2010. A molecular and co-evolutionary context for grazer induced toxin production in *Alexandrium tamarense*. PLoS ONE 5.
Wolf-Gladrow, D.A., Riebesell, U., Burkhardt, S., Bijma, J., 1999. Direct effects of CO_2 concentration on growth and isotopic composition of marine plankton. Tellus (B Chem. Phys. Meteorol.) 51, 461–476.
Wyatt, T., Jenkinson, I.R., 1997. Notes on *Alexandrium* population dynamics. J. Plankton Res. 19, 551–575.
Yoshida, T., Sako, Y., Uchida, A., 2001. Geographic differences in paralytic shellfish poisoning toxin profiles among Japanese populations of *Alexandrium tamarense* and *A. catenella* (Dinophyceae). Phycol. Res. 49, 13–21.
Zhu, M.M., Tillmann, U., 2012. Nutrient starvation effects on the allelochemical potency of *Alexandrium tamarense* (Dinophyceae). Mar. Biol. 159, 1449–1459.

Ort, Datum: _____

Versicherung an Eides Statt

Ich, _____ (Vorname, Name, Anschrift, Matr.-Nr.)

.

versichere an Eides Statt durch meine Unterschrift, dass ich die vorstehende Arbeit selbständig und ohne fremde Hilfe angefertigt und alle Stellen, die ich wörtlich dem Sinne nach aus Veröffentlichungen entnommen habe, als solche kenntlich gemacht habe, mich auch keiner anderen als der angegebenen Literatur oder sonstiger Hilfsmittel bedient habe.
Ich versichere an Eides Statt, dass ich die vorgenannten Angaben nach bestem Wissen und Gewissen gemacht habe und dass die Angaben der Wahrheit entsprechen und ich nichts verschwiegen habe.
Die Strafbarkeit einer falschen eidesstattlichen Versicherung ist mir bekannt, namentlich die Strafandrohung gemäß § 156 StGB bis zu drei Jahren Freiheitsstrafe oder Geldstrafe bei vorsätzlicher Begehung der Tat bzw. gemäß § 161 Abs. 1 StGB bis zu einem Jahr Freiheitsstrafe oder Geldstrafe bei fahrlässiger Begehung.

_____
Ort, Datum Unterschrift